UNIVERSITÀ
DEGLI STUDI
DI PADOVA

UNIVERSITA' DEGLI STUDI DI PADOVA

DIPARTIMENTO DI BIOLOGIA

SCUOLA DI DOTTORATO DI RICERCA IN : BIOSCIENZE E BIOTECNOLOGIE

INDIRIZZO: NEUROBIOLOGIA

CICLO: XXVI

ROLE OF AUTOPHAGY IN AGE-RELATED MUSCLE LOSS

Direttore della Scuola: Ch.mo Prof. Giuseppe Zanotti

Coordinatore d'indirizzo: Ch.ma Prof.ssa Daniela Pietrobon

Supervisore: Prof. Marco Sandri

Dottoranda: Francesca Lo Verso

INDEX

RIASSUNTO

Il sistema autofagico-lisosomiale è un sistema di degradazione ubiquitario e conservato tra le diverse specie. Esso viene attivato dalla cellula per degradare proteine con lunga emivita, organelli danneggiati e porzioni citoplasmatiche, che vengono sequestrate da un network di vescicole a doppia membrana, dette autofagosomi. Gli autofagosomi che contengono il materiale da degradare fondono con i lisosomi, dove il loro contenuto viene degradato e i prodotti riciclati per soddisfare la richiesta energetica cellulare. Il muscolo scheletrico è il tessuto più abbondante nei mammiferi e utilizza l'80% del glucosio presente nel corpo. Un efficiente sistema autofagico è necessario per il mantenimento della massa muscolare (Masiero et al., 2009). Durante l'invecchiamento, il tessuto muscolare subisce un inevitabile processo di atrofia, detto sarcopenia, che è indipendente dall'attività del soggetto ma si aggrava in condizioni di disuso (Rossi et al., 2008). I meccanismi coinvolti nella perdita di massa muscolare non sono ancora stati individuati con chiarezza. Poiché l'autofagia diminuisce con l'età (Tan et al., 2013), abbiamo studiato il ruolo dell'autofagia durante l'invecchiamento del tessuto muscolare.

In questo lavoro sono stati quindi caratterizzati topi knockout condizionali per il gene Atg7 ($Atg7^{-/-}$), gene che codifica per un enzima critico per la formazione degli autofagosomi (Masiero et al., 2009). In questo modo è possibile ottenere il blocco del processo autofagico in modo specifico nel muscolo scheletrico. Questi animali e i rispettivi controlli sono stati analizzati durante l'invecchiamento. I topi $Atg7^{-/-}$ muoiono prima dei controlli e, da vecchi, presentano un fenotipo miopatico, in cui le condizioni di atrofia sono esacerbate rispetto agli animali $Atg7^{-/-}$ adulti. Misure di forza *in vivo* di questi animali hanno mostrato come gli animali $Atg7^{-/-}$ risultino più deboli dei controlli; inoltre, gli animali $Atg7^{-/-}$ adulti presentano la stessa forza dei controlli vecchi, suggerendo uno stato di indebolimento precoce. Poiché il sistema autofagico è importante per la rimozione degli organelli danneggiati, abbiamo studiato i mitocondri. Durante l'invecchiamento, i mitocondri dei muscoli $Atg7^{-/-}$ si accumulano e presentano un'alterata

morfologia alla microscopia elettronica. Abbiamo quindi analizzato la loro funzionalità misurando la capacità di mantenere il potenziale di membrana mitocondriale dopo l'aggiunta di un inibitore dell'ATP sintasi. I mitocondri degli Atg7$^{-/-}$ sono risultati incapaci di mantenere il potenziale, al contrario dei controlli. L'alterata funzionalità mitocondriale induce un aumento della produzione di ROS con conseguente stress ossidativo. Mediante un approccio di proteomica in collaborazione con il Prof. Friguet dell'Univeristà di Parigi, abbiamo caratterizzato le proteine ossidate e abbiamo trovato che le proteine contrattili, actina e miosina, erano le proteine maggiormente carbonilate nei topi vecchi knockout rispetto ai controlli della stessa età. Per capire se questa alterazione contribuisse alla debolezza muscolare di questi animali abbiamo eseguito saggi funzionali in collaborazione con il gruppo del Prof. Bottinelli dell'Università di Pavia. Misurazioni della forza sulle singole fibre e della velocità di scorrimento dei filamenti di actina/miosina hanno mostrato che gli Atg7$^{-/-}$ hanno capacità contrattili minori e alterazioni nell'interazione actina/miosina.

Sebbene la presenza di fibre denervate sia fisiologica durante l'invecchiamento, gli animali adulti Atg7$^{-/-}$ presentano segni di denervazione precoce, indicata dall'aumento di espressione di markers specifici come Muscle Specific Kinase (MuSK), Acetylcholine Receptor gamma subunit (AchR-gamma) e Neural Cell Adhesion Molecule (NCAM); inoltre la loro espressione aumenta ulteriormente con l'età. Abbiamo quindi deciso di analizzare in dettaglio la giunzione neuromuscolare in collaborazione con il gruppo del Dr. Rudolf presso Karlsruhe Institute of Technology (KIT) a Karlsrhue. Esperimenti di *in vivo* imaging hanno mostrato che le giunzioni degli Atg7$^{-/-}$ sono instabili e frammentate. Tali alterazioni sono già ben evidenti in animali adulti Atg7$^{-/-}$ suggerendo nuovamente un processo di invecchiamento precoce dovuto al blocco autofagico.

Ci siamo poi focalizzati sul potenziale ruolo dello stress ossidativo nel generare e contribuire al fenotipo di questi animali. Abbiamo trattato gli animali per 30 giorni con un anti-ossidante (Trolox), analogo della vitamina E. Dopo il trattamento, le capacità contrattili di actina/miosina e di funzionalità mitocondriale sono tornate al livello dei controlli, mentre abbiamo osservato solo effetti minori sulla giunzione neuromuscolare e nessun miglioramento sull' atrofia. Questi risultati indicano che lo stress ossidativo ha sicuramente un ruolo sulla funzionalità di proteine contrattili e dei mitocondri, ma che altri fattori sono implicati nel mantenimento della giunzione neuro-muscolare e nell'atrofia. Ci siamo quindi focalizzati su fattori neurotrofici secreti dal muscolo, che fossero alterati nei topi knockout, sia negli adulti che nei vecchi. Dopo uno screening mediante qRT-PCR abbiamo individuato FGF-binding protein 1 (FGFBP1) come l'unico fattore che risultava soppressonei topi Atg7$^{-/-}$ ad entrambe le età. FGFB1 è un importante attivatore di proteine FGFs coinvolte nell'organizzazione pre-sinaptica. A questo punto per capire il ruolo di FGFBP1, abbiamo effettuato esperimenti di silenziamento e di sovra-espressione *in vivo.* Inizialmenete abbiamo ridotto l'espressione di FGFBP1 in animali di controllo per mimare il fenotipo dei topi Atg7$^{-/-}$. Due settimane di silenziamento sono state sufficienti per provocare instabilità e frammentazione della giunzione neuromuscolare. Successivamente abbiamo over-espresso FGFBP1 negli animali Atg7$^{-/-}$ per ristabilirne l'espressione ed abbiamo osservato un drastico miglioramento della stabilità della giunzione neuromuscolare. In ultimo, per far luce sul meccanismo che lega l'assenza di autofagia all'alterazione di FGFBP1, ci siamo concentrati su MuSK, una chinasi essenziale per la regolazione della maggior parte dei segnali implicati nello sviluppo e mantenimento della giunzione neuromuscolare. La localizzazione di MuSK risulta alterata negli animali Atg7$^{-/-}$ e il silenziamento di MuSK *in vivo* in animali di controllo porta all'abbattimento dell'espressione di FGFBP1.

Questi risultati suggeriscono che il mantenimento della giunzione neuromuscolare richiede la secrezione di FGFBP1 da parte del muscolo e che l'autofagia è un processo critico per la giusta localizzazione e quindi attività di MuSK.

Diversi lavori hanno dimostrato come la restrizione calorica e l'esercizio fisico migliorino la qualità della vita, siano in grado di ritardare l'insorgenza di caratteristiche proprie dell'invecchiamento ed avere effetti benefici sul mantenimento della giunzione neuromuscolare (Melov et al., 2007; Fontana et al., 2010; Sandri et al., 2013; Schiaffino et al., 2013; Coen et al., 2013; Toledo et al., 2013; Guarente, 2013). In letteratura sono presenti lavori che hanno analizzato il ruolo dell'autofagia nell'esercizio (He et al., 2012; Kim et al., 2013), essi però presentano risultati contrastanti. He et al. sostengono che l'autofagia sia richiesta per l'esercizio fisico e la regolazione dell'omeostasi del glucosio (He et al., 2009), al contario altri gruppi osservano un fenotipo opposto in animali in cui l'autofagia è assente costitutivamente nel muscolo scheletrico (Kim et al., 2013). In questo scenario, quindi, non è ancora chiaro il ruolo dell'autofagia durante l'esercizio e se gli effetti benefici dello stesso sono mediati da essa. Per investigare questo aspetto, abbiamo utilizzato animali in cui la delezione del gene Atg7, viene indotta specificamente nel muscolo scheletrico dopo somministrazione di Tamoxifen (Masiero et al., 2009). In questo modo è possibile escludere meccanismi di compensazione e adattamento presenti in modelli in cui le delezioni sono costitutive. Abbiamo deleto acutamente il gene Atg7 in animali adulti e, insieme ai rispettivi controlli, li abbiamo sottoposti ad un protocollo di esercizio concentrico su treadmill. Tuttavia non abbiamo osservato differenze nelle distanze percorse tra i due genotipi. Questo indica che l'autofagia non è richiesta per sostenere attività contrattile durante un normale esercizio concentrico.

Abbiamo, poi, sottoposto gli animali ad un protocollo di tre giorni di esercizio eccentrico, per valutare se l'autofagia fosse invece richiesta per il mantenimento del tessuto muscolare in seguito a contrazioni che inducono danno. In questo caso abbiamo osservato che gli animali $Atg7^{-/-}$ corrono di meno rispetto ai controlli e, in particolare, questa differenza risulta significativa nelle femmine. Per investigare il motivo della ridotta performance abbiamo inizialmente analizzato la morfologia, senza però osservare segni di alterazione o infiammazione. Successivamente, abbiamo valutato aspetti metabolici, ma né i livelli di glicemia e di lattacidemia, né la fosforilazione della chinasi attivata da AMP (AMPK), uno dei maggiori indicatori di stress energetico, risultano differenti tra $Atg7^{-/-}$ e controlli dopo l'esercizio.

Dato che l'autofagia è richiesta per il mantenimento del pool mitocondriale, abbiamo analizzato se la funzionalità dei mitocondri fosse alterata dopo l'esercizio. In questo caso abbiamo confermato che la delezione acuta di Atg7 causa l'accumulo di mitocondri disfunzionanti, e che la loro percentuale aumentava dopo l'esercizio. La presenza di mitocondri anomali causa un aumento dello stress ossidativo. Infatti abbiamo potuto dimostrare una maggiore carbonilazione delle proteine e aumentati livelli di produzione di ROS dopo l'esercizio, nei topi Atg7$^{-/-}$ rispetto ai controlli. Per valutare gli effetti dello stress ossidativo abbiamo trattato gli animali per sei settimane con un anti-ossidante generico N-acetil-cisteina (NAC). Sorprendentemente, il trattamento si è rivelato dannoso per la performance degli animali di controllo e in più non è stato in grado di migliorare l'attività dei topi Atg7$^{-/-}$. L'antiossidante ha causato, inoltre, l'accumulo di mitocondri disfunzionanti nei topi di controllo. Questi risultati sono stati confermati anche dopo un trattamento con un diverso anti-ossidante (Mito-TEMPO), ad azione specifica sui mitocondri.
E' riportato in letteratura che il trattamento con anti-ossidanti riduce i livelli di autofagia in animali di controllo e che livelli fisiologici di ROS svolgono funzioni critiche nel signalling cellulare (Underwood et al., 2010; Owusu-Ansah et al., 2013). Negli animali di controllo trattati con anti-ossidante sono state confermate queste evidenze, ed infatti l'autofagia era bloccata. Questa inibizione potrebbe essere la causa dell'accumulo di mitocondri disfunzionanati e della loro performance.

Questi risultati sottolineano il ruolo dell'autofagia nel mantenimento della funzionalità mitocondriale durante contrazioni eccentriche. Inoltre definiscono che l'autofagia non è richiesta per il supporto energetico durante le normali contrazioni e che AMPK e i livelli ematici di glucosio non dipendono dall' attività del sistema autofagico.

SUMMARY

Autophagy is an ubiquitous degradation system, that is conserved through species. Cells activate autophagy to degrade long-lived proteins, damaged organelles or portions of cytoplasm, that are engulfed in double-membrane vesicles called autophagosomes, that ultimately fuse to lysosomes, where the cargo is degraded and breakdown products are recycled to sustain cellular energetic demands.

Skeletal muscle is the most abundant tissue in mammals and controls 80% of the blood glucose. We have recently shown that an efficient autophagy is required for muscle mass maintenance (Masiero et al., 2009).

During ageing, muscles inevitably undergo atrophy, a process named sarcopenia (Rossi et al. 2008). Moreover, it has been reported that autophagy declines with age (Tan et al., 2013). Since the mechanisms involved in age-related muscle loss remain obscure, we investigated whether autophagy impairment contributes to sarcopenia. In this work, the muscle-specific autophagy knockout ($Atg7^{-/-}$MLC), that were recently generated in our laboratory, were characterized during ageing (Masiero et al., 2009). Aged $Atg7^{-/-}$ mice have reduced lifespan and exacerbated atrophic and myopathic phenotype. *In vivo* force measurements showed that they are weaker compared to age-matched control mice. Alteration of mitochondrial morphology is a typical feature of $Atg7^{-/-}$ muscles. Therefore, we studied mitochondrial function in adult mice. Mitochondria of $Atg7^{-/-}$ mice were dysfunctional, in fact they did not retain membrane potential upon inhibition of ATP synthase. This mitochondrial alteration induced an increase of oxidative stress. A proteomic approach on oxidized protein, in collaboration with Prof. Friguet at the University of Paris, revealed that contractile proteins, such as actin and myosin, were significantly more carbonylated when autophagy was blocked. Functional assays of force measurements on single isolated fibers and sliding properties of purified actin/myosin, performed in collaboration with Prof. Bottinelli at the University of Pavia, showed an impairment of these contractile proteins in $Atg7^{-/-}$ mice.

$Atg7^{-/-}$ mice also undergo spontaneous denervation, as confirmed by upregulation of denervation markers, such as Muscle Specific Kinase (MuSK), Acetylcholine Receptor gamma subunit (AchR-gamma) and Neural Cell Adhesion Molecule (NCAM). Moreover, in collaboration with Dr. Rudolf at Karlsruhe Institute of

Technology (KIT), in Karlsrhue, we performed *in vivo* imaging of neuromuscular junction (NMJ), that revealed NMJ fragmentation and instability in autophagy-deficient mice. These findings suggest that inhibition of autophagy specifically in muscle generates a series of events that affect NMJ and causes a precocious denervation, contributing to sarcopenia. Since oxidative stress is an important feature of Atg7$^{-/-}$ mice and is believed to contribute to ageing, we treated adult mice with an antioxidant vitamin E analogue (Trolox), for 30 days, and we monitored the effects on the phenotype of Atg7$^{-/-}$ muscles. Trolox treatment reduced the level of protein carbonylation, restored the sliding properties of actin and myosin and brought back the force to normal level. Mitochondria function was also ameliorated but we did not find any benefit on atrophy and NMJ morphology. However, there was a small amelioration on NMJ stability.

These data showed that oxidative stress contributes only to some aspects of ageing features present in Atg7$^{-/-}$ mice. Therefore, other mechanisms are involved for the atrophy and the denervation aspects. We then hypothesized that muscles release neurotrophic factors that are critical for muscle-nerve interaction and stability. Initially, we tought for neurotrophic factors that were down-regulated in autophagy-deficient muscle both in adult and old mice. qRT-PCR identified FGF binding protein 1 (FGFBP1) to be the one that was always suppressed in Atg7$^{-/-}$ mice. FGFBP1 is protein involved in the bio-activation of FGF proteins, that are important pre-synaptic organizers. In order to investigate the role of FGFBP1 in NMJ instability we used loss and gain of function approaches. Down-regulation of FGFBP1 in control mice induced instability and fragmentation of NMJ. On the contrary FGFBP1 over-expression in Atg7$^{-/-}$ muscles reduced the number of denervated fibers and restored NMJ stability. Then we investigated the connection between autophagy impairment and FGFBP1 down-regulation, by analyzing MuSK activity, a kinase that is essential for NMJ maintenance. We observed an alterated MuSK clustering in NMJ of Atg7$^{-/-}$ mice. Moreover MuSK down-regulation *in vivo* leads to FGFBP1 suppression.

These results suggest that NMJ requires the secretion of FGFBP1 neurotrophic factor that is under MuSK regulation and that autophagy is critical for a normal MuSK localization and activity.

It has been consistently demonstrated that two lifestyle adaptations, namely caloric restriction and exercise, are able to extend lifespan and, in parallel, to mitigate age-related alterations in NMJ (Melov et al., 2007; Fontana et al., 2010; Sandri et al., 2013; Schiaffino et al., 2013; Coen et al., 2013; Toledo et al., 2013; Guarente, 2013). Moreover, both these conditions promote autophagy activation in skeletal muscles and in other tissues. It has also been reported that autophagy is required for exercise itself and for training-induced adaptations in glucose homeostasis (He et al., 2012). These findings remain controversial as skeletal muscle–specific autophagy-knockout mice show the opposite phenotype (Kim et al., 2013). In this scenario, it is still unknown whether it is whole body or muscle specific autophagy that is required to sustain contraction, maintain glucose homeostasis, and trigger exercise-induced benefits. For this reason, we used Tamoxifen-inducible, muscle-specific, Atg7 knockout mice (Atg7$^{-/-}$HSA), that we have recently generated (Masiero et al., 2009), to investigate the role of autophagy in physical exercise. This inducible muscle-specific genetic model allows to minimize the chance of any adaptations and compensations that usually occur with constitutive deletion of genes. In order to investigate whether acute block of autophagy in muscle affects exercise performance, controls and autophagy-deficient mice were exercised on a treadmill. We used a concentric exercise protocol while monitoring the maximum distance ran to exhaustion. Surprisingly, we did not find any significant differences in running capacity between controls and inducible Atg7$^{-/-}$. Thus, autophagy is not required to sustain muscle contraction during concentric physical activity. We hypothesized whether a damaging eccentric-type muscle contraction might unravel a novel role for autophagy during muscle repair after exercise. So we performed repeated bouts of eccentric exercise to exhaustion for three consecutive days to induce damaging eccentric contraction in controls and inducible Atg7$^{-/-}$ animals, and found out that in these conditions, autophagy-deficient mice ran significantly less than controls. Morphological analyses did not show any sign of inflammation or myofibre degeneration, thus suggesting that impaired performance of Atg7$^{-/-}$ muscles was not due to major structural alterations. We also looked for possible energetic imbalance upon exercise, by monitoring the activity of P-AMPK, one of the major sensor of energetic stress, and by checking glucose and lactate levels in the blood. However,

no significant differences were observed, thus suggesting that autophagy is not required for metabolic regulation of skeletal muscle during exercise. Since autophagy is important for organelle quality control, we tested whether mitochondrial homeostasis was affected after exercise. Interestingly, isolated muscle fibers from inducible Atg7$^{-/-}$ animals contained dysfunctional mitochondria that well correlated with their impaired performance. Being mitochondria the main source of ROS in the cell, it was feasible to hypothesize that oxidative stress may play a role in this condition. To address that, we measured total protein carbonylation and ROS production in exercised muscles that indeed was higher in Atg7$^{-/-}$ muscles. All together these data showed that acute inhibition of autophagy led to accumulation of dysfunctional mitochondria, increased oxidative stress and reduced physical performance during eccentric contraction. Excessive oxidative stress impairs muscle function, thus potentially explaining the reduced physical performance of Atg7$^{-/-}$ mice. We therefore treated controls and inducible Atg7$^{-/-}$ mice with the anti-oxidant N-Acetyl Cysteine (NAC) for 6 weeks, and then exercised them eccentrically. Surprisingly, NAC treatment severely impaired performance of controls but did not elicit any benefit in inducible Atg7$^{-/-}$ animals. Moreover it impaired mitochondrial function of controls. This data were confirmed after treatment with another anti-oxidant (Mito-TEMPO), that was specific for mitochondria.
It has been reported that anti-oxidant treatment reduces activation of autophagy in control animals and that ROS are important for signalling pathways in the cell (Underwood et al., 2010; Owusu-Ansah et al., 2013). Our findings support these evidences, suggesting that physiological levels of ROS are important for the correct basal and stimulus-induced autophagy activation.

Our results highlight the role of autophagy in the maintenance of mitochondrial function but not in AMPK activation and exercise dependent glucose homeostasis, suggesting that autophagy is an adaptive response to exercise that ensures mitochondria-quality control during damaging contractions.

1. INTRODUCTION

1.1 SKELETAL MUSCLE

1.1.1 Structure and function

Skeletal muscle is the most abundant tissue in the whole organism, it represents almost 40% of the body weight and it is responsible for the body posture and movement. Skeletal muscle is composed by multinucleated and elongated cells called muscle fibres. Muscles fibres are organized in bundles and separated by specific membrane system. Each muscle is surrounded by a connective tissue membrane called epimysium; the muscle itself is formed by well organized bundles of muscle fibres that are grouped in fascicula and are surrounded by another layer of connective tissue, called perimysium. Within the fasciculus, each individual muscle fibre is surrounded by connective tissue called the endomysium (Figure 1).

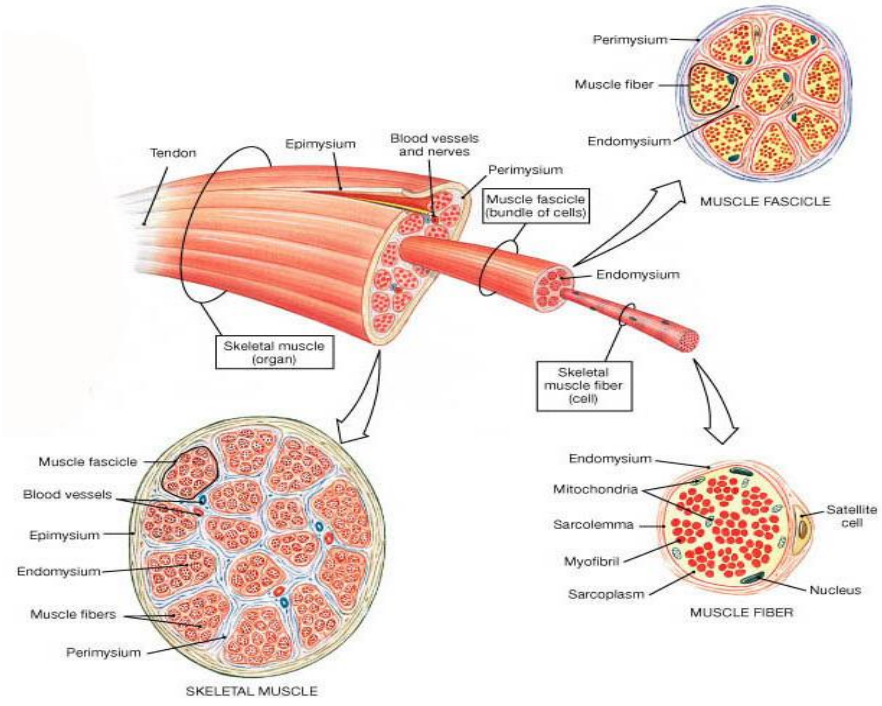

Fig.1: Schematic representation of skeletal muscle structure.

The plasma membrane surrounding muscle fibres is called sarcolemma.
Each muscle fibre is formed by thousands of myofibrils, contains contractile proteins responsible for muscle contraction. The unit of muscle contraction is called sarcomere. Its structure was described first thank to microscopy techniques that individuated isotropic (light band) and anisotropic (dark band) zones, forming the specific striated aspect of the skeletal muscle. For this reason, sarcomere is usually defined as the segment between two neighbour Z-lines, that appears as a series of dark lines. Surrounding the Z-line, there is the region of the I-band (the light band). Following the I-band there is the A-band (the dark band). Within the A-band, there is a paler region called the H-band. Finally, inside the H-band there is a thin M-line, the middle of the sarcomere. These bands are not only morphological unit but also functional, because are characterized by the presence of different contractile proteins required for muscle contraction. In fact, actin filaments (thin filaments) are the major component of the I-band and extend into the A band. Myosin filaments (thick filaments) extend throughout the A-band and are thought to overlap in the M-band. A huge protein, called titin, extends from the Z-line of the sarcomere, where it binds to the thin filament system, to the M-band, where it is thought to interact with the thick filaments. Several proteins important for the stability of the sarcomeric structure are found in the Z-line as well as in the M band of the sarcomere (Figure 2). Actin filaments and titin molecules are cross-linked in the Z-disc via the Z-line protein alpha-actinin. The M-band myosin as well as the M proteins bridge the thick filament system to the M-band part of titin (the elastic filaments). Moreover several regulatory proteins, such as tropomyosin and troponin bind myosin molecules, modulating its capacity of contraction.

Muscle contraction is due to the excitation-contraction coupling, by which an electrical stimulus is converted into mechanical contraction. The general scheme is that an action potential arrives to depolarize the cell membrane. By mechanisms specific to the muscle type, this depolarization results in an increase in cytosolic calcium that is called a calcium transient. This increase in calcium activates calcium-sensitive contractile proteins that then use ATP to cause cell shortening. Concerning skeletal muscle, upon contraction, the A-bands do not change their length, whereas

the I bands and the H-zone shorten. This is called the sliding filament hypothesis, which is now widely accepted. There are projections from the thick filaments, called cross-bridges which contain the part (head) of myosin linked to actin. Myosin head is able to hydrolyze ATP and convering chemical energy into mechanical energy. The cross bridges are mostly oriented transverse to the fibre axis in relaxed fibres, while angled at around 45 degrees in rigor.

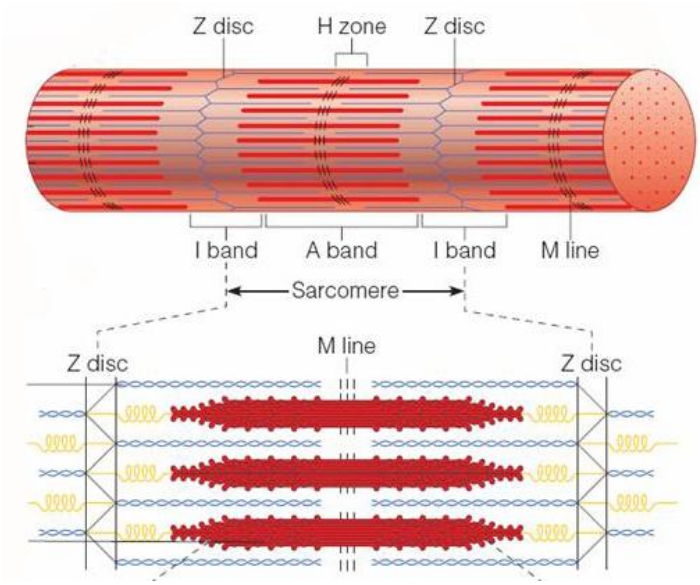

Fig.2: Schematic representation of skeletal muscle sarcomere.

To allow the simultaneous contraction of all sarcomeres, the sarcolemma penetrates into the cytoplasm of the muscle cell between myofibrils, forming membranous tubules called transverse tubules (T-tubules) (Figure 3). The T-tubules are electrically coupled with the terminal cisternae which continue into the sarcoplasmic reticulum. Thus the Sarcoplasmic Reticulum, which is the enlargement of smooth Endoplasmic Reticulum (ER) and which contains the majority of calcium ions required for contraction, extends from both sides of T-tubules into the myofibrils. Anatomically, the structure formed by T-tubules surrounded by two smooth ER cisternae is called the triad and it allows the transmission of membrane depolarization from the sarcolemma to the ER. The contraction starts when an action potential diffuses from the motor neuron to the sarcolemma and then it travels along T-tubules until it reaches the sarcoplasmic reticulum. Here the action

potential changes the permeability of the sarcoplasmic reticulum, allowing the flow of calcium ions into the cytosol between the myofibrils. The release of calcium ions induces the myosin heads to interact with the actin, allowing the muscle contraction. The contraction process is ATP dependent. The energy is provided by mitochondria which are located closed to Z line.

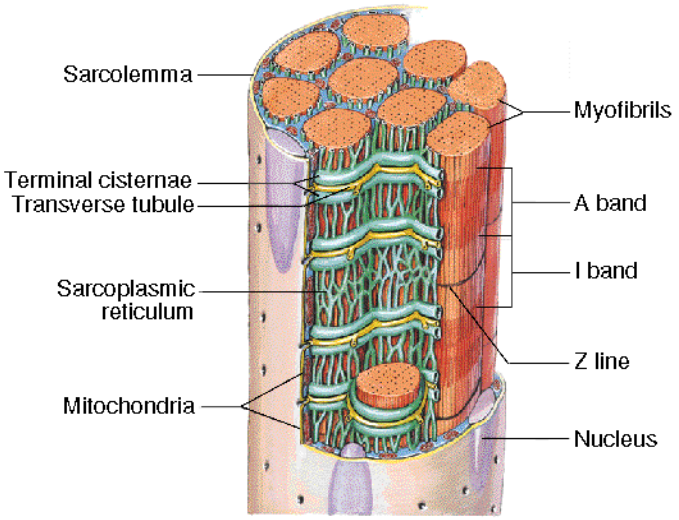

Fig.3: Schematic representation of organization of T-tubuls in skeletal muscle.

The contraction properties of a muscle depend on the fibre type composition. Mammalian muscle fibres are divided into two distinct classes: type I, also called slow fibres, and type II, called fast fibres. This classification considers only the mechanical properties. However the different fibre types also show peculiar features such as for example myosin ATPase enzymes, metabolism (oxidative or glycolitic), mitochondrial content revealed by succinate dehydrogenase (SDH) staining, and resistance to fatigue (Pette and Heilmann, 1979; Schiaffino et al., 2007). Each muscle is composed by a combination of fibre types, whose abundance affects the type of contraction the muscle undergoes (solw or fast); regarding that a muscle is defined as slow, if it containing more type I fibres, or fast, if type II fibres are more abundant. The different fibre types are also characterized by peculiar Myosin Heavy Chain (MHC) proteins expression. The fibre type I expresses the slow isoform of MHC (MHCβ or MHC1), and shows a great content of mitochondria, high levels of myoglobin, high capillary densities and high oxidative capacity. Muscles containing

many type I fibres display red colour for the great vascularisation and for the high myoglobin content. The type II, fast, myofibers are divided in three groups depending on which myosin is expressed. In fact distinct genes encode for MHC IIa, IIx (also called IId) and IIb. Type IIa myofibers are faster than type I, but they are still relatively fatigue-resistant. IIa fibers are relatively slower than IIx and IIb and have an oxidative metabolism due to the rich content of mitochondria (Schiaffino and Reggiani, 1996). Given all these characteristics, IIa fibres are also termed fast oxidative fibres. They exhibit fast contraction, high oxidative capacity and a relative fatigue resistance. The IIx and IIb fibre types are called fast-glycolitic fibres and show a prominent glycolitic metabolism containing few mitochondria of small size, high myosin ATPase activity, expression of MHC IIb and MHC IIx proteins, the fastest rate of contraction and the highest level of fatigability.

The fibre-type profile of different muscles is initially established during development independently of neural influence, but nerve activity has a major role in the maintenance and modulation of its properties in adult muscle. Indeed during postnatal development and regeneration, a default nerve activity-independent pathway of muscle fibre differentiation, which is controlled by thyroid hormone, leads to the activation of a fast gene program. On the contrary, the post natal induction and maintenance of the slow gene program is dependent on slow motoneuron activity. The muscle fibre-type then undergoes further changes during postnatal life, for example fibre-type switching could be induced in adult skeletal muscles by changes in nerve activity (Murgia et al., 2000).

1.1.2 The Nerve-Muscle connection

Neuromuscular Junction (NMJ) development and maintenance

The vertebrate skeletal neuromuscular junction (NMJ) is the connection between motor neurons and skeletal muscle.

NMJ is the most used model in the study of single synapse, because it has a clearly defined organization and it is quite accessible thanks to its relatively large size and localization. NMJ lies outside the brain and post-synaptic muscle fibre is generally innervated by one axon. Muscles are readily re-innervated following nerve damage,

allowing synaptogenesis to be studied also in adult and not only in embryonic organisms. Moreover, the bond between bungarotoxins (BGT) and AChR is able to clearly identify the localization and the morphology of NMJ.

The general structure of NMJ can be described in three zones. The pre-synaptic element is the motorneuron, it contains mitochondria and synaptic vesicles that reach the pre-synaptic membrane in correspondence of synaptic buttons. Those buttons are distributed along an elliptical area that takes the name of endplate terminal, it represent the active zone since it is where the neurotransmitter acetylcholine (ACh) is released. Muscle fibre is the post-synaptic element. It is characterized by junctional folds rich of nicotinic acetylcholine receptor (AChR) and Voltage-gated Na^+ channels. The synaptic cleft is the space between pre- and post-synaptic elements, where ACh is released from the active zone (Figure 4).

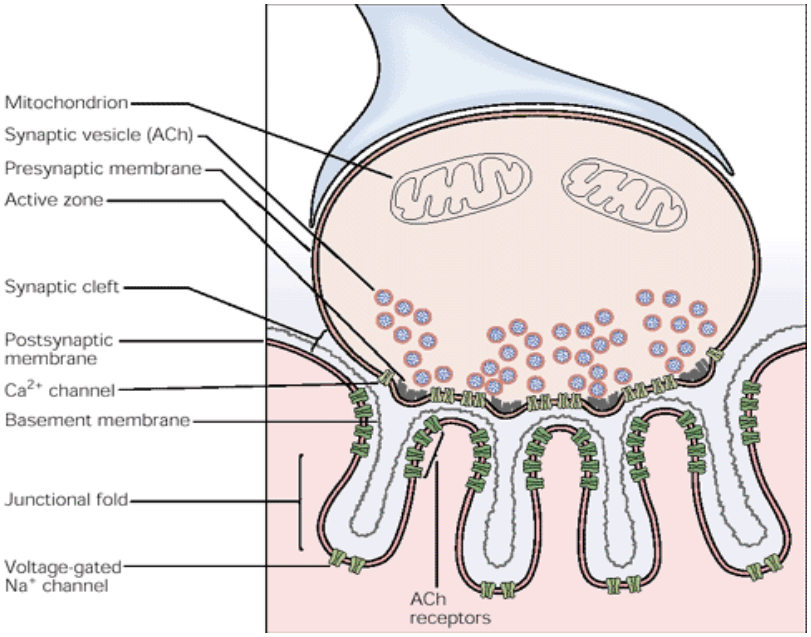

Fig.4: Schematic representation of NMJ structure, where pre-synaptic (nerve), and post-synaptic (muscle fibre) elements are described.

The generation of new synapses starts at embryonic stage (17-19 days) with the extension of motoneuron's axon, that branches to innervate a variable number of skeletal muscle fibres in a discrete central region of each one named the end-plate

band. The nerve terminal accumulates synaptic acetylcholine vesicles and other pre-synaptic components, and while both pre- and post- synaptic membranes thicken, the synaptic cleft widens. With increasing number of vesicles, the active zone starts to appear and, the expression of several genes, coding for postsynaptic proteins, including the acetylcholine receptors (AChRs), increases in the postsynaptic nuclei. The last step of this process is axon myelination and junctional fold formation in the post-synaptic element (Figure 5). These morphological changes in the nerve terminal are accompanied by increased frequency of spontaneous synaptic potential.

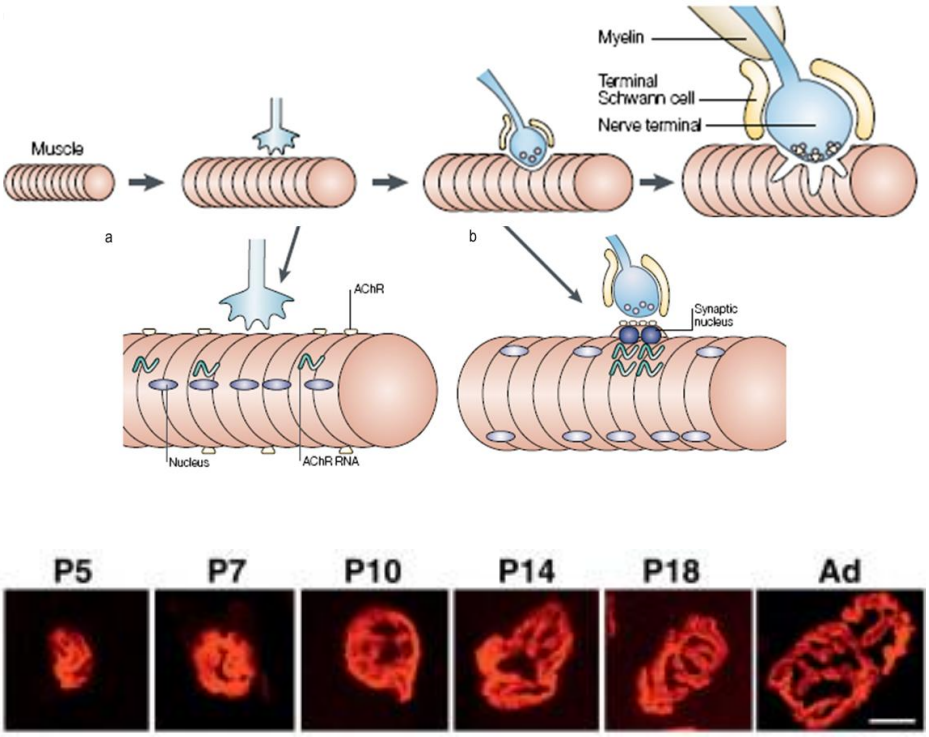

Fig.5: Morphological changes in NMJ development A) Representation of NMJ developmental stages, in details (a-b) is reported the nuclei transition from extra-synaptic to the synaptic region, where a specific transcriptional programme is activated. B) Morphological changes in NMJ that from embrionic-oval stage became pretzel-shaped in the adult and mature one (Shi et al., 2012).

The development of neuromuscular junction requires a fundamental process called muscle pre-patterning that is characterized by both muscle- and nerve-specific

dependent mechanisms. Muscle pre-patterning is the process in which AChRs aggregate at the end-plate band of muscle during the earliest stages of NMJ development at the prospective synaptic region (Figure 6). AChRs accumulate and specifically cluster in a specific region of the muscle fibre that will be where the future NMJ will originate. This process can be divided in two stages: muscle-specific processes, that start before innervation, and nerve dependent events that occur after muscle/nerve contact.

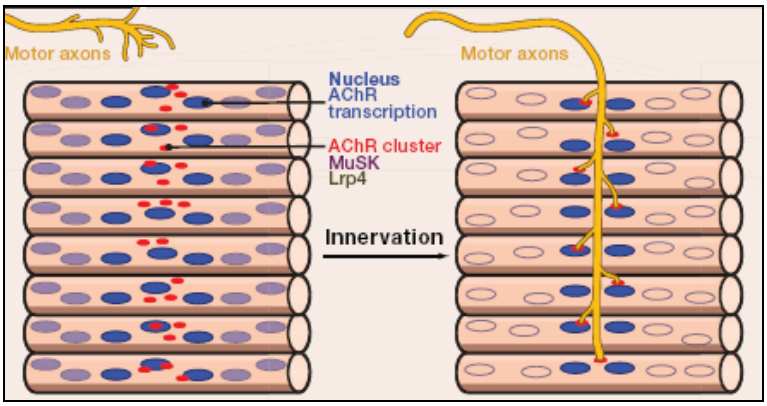

Fig.6: Representation of muscle pre-patterning (Burden, 2011).

The major factors involved in the muscle-specific part are the expression and localization of MuSK, a muscle specific tyrosine kinase receptor. Its expression is required in the central region of the end-plate, where it could be initially auto-activated itself, without any ligand. MuSK activation promotes its own clustering first (with a positive loop) and AChR later, in correspondence of the future synaptic zones (Burden, 2011). In this scenario, L-type Ca^{2+} channel DHPR receptor is also expressed in muscle, because it regulates the expression and localization of AChR and *MuSK*, through Ca^{2+} influx, not depending on the role in excitation-contraction coupling (Chen et al., 2011). Also WNT pathway, in particular with the factor WNT11, promotes clustering of AChR precursor, by binding and activating MuSK (Henríquez et al., 2011; Wu et al., 2010). At a later stage, when a growing neuron approaches the myotube, AChR clusters start to aggregate near the region of nerve contact. This means that AChR cluster become restricted to the sub-synaptic

membrane, thus disappearing from the extra-synaptic one, and that AChR subunits composition change from α_2, β, δ, γ to α_2, β, δ, ε resulting in acquisition of new channel properties (Hall and Sanes, 1993; Numberger et al., 1991). AChR-ɣ subunit is in fact a defined marker of reinnervation, because it is typical of early developmental stages of NMJ. So when the nerve establishes contact with a muscle cell, it exerts complex control over both number and distribution of AChRs.

There is another way in which nerve controls post-synaptic differentiation, in fact the system that regulates the density of extra-synaptic AChR is based on electrical activity evoked by synaptic transmission. When the nerve depolarizes the muscle, the action potential represses AChR gene transcription in extra synaptic nuclei, probably through Ca^{2+}, protein kinase C and MYOD transcription factor, thus having AChR expression specifically localized at synaptic zones. In addition, nerve terminal can also contribute with secretion of other factors that can act locally via different receptors (Wu et al., 2010; Hall and Sanes, 1993).

After the pre-patterning, post-synaptic differentiation takes place depending on the clustering of neurotransmitter (NT) receptors and scaffolding proteins. These changes are regulated by different signals including WNT pathway, and neurotrophins secreted from the nerve. An important role is played by a molecule called neuregulin that is secreted from the neuron, and binds muscle receptor ErbB to induce the activation of synaptic genes (Burden, 2002; Trinidad et al., 2000). The most important and studied signalling pathway involved in post-synaptic differentiation is the MuSK/Agrin signalling (Figure 7). MuSK, as already said, is a tyrosine kinase receptor expressed in the postsynaptic membrane of NMJ, where it co-localizes with AChRs, inducing their clustering (Kim and Burden, 2008). MuSK is activated by Agrin, a proteoglycan released from the nerve, that stimulate MuSK phosporylation, by interacting with Lrp4 and not directly with MuSK. Lrp4 is a lipoprotein receptor related protein 4, and acts as co-receptor, for the Agrin-MuSK signal. Lrp4 self-associates and interacts with MuSK also in the absence of Agrin. Binding of Agrin to Lrp4 stimulates association between Lrp4 and MuSK and increases MuSK kinase activity. Then MuSK stimulates recruitment of Dok-7 that is cytoplasmic adaptor protein expressed specifically in muscle. MuSK promotes Dok-7 tyrosine phosphorylation, and after that Dok-7 is able to form a dimer and with a

positive feedback stimulates MuSK kinase activity. Formation of a MuSK/Dok-7-signaling complex is essential to activate both a Rac/Rho-dependent and a Rapsyn-dependent pathway, which leads to the anchoring and clustering of AChRs (Burden, 2011).

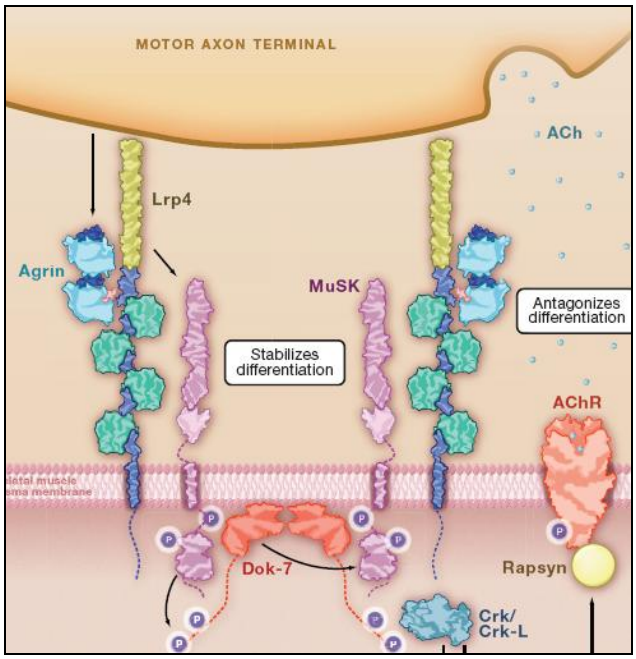

Fig.7: Representation of MuSK/Agrin signalling, that involve Dok-7 and Rapsyn as regulatory an scaffolding protein and leads to AChR clustering (Burden, 2011).

So, nerve is essential for post-synaptic differentiation and muscle tissue characterization, but in the last few years several studies have suggested an emerging larger role for the muscle, in particular in the control and maintenance of the pre-synaptic element through specific retrograde signal (Figure 8). This regulation occurs both during NMJ development and during re-innervation after injury. Different mechanisms have been identified to be clearly involved in pre-synaptic differentiation.

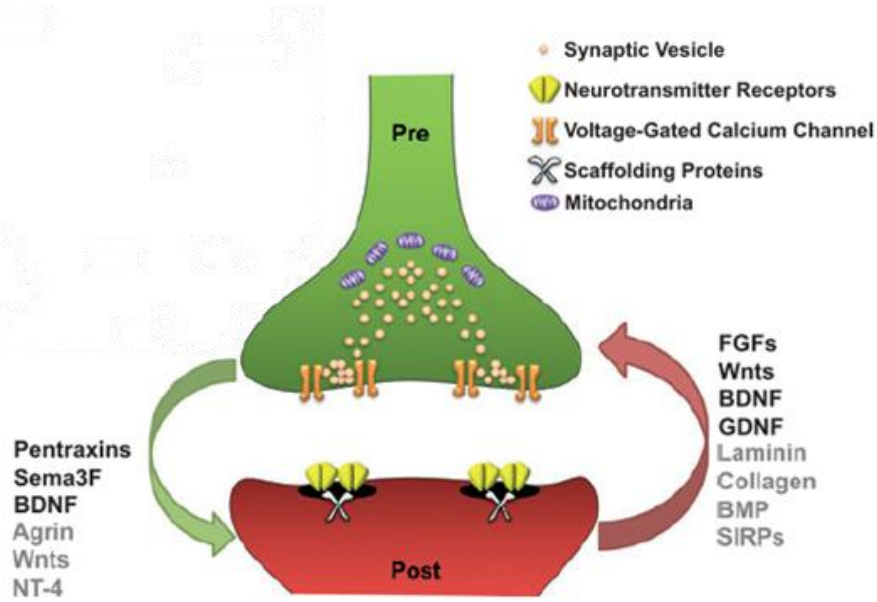

Fig.8: Signals in Nerve-Muscle communication. Several nerve-produced signals important for post-synaptic development (green arrow) and muscle-secreted retrograde factors involved in pre-synaptic development and maintenance (modified from Johnson-Venkatesh and Umemori, 2010).

Laminin beta-2 is a protein of the synaptic basal lamina, that binds voltage gated Ca^{2+} channels of the neuron mediating pre-synaptic maturation. The molecules FGF -7-10-22 are important pre-synaptic organizers, that are secreted from the muscles, bind the FGF receptor 2b and stimulate synaptic vesicle clustering and therefore the onset of the pre-synaptic terminal. Ephrin-A is a protein expressed by the muscle and contributes to the correct position of NMJ formation. In the end, Collagen IV, located at the synaptic basal lamina, is also involved in mechanisms of synaptic maintenance (Johnson-Venkatesh and Umemori, 2010; Fox et al., 2007; Burden, 2000). Finally both the muscle-specific molecules MuSK and Lrp4, besides being fundamental for muscle pre-patterning, are required for pre-synaptic differentiation (Yumoto et al., 2012; Gomez and Burden, 2011; Kim et al., 2008).

Recent studies pointed out the role of muscle tissue not only during muscle development but also concerning re-innervation mechanisms.

In has been demonstrated that after denervation or nerve injury, muscle tissue undergoes transcriptional changes trying to induce re-innervation. The most

important defined signals are the over-expression of MuSK and AChR-ɣ subunit and also miR206 that promotes the expression of FGFBP1, leading to muscle re-innervation (Williams et al., 2009). FGFBP1 is a secreted protein that interacts and potentiates the bioactivity of FGF-7, FGF-10, and FGF-22 family members (Jang and Van Remmen, 2011; Williams et al., 2009).
At present the characterization of the mechanisms of muscle-nerve communication is an open issue.

1.2 MUSCLE HYPERTROPHY AND ATROPHY

Skeletal muscle mass is orchestrated by several complex mechanisms that regulate the rate of muscle growth and muscle loss. Muscle growth is mainly due to protein synthesis, that, when exceeds, leads to muscle hypertrophy. On the contrary, excessive protein degradation, loss of organelles and cytoplasm are major causes of muscle atrophy.

Muscle Hypertrophy

Skeletal muscle hypertrophy is defined as an increase in muscle mass, which in the adult animal comes as a result of an increase in the size of pre-existing skeletal muscle fibres. This growth, as stated above, is mainly due to increased protein synthesis and concomitant decreased protein degradation. The Insulin-like growth factor (IGF-1)-AKT signalling is the major pathway that controls muscle growth. Muscle-specific IGF-1 over-expression in transgenic mice results in muscle hypertrophy and, importantly, the growth of muscle mass matches with a physiological increase of muscle strength. Furthermore, the over-expression of a constitutively active form of AKT, a downstream target of IGF-1, in adult skeletal muscle induced muscle hypertrophy. Moreover, AKT transgenic mice display muscle hypertrophy and protection from denervation-induced atrophy, showing that AKT pathway promotes muscle growth and simultaneously blocks protein degradation (Schiaffino et al., 2013). AKT pathway, in fact, controls in an opposite manner two

important downstream targets: mammalian target of rapamycin (mTOR) and glycogen synthase kinase 3 beta (GSK3β). In the first case, AKT activates mTOR, that is a key regulator of cell growth, promoting the activation of S6 kinase (S6K) and blocking the inhibition of eif4e binding protein 1 (4EBP1) on eukaryotic translation initiation factor 4E (eif4e), thus leading to protein synthesis. In the other case, the inhibition of GSK3β from AKT stimulates proteins synthesis, since GSK3β normally blocks protein translation initiated by eIF2B protein (Glass, 2005). Taken together with other observations, these results suggest that IGF-1- AKT axis is a major mediator of skeletal muscle hypertrophy. Recently, it has been reported that also TGF-β pathway contributes to regulation of muscle mass in adulthood (Sartori et al., 2013). Sartori et al. showed that when the BMP pathway is blocked or myostatin expression is increased, more Smad4 is available for phosphorylated Smad2/3, leading to an atrophy response. Therefore, under normal circumstances, a balance between these competing pathways is required to maintain muscle mass. Moreover they identify a newly characterized ubiquitin-ligase, named MUSA1, as the molecular mechanism underlying the anti-atrophic action of the BMP pathway that has a negative effect on its expression. This work provided evidences that also BMP signalling is involved in the regulation of adult muscle mass in normal and pathological situations (Sartori et al., 2013).

Muscle atrophy

Atrophy is defined as a decrease in cell size mainly due to protein degradation and then to the loss of organelles and cytoplasm as well. This is because protein turnover is dominant over cellular one during acute phases of muscle wasting, for example when sarcomeric proteins are rapidly lost during fasting, disuse, and denervation.
Muscle loss is mediated by two highly conserved pathways: ubiquitin-proteasomal system (UPS) and autophagy-lisosomal pathway (ALP).
Several evidences strongly support a major role of UPS during muscle loss. In this process Ubiquitin (Ub) is covalently attached to substrate proteins via a three-step mechanism involving the sequential actions of E1 (ubiquitin-activating enzyme), E2 (ubiquitin-conjugating enzyme) and E3 (ubiquitin ligase) enzymes. The rate limiting

enzyme of UPS is the E3 which catalyzes the transfer of ubiquitin from the E2 to the lysine in the substrate. This reaction is highly specific and the proteins, committed to ubiquitination and to proteasomal degradation, are recognized by the E3. Thus the amount and the type of proteins degraded by the proteasome is largely determined by which E3 ligases are activated in the cell (Gomes et al., 2001).

FoxO3 transcription is the key regulator of these systems, being it necessary and sufficient for the induction of autophagy in skeletal muscle *in vivo* (Mammucari et al., 2007; Zhao et al., 2007). Moreover it induces the transcription of two fundamental muscles ubiquitin-ligases: Atrogin-1 and MuRF-1 (Sandri et al., 2004; Gomes et al., 2001; Bodine, 2001). These ubiquitin-ligases were identified through gene expression profile analysis performed on different atrophic models, as part of a set of genes, called 'atrogenes', that triggered or were involved in the atrophic program. These genes encode for proteins involved in different cellular processes like energy production, transcription factors, regulators or protein synthesis and enzymes of metabolic pathways. Among the upregulated atrophy-related genes there is a subset of transcripts related to protein degradation pathways.

Together these findings indicate that muscle atrophy is a process that requires the activation of a specific transcriptional program.

1.3 AGEING IN MUSCLE TISSUE: SARCOPENIA

During ageing muscle undergoes an inevitable loss of muscle mass accompanied by loss of force, that is called sarcopenia. It has been estimated that 25% of people under the age of 70, and 40% of people aged 80 or older are sarcopenic. As people age, the strength in their muscles gradually decreases at a rate of 1-2% per year after the age of 50 and by 30-40% at the age of 70 (Rossi et al. 2008). This condition profoundly contributes to a reduced quality of life in elderly and predisposes them to an increased risk of morbidity, disability and mortality (Visser and Schaap, 2011). Despite the clinical, social and economic relevance of sarcopenia, the precise mechanisms for the age-related loss of muscle mass and function are not yet fully understood. Age-related changes in muscle are complex with key features including myofibre atrophy, profound weakness that is partially independent from muscle

mass loss, myofibre degeneration, accumulation of dysfunctional mitochondria and increased oxidative stress.

Until recently, it was thought that age-associated atrophy and weakness were secondary to motor-neuron loss in the brain or in spinal cord. However this hypothesis has been recently challenged. In fact little neuronal death occurs in most areas of ageing nervous system and there is no decline of lower motor neurons during ageing (Chai et al., 2011; Morrison and Hof, 1997). Conversely, it is emerging that the neuromuscular junctions (NMJ) and their interactions with myofibres are greatly altered during ageing, resulting in a loss of muscle innervation (Chai et al., 2011; Valdez et al., 2010). In particular, loss of nerve endings has been reported at motor endplates in both rodents and humans, indeed in the soleus muscle of aged (22-month old) rats, both pre- and post-synaptic specializations were significantly smaller compared to that of the young (8-month old) rats (Deschenes and Wilson, 2003). In this way, the muscle fibre seems to have an important role in the degeneration of motoneuron. It has been shown that reorganization of AChR plaque into multiple fragments was an occasional event that followed the degeneration of the underlying muscle fibre. Moreover, the increased prevalence of fragmented endplates in elderly was attributed to an increased incidence of sporadic muscle fibre degeneration events as the animal grew older (Li et al., 2011).

Skeletal muscle tissue is particularly vulnerable to oxidative stress, in fact being a post mitotic tissue, it uses large amount of oxygen, thus causing cumulative oxidative damage to the cell structures over time. Sarcopenic muscle degeneration is associated to an age-related oxidative stress that leads to increased mitochondrial DNA damage, lipid peroxidation and protein oxidation. A great number of studies have shown an increase in oxidized proteins at the intracellular level during senescence, this causes loss of function in the affected protein that could lead to their accumulation, compromising organ functionality (Rossi et al., 2008). Oxidative stress and decreased release of trophic factors are considered two independent and important causes that affect NMJ integrity and contribute to denervation, also during ageing process (Jang and Van Remmen, 2011). Several laboratories have

tested the impact of oxidative stress on age-related muscle wasting. In order to elucidate the direct cause and effect relation between oxidative stress and sarcopenia *in vivo*, a mouse holding homozygous deletion of an essential antioxidant enzyme Sod1 (Cu/Zn superoxide dismutase, Cu/Zn SOD) was generated (Jang et al., 2010). It has been shown that the lack of Sod1 led to age-dependent muscle atrophy with alterations in NMJs, that were similar to normal ageing muscle but occurred earlier and more frequently (Jang et al., 2010). These data indicated that maintenance of NMJ during ageing may be critically influenced by oxidative stress. For this reason it has been investigated whether mitochondrial dysfunction in the population of mitochondria associated with the NMJ may lead to altered calcium buffering and oxidative modification of key molecules in the NMJ, thus contributing to age-associated declines in neuromuscular innervation. Zhou et al. demonstrated that mitochondria adjacent to the AChR are selectively depolarized when muscle fibres are challenged by calcium in a mouse model of ALS, which exhibits significant neuromuscular degeneration (Zhou et al., 2010). In addition, other works have shown that muscle-specific over-expression of uncoupling proteins (UCP1) significantly disrupted NMJ integrity. Furthermore, it has been previously reported that isolated subsarcolemmal mitochondria of $Sod1^{-/-}$ mice have significant deficits in ATP generation and oxygen consumption, and also generate more mitochondrial ROS compared to wild-type (Jang et al., 2010).

The exchange of trophic factors is implicated in pre- and post- synaptic development as well as in the preservation of neuronal and synaptic plasticity at the NMJ. The exact role or the identity of neurotrophic and/or myotrophic factors that promote survival and maintenance of pre-synaptic and post-synaptic apparatus at the NMJ, in the context of ageing, has not been fully determined. However, recent studies indicate that a variety of trophic factors such as brain derived neurotrophic factor (BDNF), neutrophin-3 (NT-3), neutrophin-4 (NT-4), cytokines such as glial-derived neutrophic factor (GDNF) and ciliary neutrophin factor (CNTF), and other growth factors as insulin-like growth factor (IGF-1 and IGF-II) and fibroblast growth factors (FGF), play a modulatory role in neuromuscular system to a different extent during ageing (Jang and Van Remmen, 2011).

Up to now it is not known whether myofibre denervation is due to deleterious changes, such as impaired trophic factors production or increased oxidative stress, in muscle cells themselves, in neurons or both components.

Notably, two lifestyle adaptations, namely caloric restriction and exercise, have been consistently demonstrated to extend lifespan and, in parallel, to mitigate age-related alterations of NMJ (Melov et al., 2007; Fontana et al., 2010; Sandri et al., 2013; Schiaffino et al., 2013; Coen et al., 2013; Toledo et al., 2013; Guarente, 2013).
It has been shown that caloric restriction directly attenuates age-related loss of muscle mass by improving mitochondria function, which in turn, lowers the mitochondrial ROS production in $Sod^{-/-}$ mice. Those effects of caloric restriction on mitochondria contribute to the preservation of NMJ morphology, innervation of muscle fibres, and maintenance of muscle mass and structure, improving also the regenerative potential of skeletal muscle, that normally decrease with age (Jang et al., 2012).
Physical activity is known to trigger several changing in the muscle tissue such as switching of fibre type, increase in mitochondrial biogenesis, metabolic variation in glucose consumption and lactate production, activation of AMPK. AMPK is the AMP-activated protein kinase that plays an important role in cellular energy homeostasis. In fact it is involved in many different pathways and is considered the master sensor of energy imbalance, as the major regulator of metabolic switch upon stress condition. When activated, it phosphorylates its direct target, acetyl-CoA carboxilase (ACC) and contributes to translocation of the glucose transporter Glut 4 on the cell surface (Kurth-Kraczek et al., 1999). Glut 4 is a muscle specific isoform of glucose transporter, and it is normally located in intracellular storage sites, and move to the cell surface in response to insulin, muscle contraction, and other stimuli that requires an increased glucose transport (Holloszy, 2011).
Physical activity also triggers some beneficial effects on NMJ maintenance. Exercise in fact could partially reverse NMJ structural alterations that had already occurred after a denervation event (Valdez et al., 2010). Moreover since beneficial effects were observed in exercised muscles only, the ameliorated phenotype of the synapse resulted from local muscle-nerve interactions, suggesting that increased activity in

exercising muscles could lead to an up-regulation of trophic factors from muscle that would, in turn, improve synaptic maintenance (Valdez et al., 2010). These findings correlate with another work by Cheng (Cheng et al., 2013), where 21 months old mice and 18 months old mice, with reduced nerve terminal size, performed respectively 4 and 10 months voluntary wheel running. The authors found that after exercise most of the age-associated loss of nerve terminal area was prevented (Cheng et al., 2013). Furthermore, the positive effects of exercise are not limited to NMJ, but can be extended to a more general action to prevent ageing. In fact, 5 months of exercise training were sufficient to completely reverse the premature ageing phenotype of the mitochondrial DNA mutator mice, which possess a dysfunctional copy of the mitochondrial proofreading-exonuclease, polymerase gamma (Safdar et al., 2011).

It is important to consider another aspect that occurs during physical activity: contractions produce free radicals and ROS production is potentially damaging to the muscle tissues (Powers and Jackson, 2008).

Several studies tried to identify ROS sources during exercise and a number of researchers have assumed that the increased ROS generation that occurs during contractile activity is directly related to the elevated oxygen consumption that occurs with increased mitochondrial activity (Kanter et al., 1994; Urso et al., 2003). Although mitochondria are involved in ROS production upon exercise, other studies pointed out that they are not the only source of ROS in skeletal muscle during exercise. Several works found NADH-oxidase enzyme associated with the sarcoplasmic reticulum (SR) of both cardiac and skeletal muscle, and it was responsible for the superoxide production. Thus, in this case, the superoxide generation influenced calcium release by the SR through oxidation of the ryanodyne receptor (Cherednichenko et al., 2004; Xia et al., 2003).

Some recent findings proposed a new essential role for exercise-induced ROS formation, in promoting insulin sensitivity in humans, supporting the notion that anti-oxidants are detrimental for exercise-induced benefits in humans, although the mechanisms remain unclear (Ristow et al., 2011).

Even it has been widely investigated the role of ROS during exercise is still not completely clear.

1.4 THE AUTOPHAGY-LYSOSOMAL SYSTEM

The autophagy-lysosomal pathway is an evolutionarily conserved catabolic process essential for metabolic homeostasis maintenance, depending on nutrient availability. This process is responsible for the degradation of cytosolic component, long-lived proteins, damaged organelles, protein aggregates and intracellular pathogens. Autophagy in fact takes place at basal levels in all eukaryotic cells to maintain or rejuvenate function of proteins and organelles, but can also be induced by limitation of various types of nutrients, such as amino acids, growth factors, oxygen and energy as an adaptive mechanism essential for cell survival (Mizushima, 2011). During the autophagy process, the cargo that needs to be degraded is engulfed by double membranes layer called autophagosomes. These membranes have to be committed, and this requires the recruitment of ATGs proteins on the membrane, as I will explain hereafter. Then the vesicles are delivered to the lysosomes where the cargo is degraded to amino acids that supply energy requirement. This role in recycling is complementary to that of the ubiquitin-proteasome system, which degrades proteins to generate oligopeptides that are subsequently degraded into amino acids (Lecker et al., 2006).

The autophagy system is highly regulated through the action of various kinases, phosphatases, and guanosine triphosphatases (GTPases). The core protein machinery that is necessary to commit membranes to become vesicles includes two ubiquitin-like protein conjugation systems (Sandri, 2010). Moreover there is another set of proteins, that regulates the vesicle formation and their docking and fusion with lysosome (Boya et al., 2013).

There are mainly three classes of autophagy: macroautophagy, microautophagy, and chaperone-mediated autophagy (Figure 9).

Macroautophagy

Macroautophagy uses the intermediate organelle ‘‘autophagosome.’’ An isolation membrane (also termed phagophore) sequesters a small portion of the cytoplasm, including soluble materials and organelles, to form the autophagosome. The autophagosome fuses with the lysosome to become an autolysosome that degrades the material within. This process appears to be selective in targeting to degradation specific organelles such as: mitochondria (mitophagy), portions of nucleus (nucleophagy), peroxisomes (pexophagy), endoplasmic reticulum (reticulophagy), microorganisms (xenophagy), ribosomes (ribophagy) and protein aggregates (aggrephagy) (Figure 9a).

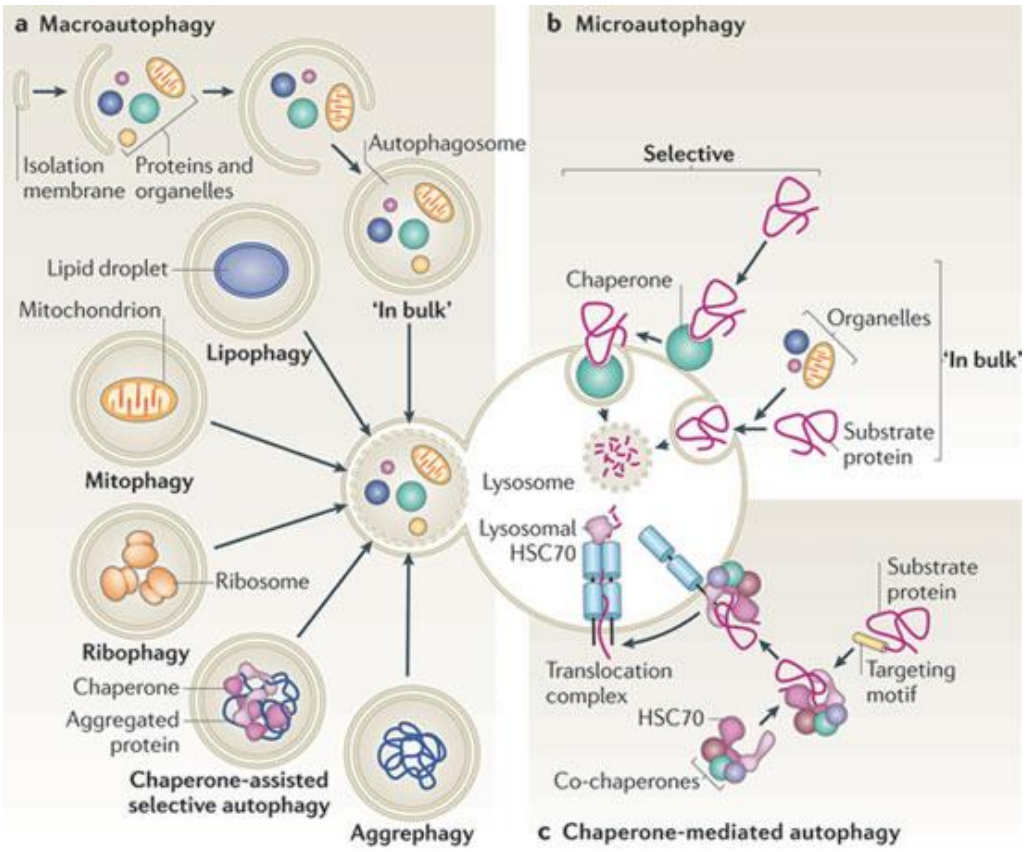

Fig.9: Scheme of the different type of autophagy: macroautophagy (a), microautophagy (b), chaperone-mediated autophagy (c) (Cuervo, 2011).

Microautophagy

In microautophagy, the lysosome itself engulfs small components of the cytoplasm by inward invagination of the lysosomal membrane. Membrane dynamics during microautophagy may be quite similar or identical to that of endosomal sorting complex required for transport (ESCRT)-dependent multivesicular body (MVB) formation, which occurs in the late endosome (Figure 9b).

Chaperone-Mediated Autophagy (CMA)

The third type of autophagy is chaperone-mediated autophagy (CMA). This class does not involve membrane reorganization; instead, substrate proteins directly translocate across the lysosomal membrane. The chaperone protein Hsc70 (heat shock cognate 70) and co-chaperones specifically recognize cytosolic proteins that contain a KFERQ-like pentapeptide. The transmembrane protein Lamp-2A, which is an isoform of Lamp-2, acts as a receptor on the lysosome, and unfolded proteins are delivered into the lysosomal lumen through a multimeric translocation complex (Mizushima, 2011) (Figure 9c).

Macroautophagy, hereafter called autophagy, is thought to be the major type of autophagy, and it has been studied most extensively compared to microautophagy and CMA.

Autophagy is activated by both caloric restriction and exercise (Grumati et al., 2010; Grumati et al., 2011a; Grumati et al., 2011b; He et al., 2012; Rubinsztein et al., 2011; Wohlgemuth et al., 2010).

Although many studies focused on these topic the mechanism that link autophagy to these lifestyle conditions is still under investigation.

1.4.1 The autophagy genes

Genetic screens in S. cerevisiae have led to the identification of a number of molecular factors essential for autophagy. There are currently over 30 genes that are primarily involved in bulk and selective types of autophagy and they have been named autophagy-related genes (ATG) (Klionsky et al., 2003). ATGs encode for

proteins that mediate the autophagic process; in particular they orchestrate the following steps: initiation, elongation, maturation and fusion of the autophagosome with the lysosome, and cargo degradation (Tan, 2013) (Table 1).

Table 1
Major proteins involved in autophagy

Mammalian autophagic proteins	Yeast homolog	Functions
Autophagosome initiation		
ULK1	Atg1	Kinase in ULK-Atg13-FIP200 complex, interfaces with mTORC1
Atg13	Atg13	Form Atg1 complex, mediates ULK1/2-FIP200 interactions
FIP200	Atg17	Form Atg1 complex, mediates ULK1/2-FIP200 interactions
Beclin 1	Atg6	PI3 K-III complex, Bcl-2–binding protein; involved in autophagosome formation
Vps34	Vps34	Form PI3 K-III complex
Autophagosome elongation		
Atg3	Atg3	E2-like enzyme for pro-LC3 (Atg8)
Atg4	Atg4	Cysteine protease cleaves Atg8 C-terminus, converts pro-LC3 (Atg8) to LC3-I, delipidates autophagosomal LC3-II
Atg5	Atg5	Form Atg5-Atg12-Atg16 complex
Atg7	Atg7	E1 ubiquitin conjugase–like enzyme in both LC3 and Atg12-Atg5-Atg16 pathways
MAP1LC3A/B	Atg8	Ubiquitin-like modifier conjugated to phosphatidyletanolamine
Atg9A/B	Atg9	Form Atg2-Atg9 complex, assists in autophagosomal assembly
Atg10	Atg10	E2 ubiquitin ligase-like enzyme in Atg12-Atg5-Atg16 pathway
Atg12	Atg12	Form Atg5-Atg12-Atg16 complex
Atg16 L1/L2	Atg16	Form Atg5-Atg12-Atg16 complex
Autophagosome maturation and fusion		
Dynein	-	Involved in microtubular transport
SNARE	-	Regulate the fusion process
Rab proteins	-	Direct the trafficking of cargoes along microtubules

Table 1: ATG proteins. The 15 conserved autophagy-related gene (Atg) proteins involved in double-membrane vesicle formation (adapted from Tan, 2013). In the left column are reported the mammalian proteins, while on the right the homologue ones in yeast.

1.4.2 Autophagy Machinery

Traditionally, it has been believed that autophagosome formation starts at phagophore assembly sites. Phagophore is an autophagosome precursor and its formation requires the class III phosphoinositide 3-kinase (PI3K) Vps34, which acts in a large macromolecular complex that also contains Atg6 (also called BECLIN1), Atg14, and Vps15 (p150) (Figure 10). Other proteins involved in the early stages of autophagy include Atg5, Atg12, Atg16, focal adhesion kinase (FAK) family-interacting protein of 200 kD (FIP200), which interacts with Atg1 (also called ULK1), and the mammalian ortholog of Atg13.

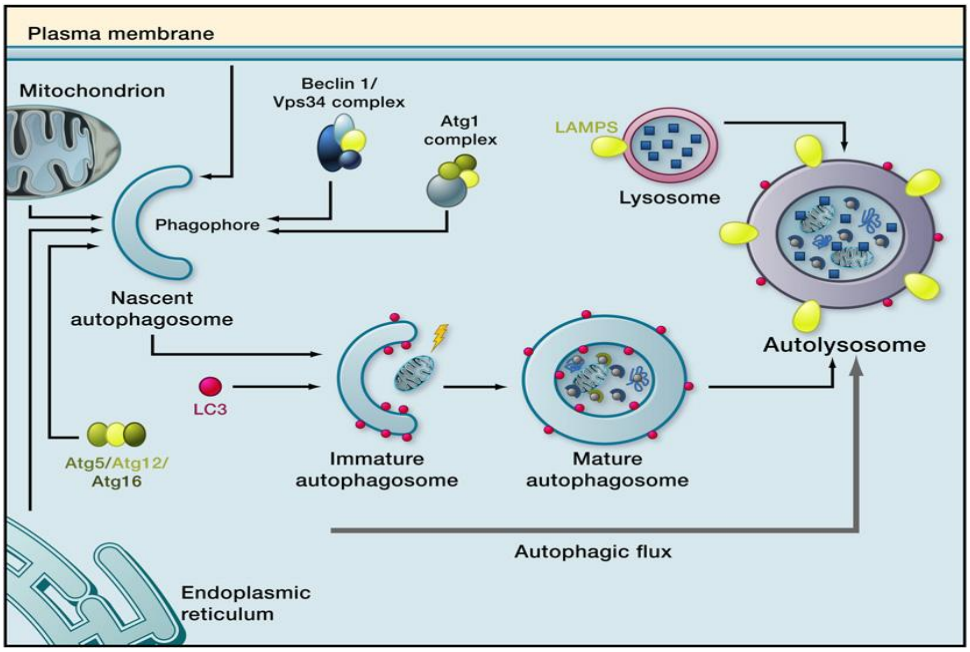

Fig.10: Possible origins for the membrane of the nascent autophagosome. This image reports the major players involved in the autophagosome formation (Rubinsztein et al., 2011).

The elongation of the autophagosomal membranes is a critical step that is associated with two ubiquitination-like reactions. In the first one, Atg12 is conjugated to Atg5 by Atg7, which is an E1 ubiquitin-like activating enzyme, and Atg10, which is an E2 ubiquitin-like conjugating enzyme. The Atg5-Atg12 conjugates interact non covalently with Atg16L1 and the whole complex associates with growing phagophores but dissociates once the autophagosomes is complete (and so the membrane is closed). In the second ubiquitin-like reaction, microtubule-associated protein 1 light chain 3 (MAP-LC3/Atg8/LC3) is conjugated to the lipid phosphatidylethanolamine (PE) with a covalent bond, by Atg7 (E1-like) and Atg3 (E2- like) to form LC3-II (Figure 11) (Rubinsztein et al., 2011). This modification results in a change of the molecular weight of LC3 that allows to distinguish by western blot the cytoplasmic soluble LC3-I, from the lipidated LC3-II isoforms. Usually, the accumulation of LC3-I or a decrease in LC3II means that autophagy is blocked.

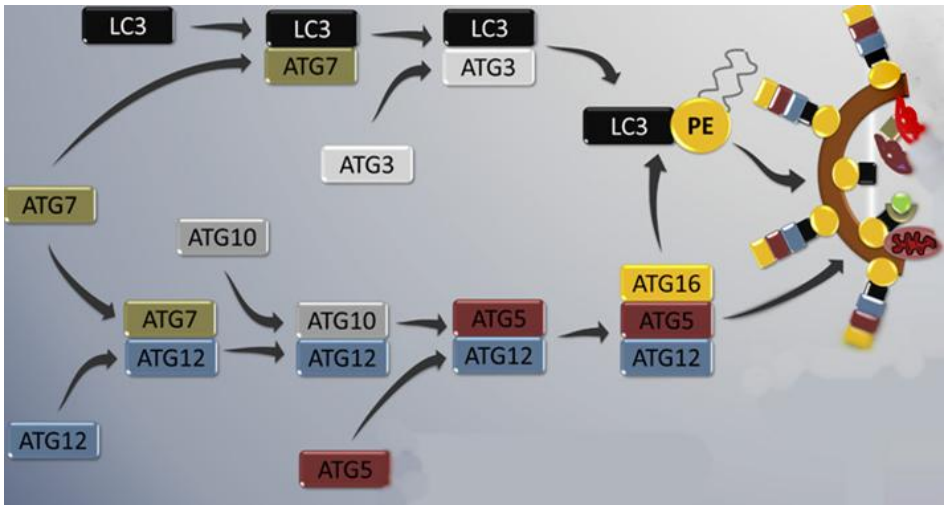

Fig.11: Ubiquitination-like reactions in the autophagosome formation: Atg12-Atg5 conjugation system and LC3 lipidation process (adapted from Kroemer et al., 2010).

LC3-II is required both on the outer and inner membranes of the nascent autophagosome. Sequestered organelles and proteins are then docked to the lysosomes for their degradation. The fusion between the outer autophagosomal membrane with the lysosomal one also determines the degradation of the inner membrane and of the proteins that are associated with it. Because of the transient nature of the autophagosomes, the lifetime of LC3 and its homologues is rather short. This feature represents the main difference between the ubiquitin-proteasome system and the autophagy-lysosome one, in fact the fate of the ubiquitin and ubiquitin-like proteins is different. While the ubiquitin proteasome pathway recycles ubiquitin molecules, the autophagy-lysosome system progressively loses the ubiquitin-like proteins, forcing the cell to replenish them in order to maintain the autophagic flux. Multiple LC3-positive autophagosomes form randomly in the cytoplasm, then they are trafficked along microtubules in a dynein-dependent manner to lysosomes, which cluster close to the microtubule organizing center (MTOC) near the nucleus. Autophagosome-lysosome fusion appears to be mediated by the SNARE proteins VAMP8 and Vti1B (Rubinsztein et al., 2011).

Selective autophagy relies on cargo-specific autophagy receptors that facilitate cargo sequestration into autophagosomes. Autophagy receptors directly interact with the structure that needs to be specifically eliminated by autophagy, as well as with the

pool of the Atg8 (yeast homologue of mammalian LC3) protein family members present in the internal surface of the growing autophagosomes. The latter interaction is mostly mediated through a specific amino acid sequence present in the autophagy receptors and commonly referred to as the LC3-interacting region (LIR) or the Atg8-interacting (AIM) motif (Figure 12). One of the most important and well known ubiquitin-associated protein that provides a link between autophagy and selective protein degradation is p62, also called sequestosome 1 (SQSTM1)(but hereafter referred as p62).

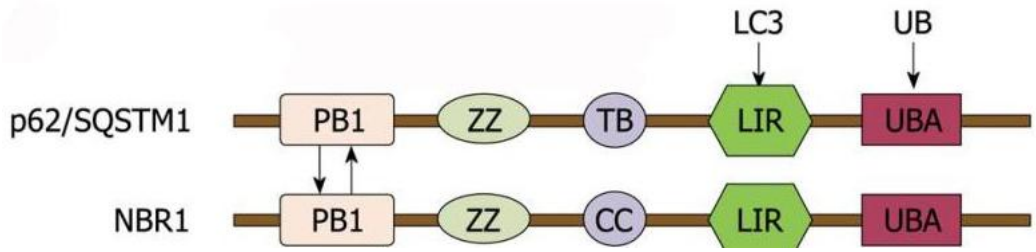

Fig.12: Cargo-specific autophagy receptors structure, here are reported the two receptors p62 and NBR1, with the main structural and interacting domain (adapted from Johansen and Lamark, 2011).

This protein is characterized by several different domains that account for its different functions. In particular it has been showed the presence of an N-terminal Phox and Bem1 (PB1), a zinc finger domain (ZZ) and a TRAF-6 binding domain (TB), moreover p62 contains LIR domain, and the C-terminal ubiquitin-associated (UBA). p62, in fact, can bind a large number of proteins through its multiple protein–protein interaction motifs. Structural analysis reveals that PB1 domain exhibits self-oligomerization, that allows the binding of different molecules, such as NBR1, that is an autophagic cargo receptor with structural similarities with p62, and it is selectively degraded by autophagy too (Johansen and Lamark, 2011). Zinc finger domain (ZZ) and TRAF-6 binding domain (TB) are important because p62 functions as scaffold protein for several signal transductions, and so these domain allow the interaction between p62 with various signalling proteins such as RIP, TRAF6, ERK, PKC, and caspase-8. For these reason p62 is involved in very different molecular pathways. As I reported before, p62 contains LIR domain, as LC3 interacting domain, and the C-terminal ubiquitin-associated (UBA) domain that can bind ubiquitinated

proteins. Recent studies have identified the LC3 recognition sequence (LRS) in murine p62, that is located between the zinc finger and UBA domains and has the same function of LIR in the human one. In this way p62 acts as a bridge between ubiquitinated proteins that has to be degraded and LC3-II located in the inner membrane of the autophagosome. Since LC3-II in the inner autophagosomal membrane is degraded together with other cellular constituents by lysosomal proteases, p62 trapped by LC3 is transported selectively into the autophagosome, and the impaired autophagy is accompanied by accumulation of p62 (Ichimura and Komatsu 2010). p62 is more linked to the autophagy-lysosome system than to the ubiquitin-proteasome system. In fact inhibition of lysosomal degradation but not proteasomal one, results in important accumulation of p62 (Bjørkøy et al., 2005; Pankiv et al., 2007). Accumulation of p62 results in self-oligomerization and formation of aggregates that contain polyubiquitinated proteins. Moreover, tissue specific inhibition of autophagy leads to a rapid and robust increase in p62 protein levels (Komatsu et al., 2007). There is crosstalk between different degradation pathways for misfolded proteins, indeed the loss of one degradation system may result in the activation of other systems. However, a high constitutive level of p62 caused by autophagy inhibition may itself contribute to an increased formation or decreased degradation of Ub-proteins. It is suggested that p62 accumulation due to autophagy inhibition delays the delivery of ubiquitinated proteins to the proteasome (Johanse and Lamark, 2011). p62 is also required in the targeting to the autophagosomes of dysfunctional mytochondria, thus being involved in the specific selective autophagy process, called mitophagy.

1.4.3 Mitophagy

Mitochondria are crucial organelles in the production of energy and in the control of signalling cascades. Moreover mitochondria are dynamic organelles, often organized in the cytoplasm as a network, a reticulum of interconnected organelles shaped by fusion (joining individual mitochondria together to become one) and fission (dividing one mitochondrion into two mitochondria) processes. When either process is blocked, the unopposed progression towards the other side of the

equilibrium defines how mitochondria appear. In mammalian cells, mitochondrial fission depends on dynamin-related protein 1 (DRP1), and FIS1, on the contrary fusion process depends on two mitofusins (Mfn1 and Mfn2) and the protein optic atrophy 1 (OPA1) (Scorrano, 2013; Hall et al., 2013). Several studies demonstrated that mitochondria shaping machinery is involved in the response of essential changes in the cell (Romanello et al., 2010; Gomes et al., 2011).

Since mitochondria are fundamental and required for several physiological pathways, a well defined mitochondria control and turnover is essential for cell homeostasis. Moreover, cells must remove damaged mitochondria to prevent the accumulation of ROS. The control of mitochondrial quality is mediated by mitophagy, a specific type of macroautophagy, that is very important in preventing ageing, neurodegenerative diseases, and other pathologies. In response to potentially lethal stress or damage, mitochondrial membranes undergo permeabilization (MMP), that constitutes one of the hallmarks of imminent apoptotic or necrotic cell death (Kroemer et al., 2007). If only a fraction of mitochondria is permeabilized, autophagic removal of damaged mitochondria can rescue the cell.

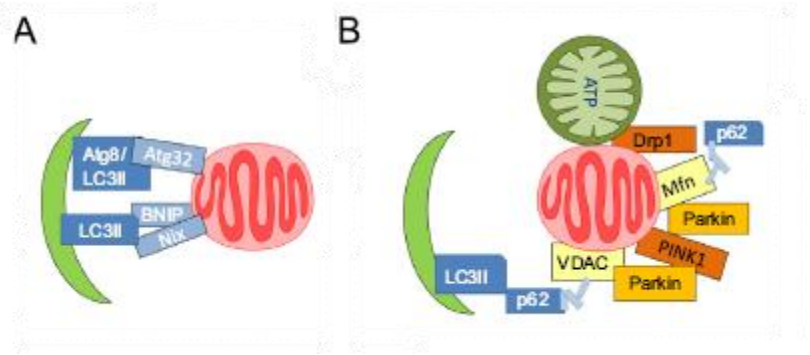

Fig.13: Mitochondrial recruitment during mitophagy: (A) Atg32 in yeast, NIX and BNIP in mammals bind mitochondria that has to be degraded, (B) moreover mitophagy can be stimulated by mitochondrial fission through DRP1 activation (adatpted Dodson et al., 2013).

The integrity of mitochondrial membrane is essential for the maintenance of the mitochondrial membrane potential, for this reason when the mitochondrial

membrane is permeabilized, mitochondria are not able to maintain the potential anymore, becoming depolarized.

The autophagic recognition of depolarized mitochondria is mediated by a voltage sensor, involving the mitochondrial kinase PINK1. Under normal condition, PINK1 is continuously recruited to the mitochondrial outer membrane and degraded through a voltage-dependent proteolysis, which leads to its removal from mitochondria first, and to proteasome-mediated degradation later (Narendra et al., 2010). Upon mitochondrial depolarization, PINK1 rapidly accumulates on the mitochondrial surface, and facilitates the recruitment of the E3 ubiquitin ligase PARKIN (Narendra et al., 2010). PARKIN ubiquitinates mitochondrial substrates including the outer membrane protein VDAC1 and Mitofusin (Mfn), recruits the autophagy adaptor molecule, p62/SQSTM1, and thus targets mitochondria for autophagic removal (Geisler et al., 2010). Mitophagy can be mediated by specific factors, such as Atg32 in yeast, NIX and BNIP in mammals, that target to mitochondria and bind to LC3 (Figure 13A); it can also be stimulated by mitochondrial fission through DRP1 activation. (Dodson et al., 2013; Lee et al., 2012)(Figure 13B).

1.4.4 Molecular signalling in autophagy

Autophagy is induced by a variety of stress stimuli, including nutrient and energy stress, ER stress, pathogen-associated molecular patterns (PAMPs) and danger-associated molecular patterns (DAMPs), hypoxia, oxidative stress, and mitochondrial damage. This signals triggers not only autophagy activation, but also several changes involved in cellular stress response.

Autophagy is mainly regulated by nutrient availability, so the insulin pathway is the major player in autophagy regulation. In condition of nutrient deprivation, in fact autophagy is activated. The best characterized regulator of autophagy is mTOR kinase that is responsible for several processes (Figure 14). It takes part to two different complexes, mTORC1 and mTORC2, that differs for the regulatory proteins, Raptor and Rictor, respectively. Moreover only mTORC1 is inhibited by Rapamycin. mTORC1 is the most involved in autophagy control. This kinase negatively regulates autophagy by inhibiting the activity of the Atg1 (ULK1) complex through directly

phosphorylating it. mTORC1 is stimulated by availability of nutrient, amino acids and growth factors, while it is inhibited when amino acids are scarce, growth factor signalling is reduced and/or ATP concentrations fall, thus resulting in de-repression of autophagy. In mammalian cells, ULK1 can also be directly phosphorylated by AMP-activated protein kinase (AMPK) in response to energy imbalance. Thus AMPK triggers autophagy by both positively regulating the Atg1(ULK1) complex and inhibiting mTOR.

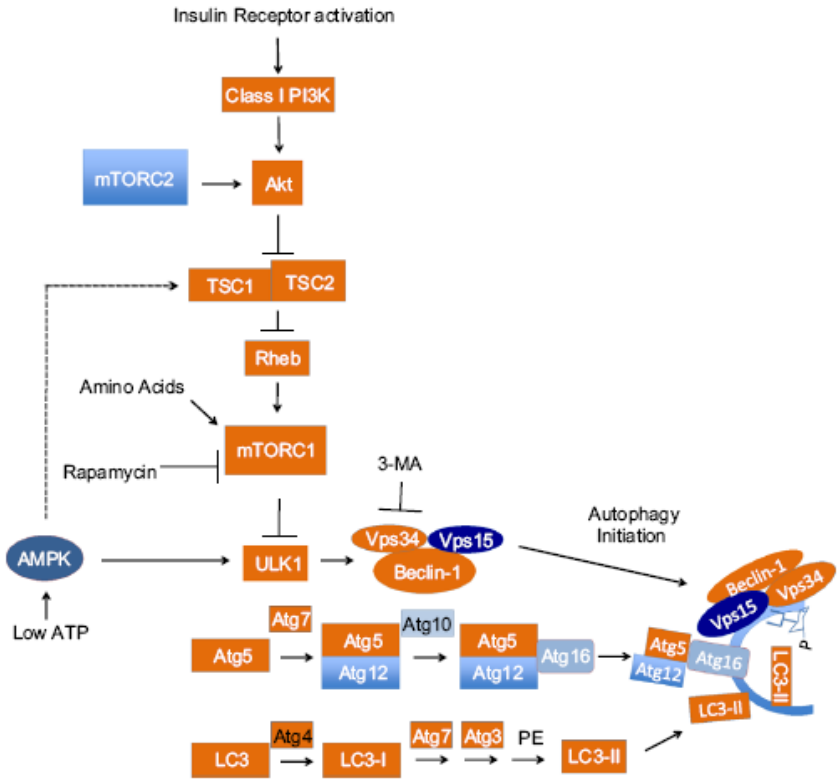

Fig.14: mTORC1-dependent signalling pathways (Dodson et al., 2013).

The phosphatidylinositol-3-OH kinase (PI(3)K) complex I is also a major point of regulation for the kinases that modulate autophagy induction. This complex contains phosphatidylinositol-3-OH kinase (PI(3)K) also called Vps34, that is the only PI3K expressed in eukaryotic cells, Beclin-1 (a mammalian homolog of yeast Atg6), p150 (a mammalian homolog of yeast Vps15), and Atg14-like protein (Atg14L or Barkor) or ultraviolet irradiation resistance-associated gene (UVRAG), and is required for the induction of autophagy. Beclin-1 is one of the subunits of the PI(3)K

complex I and its incorporation into this complex, which is essential to stimulate PtdIns3P synthesis, is dependent on other proteins, such as Bcl-2, 14-3-3 or the intermediate filament protein vimentin 1 (VMP1). The phosphorylation of BECLIN1 by the death-associated protein kinase (DAPK) or phosphorylation of Bcl-2 by the c-Jun N-terminal kinase (JNK) triggers the dissociation of the Beclin-1–Bcl-2 complex allowing Beclin-1 to associate with the PI(3)K complex I.
Furthermore, AMPK, stimulates autophagy in response to glucose starvation by phosphorylating BECLIN1 on a different residue that of the inhibitory kinases, and promotes its incorporation into the PI(3)K complex I (Boya et al 2013). In this condition, in fact, autophagy is up-regulated as compensation for the loss of key metabolites, whereas loss of autophagy or excessive autophagy may be detrimental to the cell (Dodson et al., 2013).

Some of the other regulatory molecules that induce autophagy are the eukaryotic initiation factor 2α (eIF2α), which responds to nutrient starvation, double-stranded RNA, and unfolded protein response (UPR), the major ER stress pathway (Buchberger et al., 2010; Kouroku et al., 2007).

Furthermore, mitochondria detain an important role in autophagy regulation. I have already reported that mitophagy is activated upon mitochondria damage. It is also well known that damaged mitochondria produce ROS thus increasing cell oxidative stress.
Oxidative stress reflects an imbalanced condition between reactive oxygen species (ROS) production and the capability of the cell to buffer or eliminate these molecules. In fact, ROS are formed by the incomplete reduction of oxygen and are produced at low levels under normal physiological condition as a result of mitochondria respiration and a number of other processes. The cell is able to cover this production through several antioxidant defences. When these systems are overloaded oxidative stress occurs and leads ultimately to cell death. Oxidative stress is responsible for DNA mutations, and damage of cellular components such as lipids and proteins; in particular it can lead to the non-specific post-translational

modifications of proteins, named carbonylation, and contributes to protein aggregation (Underwood et al.,2010; Rossi et al., 2008; Lee et al., 2012).
Oxidative stress has been demonstrated across several tissue types to play an important role in control of autophagy, ageing and in the progression of a multitude of diseases including neurodegeneration, cardiovascular diseases, and cancer (Lee et al. 2012). A general concept is that oxidative stress induces autophagy to remove oxidized protein (Dodson et al., 2013) and dysfunctional organelles (Figure 15). Furthermore, it has been demonstrated that anti-oxidant treatment is able to prevent or rescue protein oxidation (Whidden et al., 2010; Desaphy et al., 2010), but other studies pointed out its effect on autophagy. A recent work showed that both thiol antioxidants, in particular N-acetil-cysteine (NAC), and non-thiol antioxidants, profoundly impair both basal and induced autophagy, through different signalling pathways (Underwood et al., 2010). In fact, although thiol antioxidants inhibit mTOR, they also reduce the phosphorilation levels of JNK and BCL-2, reducing the availability of BECLIN1, that is required for autophagosome formation, thus resulting in autophagy impairment. On the contrary, non-thiol antioxidants activates mTOR, that consequently sequesters ULK-1 from autophagy pathway (Underwood et al., 2010). These findings suggest that basal level of oxidative stress is an important signal that mediates autophagy activation thus maintaining tissue homeostasis, because depletion of 'physiological ROS' in healthy cells leads to impaired autophagy and homeostatic imbalance.

Oxidative stress can also induce autophagy, through p53 activation. This is a very open topic, since there are opposite evidence regarding the role of p53, but what is known is that p53 is a tumor suppressor protein that has a dual effect on autophagy, acting both as a positive and negative regulator.
It was demonstrated that p53 induces autophagy via its transcriptional activity and acts as a negative regulator of autophagy via its cytoplasmic functions (Green and Kroemer, 2009). On the contrary, a recent work reported that cytosolic p53 leads to autophagy induction by activation of AMPK and mTOR suppression, and inhibit autophagy translocating to the nucleus and increasing transcription of TSC1, the

direct inhibitor of mTOR pathway (Dodson et al., 2013). So further works are required to clarify autophagy regulation by p53.

Other stimuli are involved in autophagy regulation, for example oxygen rate. Both hypoxia and anoxia (with oxygen concentrations <3% and <0.1%, respectively) triggers autophagy through a variety of different mechanisms. Hypoxia-induced autophagy depends on hypoxia-inducible factor, HIF, while anoxia-induced autophagy is HIF independent (Majmundar et al., 2010; Mazure and Pouyssegur, 2010).

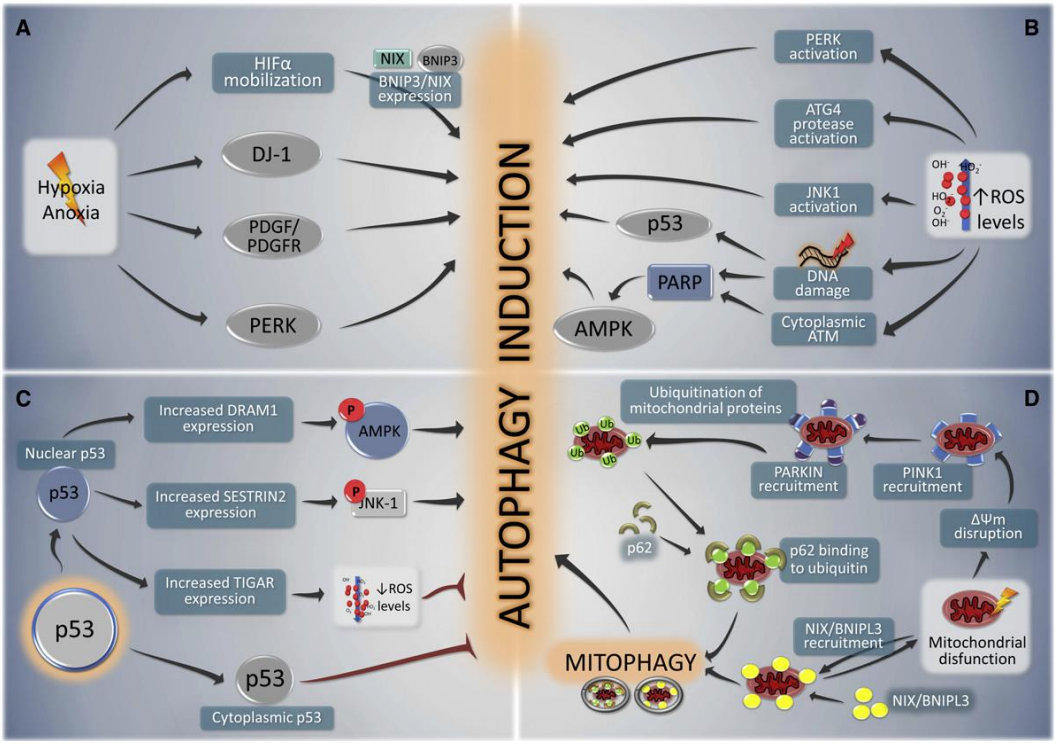

Fig.15: Representative scheme of some of the major player involved in autophagy regulation: oxidative stress, hypoxia and anoxia condition, p53, mitochondrial dysfunction (Kroemer et al., 2010).

1.4.5 Autophagy in disease

Autophagy occurs at basal levels in most tissues and contributes to the routine turnover of cytoplasmic components. In fact it is involved in development, differentiation, and tissue remodelling in various organisms. In contrast, a dramatic enhancement of autophagy can be triggered by some conditions such as starvation and hormonal stimulation as a defensive mechanism (Levine and Klionsky et al., 2004). Autophagy is also implicated in wide range of diverse human diseases. In cancer autophagy mainly acts as tumor suppressor, while clearing aggregate-prone mutant proteins in several neurodegenerative diseases. These include proteins with polyglutamine (polyQ) of Huntington's disease and spinocerebellar ataxia, mutant α-synucleins of Parkinson syndrome, and mutated tau aggregation in fronto-temporal dementia (Williams et al., 2006). Autophagy is plays a role also in muscular disorders, such as Pompe and Danon disease and X-linked myopathy, liver diseases and pathogen infection (Levine and Kroemer, 2008).

1.5 AUTOPHAGY AND MUSCLE

1.5.1 Regulation of autophagy in skeletal muscle

Autophagy is constitutively active in skeletal muscle. It is essential for proper muscle homeostasis, in fact it is required to maintain muscle mass (Masiero et al., 2009) and is a mechanism of stress-response. Autophagy is induced in skeletal muscle in the immediate post-natal period when glycogen-filled autophagosomes are abundant (Schiaffino and Hanzlikova, 1972a). The crucial role of autophagy in the newborn is demonstrated by the finding that mice deficient in autophagy genes Atg5 or Atg7 die soon after birth during the critical starvation period when transplacental nutrient supply is suddenly interrupted (Komatsu et al., 2005; Kuma et al., 2004).

FoxO3 is the master regulator of autophagy in adult muscles (Mammucari et al., 2007). Expression of FoxO3 is sufficient and required to activate lysosomal-dependent protein breakdown in cell culture and *in vivo*. Moreover several

autophagy genes including LC3, Gabarap, Bnip3, VPS34, Atg12 are under FoxO3 regulation. Gain and loss of function experiments identified BNIP3, a BH3-only protein, as a central player downstream of FoxO in muscle atrophy (Mammucari et al., 2007; Tracy et al., 2007). These studies allowed to identify the most potent autophagy inhibitor in skeletal muscles: AKT kinase. Acute activation of AKT in adult mice or in muscle cell cultures completely inhibits autophagosome formation and lysosomal-dependent protein degradation during fasting (Mammucari et al., 2007; Zhao et al., 2007; Zhao et al., 2008).

A clear pathway as been identified in muscle. In presence of nutrients IGF1/Insulin signalling pathway is activated, this leads to the activation of AKT. When AKT is phosphorylated (P-AKT), it activates mTOR, thus increasing protein synthesis rate, and blocking autophagy; on the contrary, P-AKT phosphorylates FoxO, that in this way is sequestered in the cytosol, and its transcriptional action is blocked, leading to autophagy inhibition (Figure 16, left panel). During stress or pathological conditions, such as nutrient deprivation, diabetes, cachexia, AKT signal is blocked, and in addition mTOR negative regulation on autophagy is removed. In this way, FoxO can translocate into the nucleus, promoting transcription of several genes, in particular some autophagy genes such as *Bnip3*, *LC3* and *p62*, leading to autophagy activation (Figure 16, right panel).

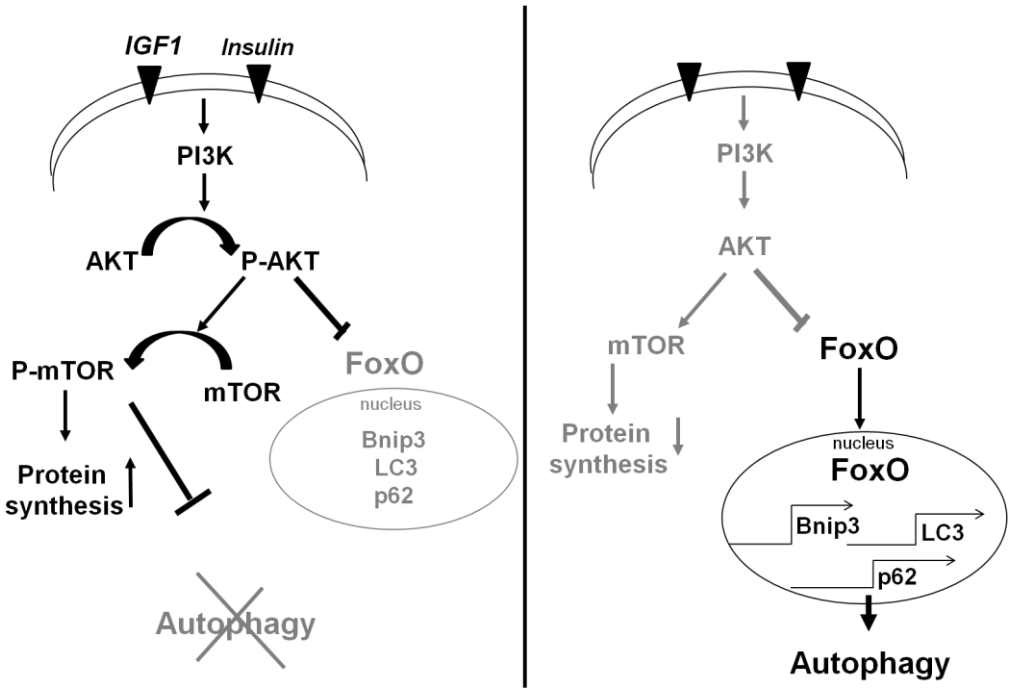

Fig.16: Regulation of autophagy in muscle tissue, in presence of IGF-1 and Insulin signals FoxO is phosphorylated by AKT and blocked outside the nucleus (on the left), during starvation or denervation AKT is not active, so FOXO can enter into the nucleus mediating transcription of the autophagy genes thus leading to autophagy activation.

1.5.2 The *in vivo* model of muscle-specific block of autophagy

During muscle denervation or muscle loss autophagy-lysosome system is severely induced (Sandri, 2008).

Electron microscopic studies previously showed that autophagy is activated in denervation atrophy (Schiaffino and Hanzlikova, 1972b) and the lysosomal proteolytic system is stimulated in different atrophic conditions, such as nutrient deprivation or disuse (Bechet et al., 2005). Furthermore among designated atrophy-related genes or atrogenes, that are upregulated during muscle loss, several belong to the autophagy-lysosome system, in particular *LC3* and *Gabarap* (Mammucari et al., 2007; Mammucari et al., 2008; Zhao et al., 2007).

After these results, it was still unclear whether activation of autophagy during muscle loss was detrimental, contributing to muscle degeneration or whether it was a compensatory mechanism for cell survival. So, in order to investigate the role of basal autophagy in muscle, in my laboratory were generated two knockout mice for the critical *Atg7* gene to block autophagy specifically in skeletal muscle (Masiero et al., 2009). Atg7-floxed mice ($Atg7^{f/f}$) were crossed with a transgenic line expressing Cre recombinase (CRE) under the control of a myosin light chain 1 fast promoter (MLC) to generate muscle-specific Atg7 knockout mice ($Atg7^{-/-}$MLC), lacking autophagy process from birth (Figure 17A). Tamoxifen-inducible muscle-specific Atg7 knockout mice ($Atg7^{-/-}$HSA) were also generated to evaluate the role of acute block of autophagy at different stages. In these mice *Atg7* gene is deleted only after Tamoxifen treatment because Cre recombinase (CRE) fused with estrogen receptor (ER) is constantly degraded. Tamoxifen binds ER thus preventing CRE degradation and mediating its localization in the nucleus, where it triggers the deletion of *Atg7* only in skeletal muscle, because it is under the control of human skeletal actin promoter (HSA) (Figure 17B).

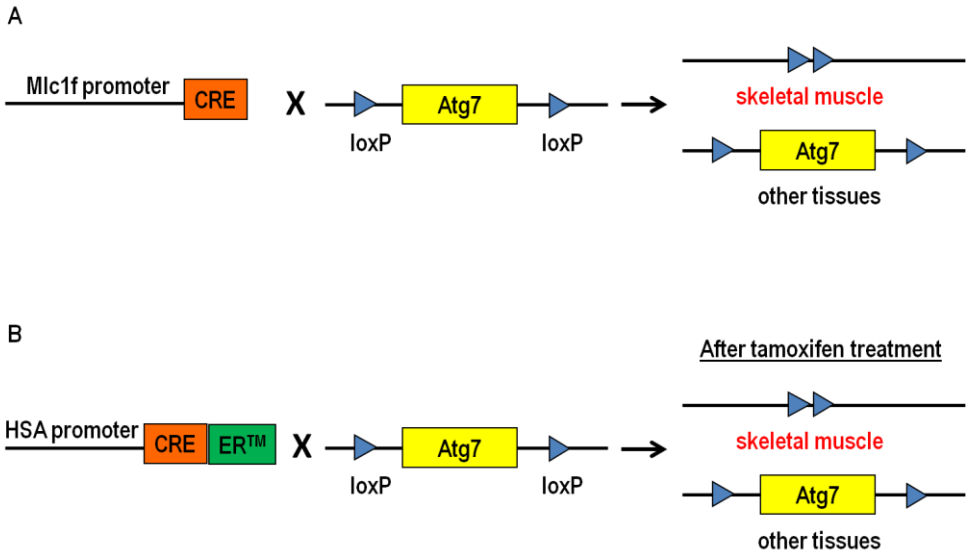

Fig.17: Schematic representation of $ATG7^{-/-}$ MLC (A) and $ATG7^{-/-}$ HSA (B) mice generation.

Autophagy block was verified by the absence of the lipidated form of LC3 (LC3-II), as it is indicated in Figure 18 (upper panel). Moreover, since p62 is no more degraded, it accumulates in autophagy deficient mice, thus leading to self-oligomerization and formation of p62 aggregates (Figure 18, lower panel).

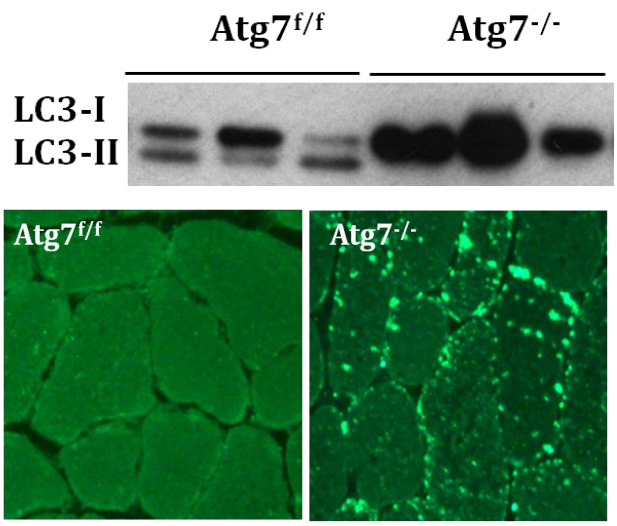

Fig.18: Block of autophagy prevents LC3 lipidation (upper panel) and induces p62 aggregates formation (lower panel).

Surprisingly, suppression of autophagy was not beneficial and instead triggers atrophy, weakness and several myopathic features (Figure 19). Atg7$^{-/-}$ MLC and HSA mice shared the same features, indicating that both prolongued (conditional model) and acute (inducible model) block of autophagy are able to induce muscle loss.

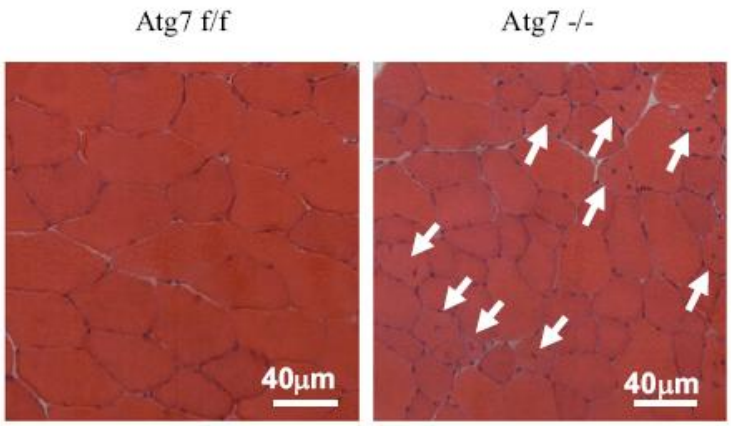

Fig.19: Myopathic phenotype observed in ATG7$^{-/-}$ MLC mice. H&E staining reveal the presence of atrophic and centernucleated myofibres in ATG7$^{-/-}$ MLC mice (Masiero et al., 2009).

Moreover deletion of *Atg7* gene causes accumulation of abnormal mitochondria and of concentric membranous structures that assemble between the myofibrils or just beneath the sarcolemma, induction of oxidative stress and activation of unfolded protein response. Together, these pathological conditions lead to myofiber degeneration.

These results indicate that autophagy is required for skeletal muscle mass maintenance and homeostasis.

1.6 AUTOPHAGY AND AGEING

Almost all ageing organisms share a gradual decrease in the activity of ubiquitin-proteasome and autophagy. Numerous pieces of evidence indicate that autophagy declines with age and this progressive reduction might cause functional deterioration during ageing (Tan et al., 2013). Recent studies in human detected down-regulation of autophagy genes (ATG5 , ATG7 , and BECN1) in the brain of old persons compared with young ones (Lipinski et al., 2010). Although different studies have established a tight connection between autophagy and ageing, a one-way cause-and-effect relationship still remains obscure (Tan et al., 2013). In mammals, the relationship between autophagy inhibition and ageing is still widely phenomenological and correlative. Conversely, robust genetic evidences in worms and flies underline such connection. Indeed, deficient expression of Atg1, Atg7, Atg8, Beclin 1 and Sestrin1 (which is also required for basic autophagy) shortens the lifespan of the fruit fly Drosophila Melanogaster and of the worm C. Elegans (Lee et al., 2010b; Rubinsztein et al., 2011; Simonsen et al., 2008). This is linked to age associated pathologies that are mainly relevant in brain, skeletal and cardiac muscles (Lee et al., 2010b). On the other hand, increased autophagy contributes to longevity and mutation of essential ATG genes prevents this effect (Melendez et al., 2003). Importantly, a recent report underlines that the ageing process can be controlled by a single tissue (Demontis and Perrimon, 2010). In fact over-expression of FoxO transcription factor or its target 4EBP1 in the skeletal muscles of flies abolishes the age-associated decline in autophagy and increases longevity while it reduces food intake and insulin release from neurosecretory cells. These data show

that maintenance of a normal autophagy level in skeletal muscle, but not in adipose tissue, positively affects whole-body metabolism (Demontis and Perrimon, 2010). FoxO3 is the a main regulator of autophagy (Mammucari et al., 2007; Mammucari et al., 2008; Zhao et al., 2007) and, interestingly, genetic variations in the human FoxO3 have been linked to longevity in multiple population studies (Kenyon, 2010).

As I reported before, sarcopenia can be defined as ageing of muscle tissue. In mammals the role of autophagy during sarcopenia is still controversial, because either impaired or excessive autophagy have been associated to it (Wenz et al., 2009; Wohlgemuth et al., 2010). Among all the studies done, loss-of-function experiments that support the involvement of autophagy in ageing sarcopenia are still lacking.

1.7 AUTOPHAGY AND EXERCISE

As I reported before, physical exercise is an important lifestyle practice that induces a multitude of beneficial adaptations both in humans and rodents. Regular physical activity has been demonstrated to improve glucose and lipid homeostasis, maintain muscle mass and delay ageing (Melov et al., 2007; Fontana et al., 2010; Sandri et al., 2013; Schiaffino et al., 2013; Coen et al., 2013; Toledo et al., 2013). Although the positive effects of exercise are undisputed, the underlying mechanisms are still under vigorous investigation, in particular the possible link with autophagy.

Previous work revealed that an acute bout of exercise is sufficient to induce autophagy in skeletal muscle (Grumati et al., 2011). Others have further confirmed these findings reporting that physical activity-induced adaptations that may be mediated by the activation of autophagy (He et al., 2012; Kim et al., 2013).

Mice with defective stress-induced autophagy, but proper basal autophagy, were found to run significantly less on a treadmill than the wild types (He et al., 2012). Moreover, these mice do not obtain the same exercise-mediated benefits and were not protected from high fat diet-induced glucose intolerance. This supports that exercise-induced metabolic rejuvenation occurs through the stimulation of autophagy. Moreover, He et al. identified AMPK as a potential player in the exercise-induced autophagy-mediated metabolic improvements. In their hands, AMPK

activation presumably leads to the up-regulation of the glucose transporter, GLUT4, at the muscle membrane, thus increasing the capacity for muscular glucose uptake (He et al., 2012). However, the signalling cascade responsible has not been elucidated yet. These findings remain controversial as skeletal muscle–specific autophagy-knockout mice show the opposite phenotype. These mice appear to have an improved metabolic profile and increased sensitivity to insulin, that protects them from diet-induced obesity (Kim et al., 2013). These contrasting results may be due to the difference in tissue specific versus general autophagy disturbance and, therefore, highlight a potential cell autonomous regulation, which has yet to be investigated.

In conclusion, it is still unknown whether it is whole body or muscle-specific autophagy that is required to sustain contraction, maintain glucose homeostasis, and trigger exercise-induced benefits.

1.8 AIM OF THE WORK

It is widely accepted that autophagy declines with age and this progressive reduction might have a role in the functional degeneration of tissues, but a direct causative relationship still remains undefined. Moreover, the role of autophagy during ageing of muscle tissue, in mammals, is still controversial and loss-of-function experiments that support its involvement are still lacking.

In order to investigate the role of autophagy inhibition in skeletal muscle during ageing, we mimic that condition *in vivo*, through muscle-specific block of autophagy process.

My work is focused on the characterization of muscle-specific aged autophagy knockout mice (Atg7$^{-/-}$MLC).

Moreover, since it is known that exercise has a beneficial effect on ageing features and moreover it is able to reactivate autophagy in elderly, we wanted to understand whether these beneficial effects are triggered by autophagy, and so indentify the role of autophagy during muscle contraction. It is known that autophagy is activated upon exercise, but the effects of this induction are still controversial. In fact, whether it is whole body or muscle specific autophagy that is required to sustain contraction, maintain glucose homeostasis, and triggers exercise-induced benefits, remains unknown.

In order to clarify this issue, we used muscle-specific inducible autophagy deficient mice (Atg7$^{-/-}$HSA), to minimize the chance of any adaptations and compensations that occur with constitutive deletion of genes.

2. MATERIALS AND METHODS

2.1 GENERATION OF MUSCLE-SPECIFIC ATG7 KNOCKOUT MICE

Muscle-specific $Atg7^{-/-}$ MLC and $Atg7^{-/-}$ HSA mice generation have been previously described by Masiero et al., 2009. Briefly Atg7 floxed mice $Atg7^{f/f}$ (Komatsu et al., 2005) were crossed with transgenic mice expressing Cre-recombinase (CRE) under the control of a Myosin Light Chain 1 fast promoter (MLC-1f), that is expressed only in skeletal muscle during the embryonic development. In order to obtain inducible muscle specific Atg7 knockout mice, Atg7 floxed mice (Komatsu et al., 2005) ($Atg7^{f/f}$) were crossed with transgenic mice expressing a Cre-recombinase fused with a modified estrogen receptor domain (Cre-ER™) driven by Human Skeletal Actin promoter (HSA) (Schuler et al., 2005). In order to induce the deletion of Atg7 gene we treated animals with Tamoxifen food (Harlan) for 9 weeks. We characterized muscle-specific autophagy deficient ($Atg7^{-/-}$) and control ($Atg7^{f/f}$) mice. We analized adult (2, 5 and 10 months old) and aged (26 months old) mice.

2.1.1 Genotyping of muscle specific Atg7 knockout mice

Mice were identified by analyzing the presence of Cre-recombinase on genomic DNA by PCR .

We used a lysis buffer containing Tris-HCL 1M pH 7.5 and Proteinase K 10mg/mL (Life Technologies).

The samples were denaturated by incubation for 1 hour at 57°C and then the proteinase K was inactivated at 99°C for 5 minutes. For the PCR reaction we used the following primers and program:

Primers:

NSP-780: CACCAGCCAGCTATCAACTCG

NSP-979: TTACATTGGTCCAGCCACCAG

We prepared a 20 µl total volume mix for each sample with:
Template DNA: 2 µl
Primer NSP-780 (10 µM): 0.2 µl
Primer NSP-979 (10 µM): 0.2 µl
GoTaq Green master mix 2X (Promega): 10 µl
Water

Program:
step 1: 94° C for 3 minutes
step 2: 94° C for 45 seconds
step 3 61° C for 30 seconds
step 4 72°C 1 minute
step 5: go to step 2 for 40 times
We detected Cre-recombinase DNA (200 bp) with a 2% agarose gel (Figure 1).

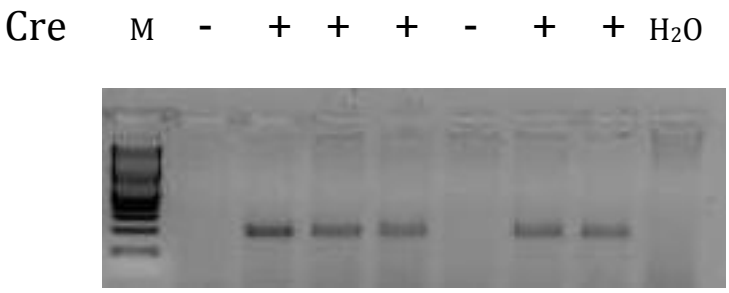

Fig. 1: Representative image of eletrophoretic run of DNA, mice in which the deletion of Atg7 occurred, resulted Cre positive.

2.2 *In vivo* SKELETAL MUSCLE ELECTROPORATION

Experiments were performed on adult $Atg7^{fl/fl}$ or $Atg7^{-/-}$ mice tibialis anterior (TA) or flexor digitorium brevis (FDB). The animals were anesthetized by an intraperitoneal injection of xylazine (Xilor) (20 mg/Kg) and Zoletil (10 mg/Kg).
Tibialis anterior (TA) muscle was isolated through a small hindlimb incision, and DNA was injected along the muscle length. Electric pulses were then applied by two

stainless steel spatula electrodes placed on each side of the isolated muscle belly (50 Volts/cm, 5 pulses, 200 ms intervals). Muscles were analyzed 14 days later. No evidence of necrosis or inflammation as a result of the transfection procedure were observed (Sandri et al., 2004 and Donà et al., 2003).
Tibialis Anterior of $Atg7^{-/-}$ MLC mice were transfected with FGFBP1-V5 (20 μg) and GFP (5 μg) plasmids. Tibialis Anterior of control mice were transfected with oligos (25 μg) for knocking down experiments.

FDB electroporation did not require muscle isolation. We injected 5 μl of Hyaluronidase (2mg/ml)(Sigma-Aldrich) in the feet of anesthetized mice, to soften muscle tissue underneath the epidermis. We waited 50 minutes to inject DNA and after 10 minutes electric pulses were applied by two stainless needles placed at one cm from each other (100V/cm) (100 Volts/cm, 20 pulses, 1 s intervals). Muscles were analyzed 7 days later. No evidence of necrosis or inflammation were observed after the transfection procedure. FDB of $Atg7^{f/f}$ HSA and $Atg7^{-/-}$ HSA mice were transfected with roGFP plasmid (15 μg).

2.3 MEASUREMENTS OF MUSCLE FORCE *IN VIVO*

Muscle force was measured in a living animal as previously described (Blaauw et al., 2008). We performed this experiment in collaboration with Bert Blaauw (VIMM, Padua). Briefly gastrocnemius (GCN) muscle contractile performance was measured *in vivo* using a 305B muscle lever system (Aurora Scientific Inc.) in anaesthetized mice. Contraction was elicited by electrical stimulation of the sciatic nerve. The torque developed during isometric contractions was measured at stepwise increasing stimulation frequency, with pauses of at least 30 seconds between stimuli to avoid effects due to fatigue. Duration of the trains never exceeded 600 ms. Force developed by plantar flexor muscles was calculated by dividing torque by the lever arm length (taken as 2.1 mm).

2.4 HISTOLOGY ANALYSES AND FIBRE SIZE MEASUREMENTS

Muscles were collected and directly frozen by immersion in liquid nitrogen. Then we cut muscle cryosections by using Cryostat (Leica CM 1950), 10µm thick for histology and 7µm thick for immunostaining analyses. TA Cryosections, 10µm thick, were used to analyze tissue morphology with different methods, listed below. Images were collected with an epifluorescence Leica DM5000B microscope, equipped with a Leica DFC300-FX digital charge-coupled device camera, by using Leica DC Viewer software.

For electron microscopy, we used conventional fixation-embedding procedures based on glutaraldehyde-osmium fixation and Epon embedding.

2.4.1 Haematoxylin and Eosin staining (H&E)

Haematoxylin colors basophilic structures that are usually the ones containing nucleic acids, such as ribosomes, chromatin-rich cell nuclei, and the cytoplasmc regions rich in RNA. Eosin colors eosinophilic structures bright pink. The eosinophilic structures are generally intracellular or extracellular protein.

The methods consist of:

Materials	Time
3 washes in PBS	5 minutes each
Harris Haematoxylin (Sigma-Aldrich)	1 minute
Wash in running tap water	3 minutes
Eosin Y Solution Alcoholic (Sigma-Aldrich)	1 minute
Ethanol 50%	30 seconds
Ethanol 70%	30 seconds

Ethanol 100%	5 minutes
Ethanol 100%	10 minutes
Xilen	3 minutes
Mount with Eukitt (Sigma-Aldrich)	

2.4.2 Succinate dehydrogenase (SDH)

The succinate dehydrogenase is an enzyme complex, bound to the inner mitochondrial membrane. With this staining it is possible to evaluate approximately the quantity of mitochondria present in the muscle fibres, through colorimetric evaluation. The reaction gives a purple coloration in the oxidative fibres. The sections were incubated for 30 minutes at 37°C with SDH solution (0.2M sodium succinate) (Sigma-Aldrich), 0.2M phosphate buffer (Sigma) ph 7.4 and 50mg of nitro blue tetrazolium (NBT)(Sigma-Aldrich). After the incubation, the sections were washed 3 minutes with PBS and then mounted with Mounting medium (Dako).

2.4.3 Fibre Cross-Sectional Area (CSA)

Fibre Cross-Sectional Area was measured, by using ImageJ software (National Institutes of Health). All data are expressed as the mean SEM (error bars). Comparisons were made by using t test, with $*P<0.05$ being considered statistically significant.

2.5 IMMUNOHISTOCHEMISTRY ANALYSES

TA muscle cryosections, 7 μm thick, were processed for immunostaining. All data are expressed as the mean SEM (error bars). Comparisons were made by using t test, with $*P<0.05$ being considered statistically significant.

2.5.1 NCAM staining

Muscle cryosections were fixed with Methanol -20°C, treated with 0,1% Triton for 5 minutes and incubated in blocking solution (0.5% BSA, 10% goat serum in PBS) at room temperature (RT) for 40 minutes. Samples were then incubated with the primary antibody against NCAM (Millipore) (dilution 1:200) at 4°C over-night. Then the sections were washed with PBS three times for 5 minutes and incubated with the anti-rabbit-Cy3-conjugated secondary antibodies (dilution 1:200) at 37°C for 1 hour (Life Technologies). After the washes and incubation with DAPI, that labels nuclei, slides were mounted with mounting medium (Dako).

2.5.2 MuSK staining

Cryosections were fixed with PFA 4%, treated with 0,1% Triton for 5 minutes and incubated in blocking solution (0.5% BSA, 10% mouse serum in PBS) at RT for 40 minutes. After that samples were incubated with the primary antibody against MuSK (kind gift from M. Ruegg), at 4°C over-night (dilution 1:200). Sections were then washed with PBS three times for 5 minutes and incubated with the anti-rabbit-Cy3-conjugated secondary antibodies (dilution 1:200) at 37°C for 1hour (Life Technologies). After the washes, sections were incubated with anti-Bungarotoxin-Alexa 488 (dilution 1:500) from Life Technologies at 37°C for 1 hour. After the washes and incubation with DAPI, slides were mounted with mounting medium (Dako).

2.5.3 IgG staining

Cryosections were incubated in blocking solution (0.5% BSA, 10% goat serum in PBS) at RT for 20 minutes. Samples were then incubated with anti-mouse-Cy3-conjugated secondary antibodies (dilution 1:200) at 37°C for 1hour (Life Technologies). After the wash and incubation with DAPI, slides were mounted with mounting medium (Dako).

2.6 IMMUNOBLOTTING

Cryosections of 20 μm of TA muscles were lysed with 100 μl of a buffer containing 50 mM Tris pH 7.5, 150 mM NaCl, 10 mM MgCl2, 0.5 mM DTT, 1 mM EDTA, 10% glycerol, 2% SDS, 1% Triton X-100, Roche Complete Protease Inhibitor Cocktail and Sigma Protease Inhibitor Cocktail. After incubation at 70°C for 10 minutes and centrifugation at 11000 g for 10 minutes at 4°C, the surnatant protein concentration was measured using BCA protein assay kit (Pierce) following the manufacturer's instructions.

2.6.1 Protein gel Electrophoresis

The extracted proteins from TA muscle were solubilized in Loading buffer composed by 5μl of 4X NuPAGE® LDS Sample Buffer (Life Technologies) and 1μl of 20X DTT (Life Technologies). The volume of each sample was brought to 20μl with TBS 1X. The samples were denaturated at 70°C for 10 minutes.

Samples were loaded on SDS 4-12% precast polyacrylamide gels (NuPAGE Novex-Bis-tris-gels) or in SDS 3-8% depending on the protein to be analyzed (Life Technologies). The electrophoresis was run in 1X MES Running buffer or 1X Tris-Acetate Running buffer respectively (Life Technologies) for 1 hour and 30 minutes at 150V constant.

2.6.2 Transfer of the protein to the PVDF membrane

After the electrophoretic run, proteins were transferred from gels to PVDF membranes, previously activated with methanol. The gel and the membrane were equilibrated in Transfer Buffer. The Transfer Buffer was prepared as follows: 50 ml of 20X NuPAGE® Transfer buffer (Life Technologies), 1 ml of 10X NuPAGE® Antioxidant (Life Technologies), 200 ml of 20% Methanol (Sigma-Aldrich). The volume was brought to 1l with distilled water. The blotting was obtained by applying a current of 400mA for two hours at 4°C. To evaluate the efficiency of the transfer, proteins were stained with Red Ponceau 1x (Sigma-Aldrich). The staining was easily reversed by washing with distilled water.

2.6.3 Incubation of the membrane with antibodies

Once the proteins were transferred on PVDF membranes, the membranes were saturated with Blocking Buffer (5% no fat milk powder solubilized in TBS 1X with 0.1% TWEEN) for 1 hour at room temperature and were incubated overnight with various primary antibodies at 4°C . Membranes were then washed 3 times with TBS 1X with 0.1% TWEEN at RT and incubated with secondary antibody-HRP Conjugate (Bio-Rad), for 1 hour at room temperature.

Immunoreaction was revealed by SuperSignal West Pico Chemiluminescent substrate (Pierce) and followed by exposure to Xray film (KODAK Sigma-Aldrich).

Antibodies	**Companies**	**Catalogue number**
Anti-ATG7	Sigma-Aldrich	A2856
Anti-p62	Sigma-Aldrich	P0067
Anti-LC3	Sigma-Aldrich	L7543
anti-V5	Life technologies	46-0705
anti-βtubulin	Sigma-Aldrich	T8328
anti-GAPDH	Abcam-Aldrich	AB8245
anti-pan actin	Sigma-Aldrich	AC40
anti-GFP	Life technologies	A11122
anti-NCAM	Millipore	AB5032
Secondary Antibodies		
anti- mouse	Biorad	170-6516
anti-rabbit	Biorad	170-6515

Tab. 1: Antibodies used for western blot analyses.

All the peroxidase-conjugated secondary antibodies were from Bio-Rad. Blots were stripped using Stripping Solution, containing 25mM glycine and 1% SDS, pH 2.

2.7 FUNCTIONAL ASSAYS ON SINGLE MUSCLE FIBRES

All these experiments were done in collaboration with the group of Prof. Bottinelli (Physiology department, University of Pavia).

2.7.1 Single fibre dissection and experimental set-up

The method used for single muscle fibres dissection, the solutions and the experimental set-up have been previously described (Bottinelli et al., 1996). Briefly, after animal sacrifice, muscle bundles were prepared and stored at -20°C. On the day of the experiment, single muscle fibres were dissected from a bundle with the help of a stereomicroscope. Segments of muscle fibres were chemically skinned and attached in the experimental setup. Relaxing (5mM EGTA pCa 9.0), pre-activating (0.5mM EGTA pCa 9.0) and activating (pCa 4.5) solutions were prepared as previously described (Bottinelli et al., 1996). The set up was placed on the stage of an inverted microscope (Axiovert 10, Zeiss, Germany) which allowed us to view the fibre at x 320 magnification. In this way, we measured the force generated by each fiber and their speed of contraction. The signals from the force and displacement transducer were fed into a personal computer and analyzed by a data analysis software (Spike 2, CED,Cambridge, UK).

2.7.2 Single fibre analysis

Single fibre analysis was performed as previously described (Bottinelli et al., 1996). The experiments were performed at the temperature of 12°C. Sarcomere length was determined and set at 2.5µm. The cross sectional area (CSA) of the fibres was determined without correction for swelling. Absolute (Po) and specific force (Po/CSA) of the fibres were determined. At the end of the mechanical experiment fibres were put in 20 µl of Laemmli buffer and stored at –20 °C for subsequent electrophoretic analysis of myosin heavy chains (MHC) isoform content.

2.7.3 Contractile proteins for IVMA

Myosin extraction from bulk muscles

Myosin isoform 2B was extracted from bulk gastrocnemius muscles of mice according a procedure previously described in detail (Canepari et al., 2000) and used to prepare heavy meromyosin fraction (HMM).

Heavy meromyosin (HMM) preparation

HMM was obtained by a proteolytic digestion with α-chimotrypsin of myosin according to a modification of the method of Margossian and Lowey (Margossian and Lowey, 1982) previously described in detail (Canepari et al., 2000).

Actin preparation

G Actin was extracted as described by Pardee and Spudich (Pardee and Spudich, 1982) from acetone powder prepared from the residues of mice muscles after myosin extraction. After polymerization, F actin was labeled by incubation for several hours with rhodamine-phalloidine (Molecular Probes R415) as described by Kron et al (Kron et al., 1991).

2.7.4 *In Vitro* Motility Assay (IVMA)

In this assay actin and myosin are purified, then actin is labeled with rhodamine falloidine and allowed to move over myosin molecules that were previously linked onto a glass slide. When ATP is added, the actin-myosin complexes move out from the in rigor state and the actin movement and velocity of sliding on myosin is measured.

Myosin (or HMM) was diluted to 0.1 mg/ml in a high (or low) ionic strength buffer and infused in a flow cell treated with nitrocellulose and prepared according to Anson et al (Anson et al., 1995). The IVMA analysis was performed according to Canepari et al. (Canepari et al., 2000; Canepari et al., 1999) at the temperature of 25°C. The composition of the experimental buffer was MOPS 25mM (pH=7.4 at 25°C), KCl 25mM, MgCl2 4mM, EGTA 1mM, DTT 1mM, glucose oxidase 200 μ/ml, catalase 36μg/ml, glucose 5 mg/ml, ATP 2mM. Average velocities of actin filaments

were determined for each myosin and HMM sample, the velocities of at least 50 filaments were measured and their distribution characterized according to parametric statistics.

2.8 *IN VIVO* MICROSCOPY AND ANALYSIS OF ACHR TURNOVER AND NMJ FRAGMENTATION

We performed these experiments in collaboration with the group of Dr. Rudolf (KIT-Karlsruhe Institute of Technology, Karlsruhe). Bungarotoxin-Alexa 488 (1:100 dilution from 1mg/ml stock solution) (Life Technologies) was injected in the TA of an anesthetized mice, then after 10 days, a second injection of Bungarotoxin-Alexa 594 was performed in the same TA muscle of each mice. Mice that were previously transfected with specific plasmids had the first injection after 5 days of transfection. *In vivo* microscopy of mice was performed under anesthesia using Xylazine (Xilor) (20 mg/Kg) and Zoletil (10 mg/Kg) on a Leica SP2 confocal microscope equipped with a 63x 1.2 N.A. water immersion objective, essentially as described previously (Roder et al., 2010; Roder et al., 2008). Automated analysis of AChR turnover and NMJ fragmentation used algorithms described earlier (Roder et al., 2010).

2.9 GENE EXPRESSION ANALYSIS

Quantitative Real-time PCR was performed with SYBR Green chemistry (Applied Biosystems). SYBR green is a fluorescent dye that intercalates into double-stranded DNA and produces a fluorescent signal. The Real-Time PCR Instrument allows real time detection of PCR products as they accumulate during PCR cycles and create an amplification plot, which is the plot of fluorescence signal versus cycle number. In the initial cycles of PCR, there is little change in fluorescence signal. This defines the baseline for the amplification plot. An increase in fluorescence above the baseline indicates the detection of accumulated PCR products. A fixed fluorescence threshold can be set above the baseline. The parameter Ct (threshold cycle) is defined as the fractional cycle number at which the fluorescence passes the fixed threshold. So the

higher the initial amount of the sample, the sooner the accumulated product is detected in the PCR process as a significant increase in fluorescence, and the lower is the Ct value.

2.9.1 Quantification of the PCR products and determination of the level of expression

A relative quantification method were used to evaluate the differences in gene expression, as described by Pfaffl (Pfaffl, 2001). In this method, the expression of a gene is determined by the ratio between a test sample and a housekeeping gene. The relative expression ratio of a target gene is calculated based on the PCR efficiency (E) and the threshold cycle deviation (ΔCt) of unknown samples versus a control, and expressed in comparison to a reference gene.

The mathematical model used for relative expression is represented in this equation:

$$\text{Ratio} = \frac{(E_{\text{target}})^{\Delta Ct}}{(E_{\text{reference}})^{\Delta Ct}}$$

The internal gene reference used in our real time PCR was pan-actin, whose abundance did not change under the experimental conditions.

2.9.2 Primer pairs design

Gene-specific primer pairs were selected with Primer Blast software (http://www.ncbi.nlm.nih.gov/tools/primer-blast/). Primer pairs were selected in a region close to the 3'-end of the transcript, and amplified fragments of 150-250bp in length. To avoid the amplification of contaminant genomic DNA, the target sequences were chosen on distinct exons, separated by a long (more than 1000bp) intron. The melting temperature was chosen to be of about 58-60° C. The sequences of the primer pairs are listed in Table 2.

qRT-PCR primer	Oligo Sequence (5'-3')
m-AchRγ	Fw: CAGTGGGGGACCTAGAAACA Rev: ACCTTTCCAATCCACAGCAC
m-MuSK	Fw: ATCACCACGCCTCTTGAAAC Rev: TGTCTTCCACGCTCAGAATG
m-FGFBP1	Fw: CGCACGCTGCGCAAACAGAA Rev: TCCACGTGCGTTGGGGTTCA
m-Neurotrophin 3	Fw: GCCAGGCCGGTCAAAAACGG Rev: TCCAGCGCCAGCCTACGAGT
m-GDNF	Fw: TCGCGCTGACCAGTGACTCCAA Rev: GGAAGCGCTGCCGCTTGTTT
m-BDNF	Fw: AATGGCCCTGCGGAGGCTAA Rev: AGGGTGCTTCCGAGCCTTCCTT
m-PAN-ACTIN	Fw: CTGGCTCCTAGCACCATGAAGAT Rev: GGTGGACAGTGAGGCCAGGAT
m-h-GAPDH	Fw: TGCACCACCAACTGCTTAGC Rev: GGCATGGACTGTGGTCATG
h-FGFBP1	Fw: TCAGAACAAGGTGAACGCCCAGC Rev: GTGAGCGCAGATTCCGGGCA

Tab. 2: Sequence of primers used in q-RT-PCR analyses.

2.9.3 Extraction of total RNA

Total RNA was isolated from TA using Trizol (Life Technologies) following the manufacturer's instructions.

2.9.4 Synthesis of the first strand of cDNA

400ng of total RNA was reversly transcribed with SuperScript™ III (Life Technologies) in the following reaction mix:
Random primer hexamers (50ng/µl random): 1µl
dNTPs 10 mM: 1µl
H2O Rnase-free: 8.5µl

The samples were mixed and briefly centrifuged and denaturised by incubation for 5 minutes at 65°C to prevent secondary structures of RNA.

Samples were incubated on ice for 2 minutes to allow the primers to align to the RNA, and the following components were added sequentially:
First strand buffer 5X (Life Technologies): 5µl

DTT 100mM: 2µl
RNase Out (Life Technologies): 1µl
SuperScriptTM III (Life Technologies): 0.5µl
The volume was adjusted to 20ul with RNase free water.
The used reaction program was:
step1: 25°C for 10 minutes
step2: 42°C for 50 minutes
step3: 70°C for 15 minutes
At the end of the reaction, the volume of each sample was adjusted to 50ul with RNase free water.

2.9.5 Real-Time PCR reaction

1µl of diluted cDNAs was amplified in 10µl PCR reactions in a ABI Prism 7000 (Applied Biosystem) thermocycler, coupled with a ABI Prism 7000 Sequence Detection System (Applied Biosystems) in 96-wells plates (Micro Amp Optical, Applied Biosystems). In each well 5ul Sample mix and 5ul reaction mix were mixed.
Sample mix was prepared as follows for 5 µl total volume:
Template cDNA: 1 µl
H2O Rnase-free: 4 µl

The SYBR Green qPCR (Applied Biosystem) was used for the Real-Time PCR reaction as follows:
SYBR Green qPCR (Applied Biosystem): 4.8µl
Mix Primer forward /reverse 50mM: 0.2µl

The PCR cycle used for the Real-Time PCR was:
step 1: 95° C for 15 minutes
step2: 95° C for 25 seconds
step3: 58° C for 1 minute
step4: go to step 2 for 40 times

2.10 PLASMID CLONING

The cloning strategy required insertion of the DNA of intrest in a specific plasmid. Then competent bacteria (Top 10) (Life Technologies) were transformed and the plasmid was purified first with Mini-prep kit (Machery-Nagel) and then, to increase the quantity of DNA, in particular for *in vivo* transfection, we prepared Maxi-prep (Qiagen) following the manufacturer's instructions. Final DNA concentration was quantified by Nanovue Plus (GE Haelthcare).

2.10.1 FGFBP1 cloning

FGFBP1 was amplified from mouse cDNA by PCR using the following primers Fw: ACCATGAGACTCCACAGCCTC and Rev: GCATGATGTCGCCTGTAACAT. The PCR fragments then were cloned into pcDNA3.1-V5-HISTOPO vector (Life Technologies).

2.10.2 *In Vivo* RNAi

Oligos were cloned into Life Technologies BLOCK-IT Pol II miR RNAi Expression Vectors. For validation of shRNA constructs, C2C12 cells were maintained in DMEM/10%FBS and transfected with shRNA constructs using Lipofectamine 2000 (Life Technologies) according to manufacturer's instructions. Cells were lysed 24 hours later, and immunoblotting was performed as described below. The sequences of the Oligos Used for shRNA Production are listed in the Table 1:

shRNA oligos	**Oligo sequence (5'-3')**
FGFBP1-oligo 1	Fw: TGCTGTATTCTGGGCCTTCCCTAACGGTTTTGGCCACTGACTGACCGTTAGGGGGCCCAGAATA Rev: CCTGTATTCTGGGCCCCCTAACGGTCAGTCAGTGGCCAAAACCGTTAGGGAAGGCCCAGAATAC
FGFBP1-oligo 2	Fw: TGCTGTGCACTGGACCTTCAGGCTGAGTTTTGGCCACTGACTGACTCAGCCTGGGTCCAGTGCA Rev: CCTGTGCACTGGACCCAGGCTGAGTCAGTCAGTGGCCAAAACTCAGCCTGAAGGTCCAGTGCAC
FGFBP1-oligo 3	Fw: TGCTGTTCTGAGAACGCCTGAGTAGCGTTTTGGCCACTGACTGACGCTACTCACGTTCTCAGAA Rev: CCTGTTCTGAGAACGTGAGTAGCGTCAGTCAGTGGCCAAAACGCTACTCAGGCGTTCTCAGAAC
FGFBP1-oligo 4	Fw:TGCTGTTAGCATGATGTCGCCTGTAAGTTTTGGCCACTGACTGACTTACAGGCCATCATGCTAA Rev: CCTGTTAGCATGATGGCCTGTAAGTCAGTCAGTGGCCAAAACTTACAGGCGACATCATGCTAAC

MuSK-oligo 1	Fw: TGCTGAAATATGGCAGTCTTGTGCAGGTTTTGGCCACTGACTGACCTGCACAACTGCCATATTT Rev: CCTGAAATATGGCAGTTGTGCAGGTCAGTCAGTGGCCAAAACCTGCACAAGACTGCCATATTTC
MuSK-oligo 2	Fw: TGCTGTTAGGTTTCATCTTCACTTGCGTTTTGGCCACTGACTGACGCAAGTGAATGAAACCTAA Rev: CCTGTTAGGTTTCATTCACTTGCGTCAGTCAGTGGCCAAAACGCAAGTGAAGATGAAACCTAAC

Tab. 3: Sequence shRNA used for in vivo transfection

2.10.3 Cell culture and transient transfection

C2C12 myogenic cell line were cultured in DMEM (GIBCO-Life Technologies) supplemented with 10% foetal bovine serum. Myoblasts were transfected using Lipofectamine 2000 (Life Technologies) according to the manufacturer's instructions.

2.11 PROTEIN CARBONYLS DETECTION

We used the Oxyblot assay to evaluate ongoing protein carbonylation in skeletal muscle. Extensor Digitorum Longus (EDL) muscles were lysed in lysis buffer with 50mM of DTT. The composition of the lysis buffer is similar to that used for protein extraction. The samples were then incubated at 70°C for 10 minutes in a termomixer, and centrifuged at 11000 g for 10 minutes at 4°C. Then 15 μg of protein lysates were derivatized with 2,4dinitrophenylhydrazine (DNPH) solution and then neutralized. This way the samples can be separated on SDS-PAGE (12% (v/v) polyacrylamide) and electro blotted onto nitrocellulose membranes. After blocking, membranes were incubated with anti-DNP antibody (Sigma-Aldrich), washed, and incubated with peroxidase conjugated anti-rabbit IgG antibodies. Immunoreaction was revealed by SuperSignal West Pico Chemiluminescent substrate (Pierce) and followed by exposure to Xray film (KODAK Sigma-Aldrich). Quantification analysis was performed with ImageJ Software and all values were normalized for the housekeeping gapdh.

2.12 EXERCISE PROTOCOL

$Atg7^{f/f}$ and $Atg7^{-/-}$ HSA mice performed one day of concentric exercise on a treadmill (LE 8710 Panlab Technology 2B, Biological Instruments), with 10 degrees incline, at increasing velocity, according to the protocol of acute exercise previously described (He et al., 2012).

The eccentric training protocol consisted of 3 days running to exhaustion, with a 10 degree decline, at increasing velocity, according to the protocol of exercise previously described (He et al., 2012).

Briefly, exercise consists in 17 cm/sec for 40 minutes, 18 cm/sec for 10 min, 20 cm/sec for 10 min, 22 cm/sec for 10 min, and then increasing velocity of 1cm/sec and or 2 cm/sec alternatively every 5 minutes, until they were exhausted. Exhaustion was defined as the point at which mice spent more than 5 s on the electric shocker without attempting to resume running.

Total running distance and time were recorded for each mouse. All procedures are specified in the projects approved by the Italian Ministero Salute, Ufficio VI (authorization numbers C65).

2.13 ANTI-OXIDANT TREATMENT

$Atg7^{f/f}$ and $Atg7^{-/-}$ MLC mice were intraperitoneally injected with Trolox (Sigma-Aldrich) 30mg/kg daily for four weeks. Trolox is a general anti-oxidant because it is an analogue of vitamin E.

Females $Atg7^{f/f}$ and $Atg7^{-/-}$ HSA mice were treated with N-Acetyl-Cysteine (NAC) (Sigma-Aldrich A9165), for 6 weeks. We used 1% NAC drinking water for 5 weeks and 2% NAC drinking water for the last week. The treatment was also maintained during exercise training. NAC is a general anti-oxidant because it is a thiol antioxidant.

Another group of females $Atg7^{f/f}$ and $Atg7^{-/-}$ HSA mice were then treated with intraperitoneal injections of Mito-TEMPO (Enzo Life Science) 1.4 mg/kg daily for 7 days. Mito-TEMPO is a specific anti-oxidant, because it is a mitochondria-targeted superoxidant dismutase mimetic (Dikalova et al., 2010).

2.14 ANALYSES OF MITOCHONDRIAL MEMBRANE POTENTIAL IN ISOLATED SINGLE FIBRES

Mitochondrial membrane potential was measured in isolated fibres from flexor digitorum brevis (FDB) muscles. FDB muscle was incubated in a DMEM (GIBCO-Life Technologies) and Collagenase (4mg/ml)(GIBCO-Life Technologies) solution for about one hour and 45 minutes at 37°C. Then single fibres were dissected with the pipet with the help of a stereomicroscope. Mitochondrial membrane potential was measured by epifluorescence microscopy based on the accumulation of TMRM fluorescence as previously described (Romanello et al., 2010). Single fibres were incubated with TMRM (Tetramethylrhodamine, methyl ester)(Life Technologies) a fluorescent lipophilic cationic molecule that accumulates in mitochondria in a potential-dependent manner. The solution contains also glucose (3,5 g/l), to sustain the fibres during the experiment and Cyclosporin H (8mM) (Enzo Life Science), to block mitochondrial pumps, that would transport TMRM outside the mitochondria. In this experiment we need to perturbed the system with Oligomycin (4 μM)(Sigma-Aldrich), that is an ATP-syntase inhibitor, because ATP-synthase can reversely transport protons across the inner mitochondrial membrane, so maintaining the potential also in dysfunctional mitochondria. For this reason, only this treatment allow us to detect real dysfunctional mitochondria, that would inevitably dissipate the potential, loosing TMRM signal. At the end, we add an uncoupling agent FCCP (Trifluorocarbonylcyanide Phenylhydrazone) (4 μM)(Sigma-Aldrich), as experimental control. All the images were analyzed with ImageJ Software, and we considered fibres as depolarized when they have lost more than 10% of the initial value of TMRM fluorescence.

2.15 MITOCHONDRIAL OXIDATIVE STRESS MEASUREMENT

Mt-roGFP1 is an indicator of mitochondrial redox status (Dooley et al., 2004; Hanson et al., 2004). It measures the thiol/disulfide equilibrium in the mitochondrial matrix. We transfected FDB muscles of females $Atg7^{f/f}$ and $Atg7^{-/-}$ HSA mice with mt-roGFP

plasmid, that is targeted to the mitochondria, one week before exercise. Then we measured the fluorescence in single muscle fibres, that were isolated prior to and after exercise. Mt-roGFP1 fluorescence (excitation: 405 and 480 nm, emission: 535 nm, 20X objective) was measured for 5 minutes every 10 seconds. The ratio of fluorescence intensities (exc. 405/480) were computed. Records were analyzed with ImageJ Software.

2.16 BLOOD METABOLITES QUANTIFICATION

This analysis was performed in collaboration with the group of Prof. Avogaro (Venetian Institute of molecular medicine, VIMM, Padova). Blood samples were collected before exercise and immediately after the 3 days of exercise. Blood was collected from the orbital sinus in heparin-coated pasteur pipettes and centrifuged immediately after collection. Plasma samples were kept at -20°C until dosing.
Blood glucose and lactate levels were measured with an YSI 2300 STAT Plus™ Glucose & Lactate Analyzer (YSI Life Sciences, Yellow Springs, OH) according to the manufacture's instruction. Free fatty acids (FFAs) and beta-hydroxybutyrate were dosed using an automated spectrophotometer Cobas Fara II (Roche) according to the manufacture's instruction.

2.17 STATISTICAL ANALYSES

Survival probability evaluated by using Kaplan-Meier method. Comparison of $Atg7^{f/f}$ and $Atg7^{-/-}$ survival curves was performed by both Mantel-Cox and Gehan-Breslow-Wilcoxon tests.
Comparisons were made by using t test, with $p<0.05$ being considered statistically significant (*$p<0.05$, **$p<0.01$, ***$p<0.001$). Values are indicated in the graphs by mean +/- standard error.

3. RESULTS

PART I

3.1 ANALYSIS OF AUTOPHAGY PROCESS DURING AGEING

Initially we identified the level of the autophagy-lysosome pathway during ageing; for this reason we monitored autophagy in control animals, analyzing both adult (10 months old) and aged mice (26 months old). As indicator of autophagy, we analyzed ATG7 and LC3 protein levels. Aged mice showed a decrease of ATG7 and LC3 lipidation suggesting that autophagy is not only reduced, but impaired during ageing (Figure 1A). We also evaluated autophagy level in human biopsies from young (25 years old), old sedentary (70 years old), and old sportsmen (70 years old), that confirmed the finding observed in mice. LC3 lipidation and Atg7 level were dramatically reduced in old sedentary subjects (Figure 1B). Moreover, it is important to underline that autophagy is reactivated through physical exercise in elder people.

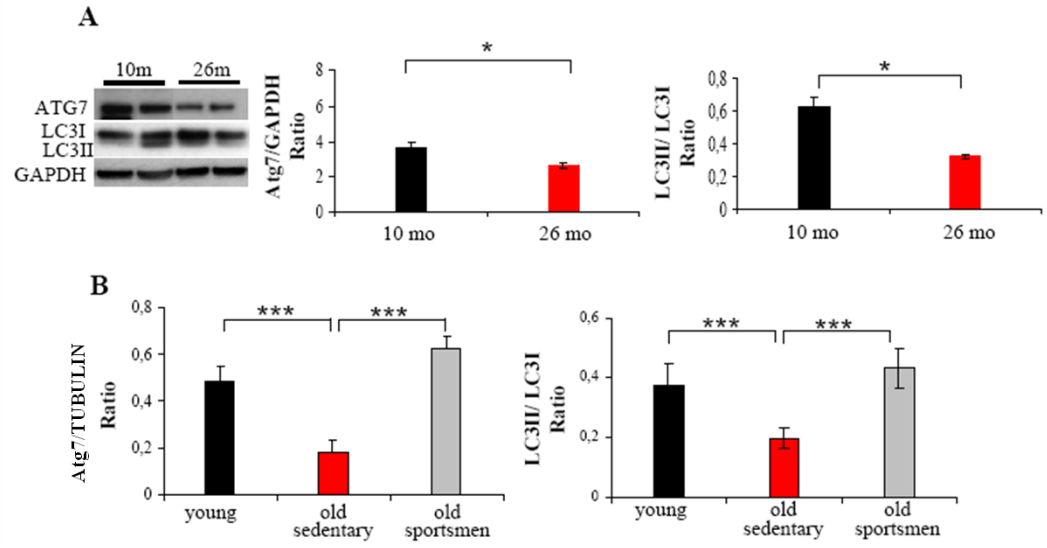

Fig. 1: Levels of autophagy proteins in aged mice (A) human biopsies (B). (A) Representative immunoblotting for the critical E1-like enzyme, ATG7, LC3-II and LC3-I on muscle extracts from gastrocnemius of 10 and 26 months old mice. The graphs show the quantification of Atg7

*protein and the LC3-II/LC3-I ratio. Values are mean +/- s.e.m., n=4 per condition, *p<0.05. (B) Ageing reduces, while exercise maintains expression of ATG7 and LC3 lipidation in humans. The graphs show the quantification of ATG7 protein and LC3-II/LC3-I ratio revealed by immunoblotting on muscle biopsies. Values are mean +/- s.e.m., n=6 young, n=10 old sedentary and n=4 senior sportsmen, ***p<0.0001.*

3.2 AUTOPHAGY INHIBITION EXACERBATES THE FEATURES OF AGEING SARCOPENIA

In order to understand the role of autophagy during ageing we characterized muscle-specific autophagy deficient mice, hereafter reported as $Atg7^{-/-}$ and control animals ($Atg7^{f/f}$). We analized adult mice (2, 5 and 10 months old) and aged ones (26 months old). Initially we monitored lifespan expecting that the inhibition of the second major protein degradation pathway would ameliorate the atrophic condition associated with ageing. Surprisingly $Atg7^{-/-}$ mice showed a significant reduction of survival (Figure 2A). Then we characterized the typical features of sarcopenia in these mice. We first monitored muscle morphology and measured muscle mass. H&E staining of aged animals revealed the presence of atrophy, center-nucleated fibres and inflammation in Atg7 deficient muscles compared to age-matched controls (Figure 2B). Fibre size was dramatically reduced in $Atg7^{-/-}$ and fibres displayed a great variability in dimension. In particular, we found extremely small fibers that made them hardly detectable (Figure 2C). We confirmed that those fibres were adult atrophic myofibres, and not regenerating fibers, as revealed by the absence of embryonic or neonatal isoforms of Myosin Heavy Chain, two markers or regeneration (data not shown). In order to quantify the atrophic condition we measured the fibre cross sectional area (CSA). CSA measurements confirmed that aged $Atg7^{-/-}$ presented an exacerbated atrophic phenotype compared to age matched controls (Figure 2D). Further analyses revealed that atrophy was exacerbated in glycolytic fibres (Figure 2E). The deterioration of $Atg7^{-/-}$ muscle was also confirmed by the significant increase of centre-nucleated fibres (Figure 2F), that are considered a typical sign of myopathy.

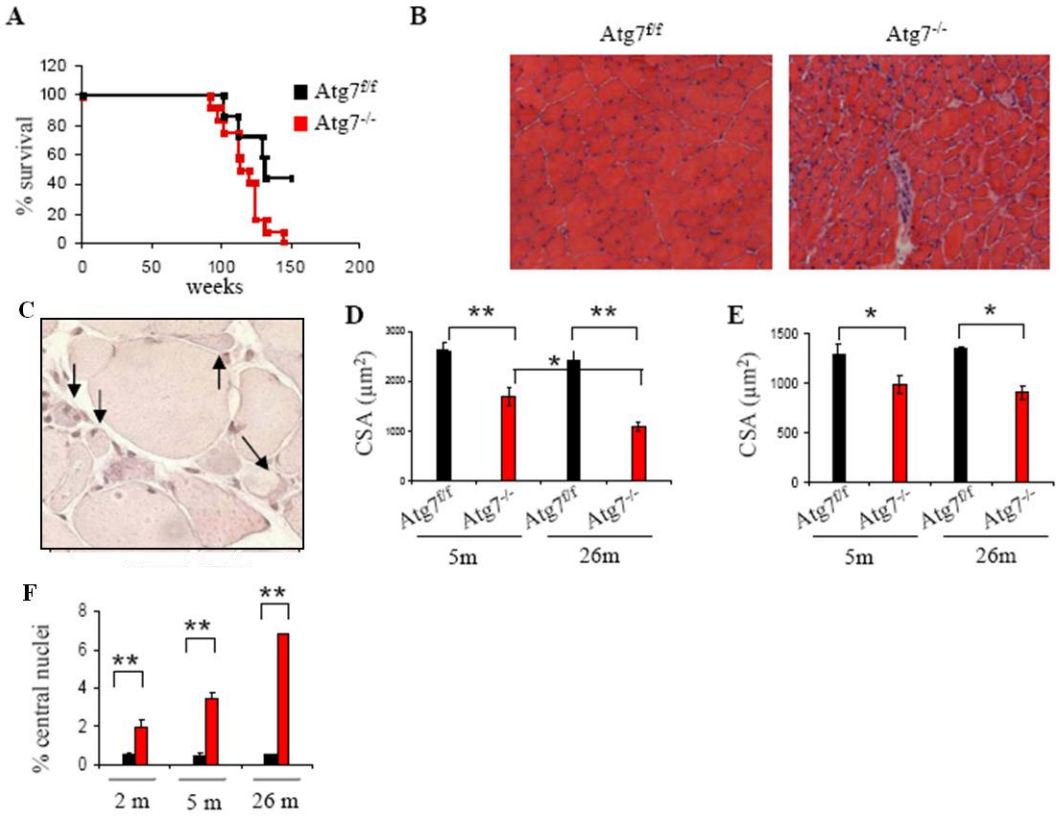

*Fig. 2: (A) Surival curve of autophagy deficient mice, they die earlier compared to control ones. Survival probability evaluated by using Kaplan-Meier method. Comparison of Atg7$^{f/f}$ and Atg7$^{-/-}$ survival curves was performed by both Mantel-Cox and Gehan-Breslow-Wilcoxon tests. (n>10 for each group) (p<0.05). (B-F) Atg7$^{-/-}$ are myopathic and atrophic as revealed by H&E staining and measure of CSA and centre-nucleated fibres. Values are mean +/- s.e.m., n>4 for each group, *p<0.05 **p<0.01.*

Considering that atrophy is often associated with a decrease in functionality we measured muscle force *in vivo*. In this assay, increasing electrical stimuli are applied to sciatic nerve of an anesthetized mouse in order to induce muscle contraction, and so force generation untill the maximum tetanic force is reached. In this way it is possible to measure the maximum force generated by a single muscle in living animals. We found that Atg7$^{-/-}$ muscles were weaker than controls in adulthood and in aged mice (Figure 3 A-B). This result indicated that Atg7 deficient muscles had an impaired functionality. Interestingly, the strength of adult Atg7$^{-/-}$ mice was

comparable to the force generated by 26 months old controls suggesting an ongoing precocious ageing. Given that muscle atrophy and weakness are exacerbated in autophagy-deficient muscles, and that a decline in innervation and loss of motor units are known to be important endogenous causes of sarcopenia, we tested whether the ageing-associated muscle loss was due to a possible ongoing denervation process. We first evaluated the expression pattern of Neural Cell Adhesion Molecule (N-CAM), that is a well defined re-innervation marker. NCAM localizes specifically at the neuromuscular junction (NMJ) level in innervated myofiber, but after denervation it is expressed along the entire fibres. Therefore, NCAM localization is used as a marker of denervation. As expected, aged control animals showed some NCAM positive however autophagy-deficient muscles displayed 5-7 fold more NCAM-positive fibres when compared to age-matched controls in both adulthood and elderly (Figure 3 C-E).

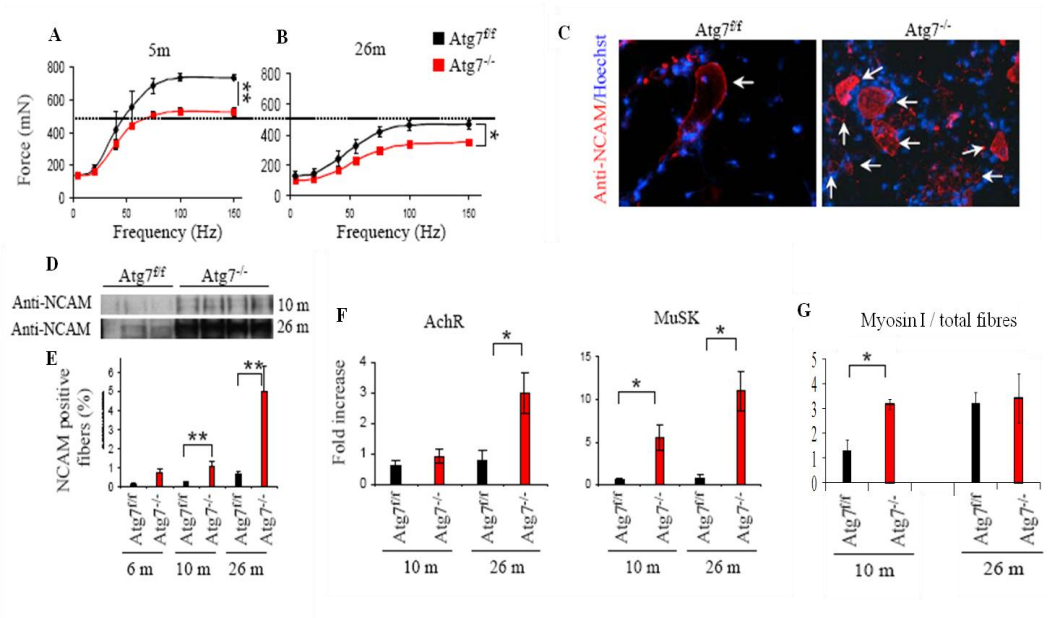

*Fig. 3: (A) Atg7$^{-/-}$ mice show a profound decrease in maximal force generation in adult animals. Values are mean +/- s.e.m., (n=5), **p<0.01. (B) Ageing reduces force production in both Atg7$^{f/f}$ and Atg7$^{-/-}$ mice, therefore aggravating the already profound weakness of Atg7$^{-/-}$ mice. Values are mean +/- s.e.m., n=4, *p<0.05. (C) Representative images of immunostaining for NCAM in aged mice. (D) Immunoblotting for NCAM protein on muscle extracts from adult and aged GCN muscles. Atg7$^{-/-}$ muscles express higher levels of NCAM than age-matched Atg7$^{f/f}$. (E)*

*Quantification of NCAM-positive fibers. Values were normalized for the total number of myofibers in muscle section (at least 4 muscles per group were analysed, **p<0.01). Atg7$^{-/-}$ mice are characterized by much higher age-dependent increase in NCAM positive fibers than age-matched Atg7$^{f/f}$. (F) Expression levels of acetylcholine receptor (AChR) ɣ-subunit (left), and MuSK (right). MuSK and AChR are up-regulated in adult and aged Atg7$^{-/-}$ muscles (*p<0.05, n>5). (G) Quantification of Myosin type I fibres, that is a typical hallmark of ageing. Adult Atg7$^{-/-}$ showed a number of Myosin type I fibres comparable to aged control mice. Values were normalized for the total number of myofibers in muscle section (at least 4 muscles per group were analysed, *p<0.05)*

We then monitored the expression of two other markers of denervation, MuSK and acetylcholine receptor (AChR) ɣ-subunit that are strongly induced upon denervation. Notably, both these genes were significantly more induced in Atg7-deficient muscles (Figure 3F). We also evaluated the number of myosin type I fibres, that is another marker of ageing. Indeed we found an increased number of these fibres in adult autophagy deficient mice when compared to aged-matched controls, (Figure 3G), suggesting an precocious ageing process in adult Atg7$^{-/-}$ mice.

To further investigate this aspect, we analyzed NMJ morphology and stability in living animals. This was possible trough an *in vivo* imaging approach that used the two photon confocal microscopy. In this assay Acetylcholine Receptors (AChR) of tibialis anterior (TA) muscle were pulse-labeled with a-bungarotoxin conjugated with different fluorophores, in these way, colour shows both shape and stability of NMJ. In fact the colour prevalence of first or second injected fluorophore indicates old or new receptors, respectively. A shift in the fluorescence reveals an instability of NMJ. Automated image analysis showed an significant increase of fragmented NMJ in adult Atg7$^{-/-}$ mice and a higher new receptor/old receptor ratio (Figure 4A-B). Moreover it is interesting notice that while in controls the changes in NMJ morphology and stability progressively worsen with age, this was not the case in Atg7$^{-/-}$. Notably, NMJs of both adult and aged Atg7$^{-/-}$ animals showed significantly more fragmentation and AChR turnover than 26 months aged control animals (Figure 4C). Indeed, while in control animals the amount of fragmented NMJs increased from 24.0 ± 1.8% (mean ± SEM, n = 4) in adult to 40.1 ± 11.6% (mean ±

SEM, n = 2) in aged mice, Atg7$^{-/-}$ muscles exhibited 70.7 ± 4.5% (mean ± SEM, n = 6) and 77.4 ± 2.7% (mean ± SEM, n = 6) fragmented synapses.

An important kinase specifically localized in postsynaptic region of NMJ is Muscle Specific Kinase (MuSK). MuSK controls a plethora of signalling pathways that are important for NMJ development and stability. The specific localization of MuSK in correspondence of NMJ is essential for its correct function. For this reason, we checked whether alteration in autophagy might also affect MuSK localization. Immunohistochemistry on control muscle sections revealed that most of MuSK signal correctly co-localized with AChR at the plasma membrane. Importantly, absence of autophagy caused a significant loss of MuSK at the myofiber plasma membrane and a concomitant enrichment of internalised MuSK protein (Figure 4D, E). Therefore, this set of experiments suggests that block of autophagy leads to precocious appearance of morphological and physiological features of denervation.

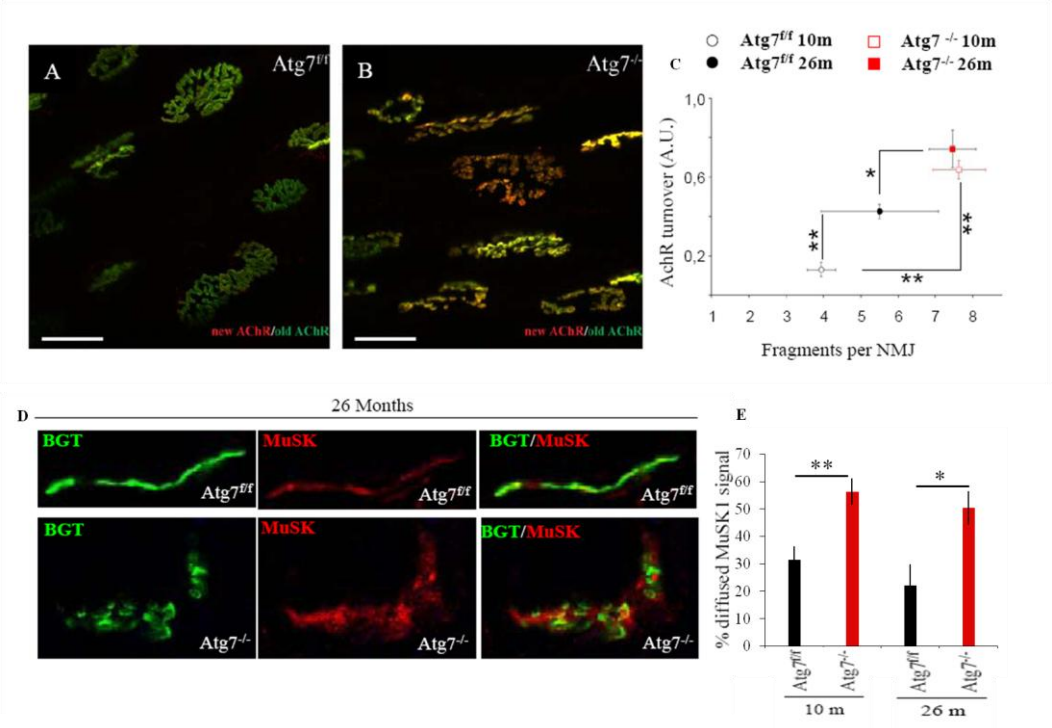

Fig. 4: (A) (B) Representative images of Atg7$^{f/f}$ and Atg7$^{-/-}$ neuromuscular junctions (NMJ) obtained using confocal in vivo microscopy. Muscles were in vivo pulse-labelled with bungarotoxins (BGT) conjugated with different fluorophores. BGT-AlexaFluor647 (shown in

*green) was injected 10 days before microscopy thus identifying stable AChR, while BGT-AlexaFluor555 (shown in red), injected 1 hour prior to microscopy, identifies newly incorporated AChR. Micrographs show representative maximum z-projections of confocal in vivo images of NMJs from Atg7$^{f/f}$ (A) and Atg7$^{-/-}$ (B). (C) Quantification of the AChR turnover as a function of NMJ fragmentation of adult and aged Atg7$^{f/f}$ versus Atg7$^{-/-}$. Analysis was done using custom-made algorithms as described previously (Roder et al., 2010). Data from at least 4 muscles per group, **p<0.01, *p<0.05. (D) Immunohistochemistry of MuSK expression on aged Atg7$^{f/f}$ and Atg7$^{-/-}$ myofibers. Upper panel shows normal pattern of NMJs in Atg7$^{f/f}$ mice, where MuSK (red) localizes to NMJ, revealed by BGT-AlexaFluor647 (green). Lower panel shows MuSK (red) that accumulates inside myofibers at the level of NMJ (green). (E) Quantification of the amount of diffused MuSK staining normalized over the total number of MuSK positive NMJs is higher in Atg7$^{-/-}$ than Atg7$^{f/f}$; **p<0.01.*

3.3 AUTOPHAGY INHIBITION ENHANCES OXIDATIVE STRESS AND MITOCHONDRIAL DYSFUNCTION

During ageing accumulation of dysfunctional mitochondria occurs thus contributing to an increased production of reactive oxygen species (ROS) and oxidative stress. It has been shown that adult autophagy-deficient mice present abnormal mitochondria, so we monitored mitochondria morphology in aged muscles. Succinate dehydrogenase (SDH) staining revealed an accumulation of mitochondria in aged autophagy deficient mice (Figure 5A). Electron microscopy showed an abnormal mitochondria morphology with cristae (Figure 5B). Since altered morphology is often associated with impairment in function we analyzed mitochondria functionality by evaluating their capability to maintain membrane potential. We performed TMRM assay on flexor digitorium brevis (FDB) single muscle fibres of adult mice (10 moths old). We did not perform the same assay in aged mice because of technical difficulties due to the condition of muscle tissue. While control mitochondria maintain membrane potential, after oligomycin addition, mitochondria of Atg7$^{-/-}$ did lose the potential (Figure 5C), thus revealing mitochondria dysfunction of Atg7$^{-/-}$ mice. Impairment in function leads to exacerbated ROS production, that we monitored by evaluating overall protein

carbonylation, that indeed was increased in Atg7$^{-/-}$ mice (Figure 5D). Atg7$^{-/-}$ muscles showed two-fold increase of carbonylated proteins when compared to age-matched controls.

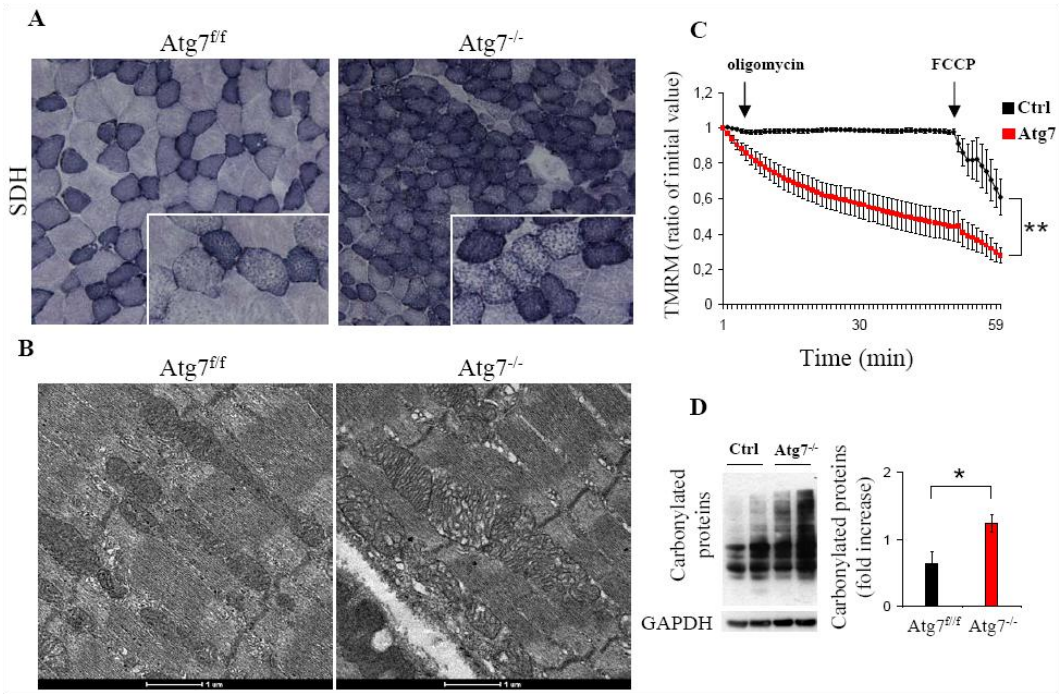

*Fig. 5: (A) SDH staining on serial sections of aged Atg7$^{f/f}$ and Atg7$^{-/-}$ muscles (TA) shows an accumulation of abnormal mitochondria in Atg7$^{-/-}$ myofibers. (B) Electron microscopy images of EDL muscles from aged Atg7$^{f/f}$ and Atg7$^{-/-}$ mice show accumulation of abnormal mitochondria displaying alterations in size, cristae morphology and matrix density. (C) Measurement of mitochondrial membrane potential. Isolated FDB muscle fibres from adult Atg7$^{f/f}$ and Atg7$^{-/-}$ mice were loaded with TMRM, that accumulates in healthy mitochondria that are able to maintain membrane potential. Atg7$^{-/-}$ mitochondria dissipate membrane potential. TMRM staining was monitored in at least 20 fibers per group (** p<0.001). (D) Overall protein carbonylation of aged Atg7$^{f/f}$ and Atg7$^{-/-}$ muscles, revealed by Oxyblot. A representative immunoblot for carbonylated proteins is depicted on the left, and densitometric quantification of the carbonylated proteins is in the graph on the right. Aged Atg7$^{-/-}$ mice show higher ongoing protein carbonylation than Atg7$^{f/f}$. (n=5, *p<0.05).*

Next we performed proteomic approach on carbonylated proteins to determine which proteins were oxidized in aged control compared to aged Atg7$^{-/-}$ mice. The

analyses revealed that mitochondrial and sarcomeric proteins, including actin, are indeed more carbonylated in aged Atg7$^{-/-}$ than controls. Since oxidative stress is believed to affect force generation, its enhancement might contribute to the ageing-dependent weakness.

Therefore, we studied this correlation at molecular level on single muscle cells in adult mice. Morphological and functional analyses on isolated single skinned fibres confirmed that autophagy-deficient muscle cells are more atrophic and generate less force (Figure 6A). Thus, not only the muscles become smaller but there is a general impairment in fibre contraction, which leads to profound weakness. Post-translational modifications of contractile proteins induced by ROS could also affect the specific interaction between actin and myosin. In order to investigate that, first we checked the carbonylation level of actin and myosin. We found an increased carbonylation level of contractile proteins in Atg7$^{-/-}$ compared to control (Figure 6B). Then we purified actin and myosin molecules and tested with an *in vitro* motility assay approach. Actin sliding velocity on both Myosin and HMM (a myosin proteolitic fraction able to move faster the actin filaments) of Atg7$^{-/-}$ mice was significantly slower compared to control (Figure 6C), confirming that autophagy block induces a functional alteration of contractile proteins.

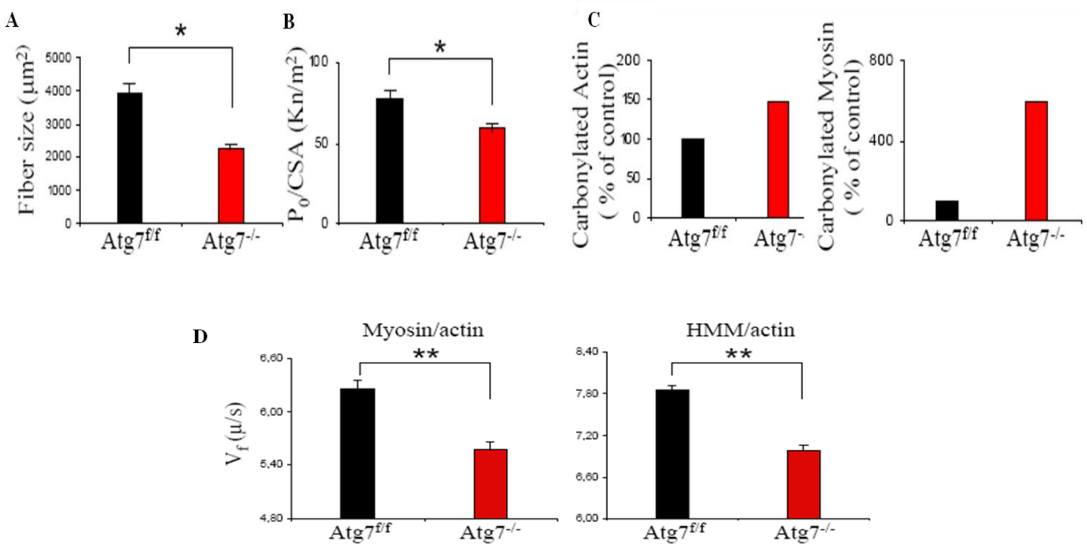

Fig. 6: (A) (B) In vitro analysis of isolated skinned muscle fibers from GCN muscles of Atg7$^{f/f}$ and Atg7$^{-/-}$. (A) Single Atg7$^{-/-}$ myofibers are more atrophic and weaker (B) than Atg7$^{f/f}$ counterpart

*(at least 20 fibers for each condition, * p<0.05). (C) Carbonylation of Actin (on the left) and Myosin (on the right) proteins, extracted from Atg7$^{f/f}$ and Atg7$^{-/-}$ GCN. Atg7$^{-/-}$ show higher carbonylation than Atg7$^{f/f}$. (D) In vitro motility assay reveals reduced actin sliding velocity (Vf) on myosin (left panel) and HMM (right panel) extracted from adult Atg7$^{-/-}$ muscles in comparison with Atg7$^{f/f}$. Reduced actin sliding velocity was statistically significant in Atg7$^{-/-}$ (n=4 per condition, *p<0.05) on both myosin and HMM*.

Since it has been demonstrated that oxidative stress might contribute to weakness and sarcopenia (Jang and Van Remmen, 2011), we wanted to test the role of oxidative stress in age-dependent muscle weakness. We treated adult animals (10 months) for four weeks with Trolox, a cell-permeable water-soluble derivative of vitamin E with general antioxidant properties. The treatment successfully reduced the amount of total carbonylation on muscle protein extracts (Figure 7A). Then, we evaluated the effect of Trolox on mitochondria functionality. Anti-oxidant treatment blocked the oligomycin-dependent mitochondrial depolarization of Atg7 knockout animals (Figure 7B). Therefore, proteomic and functional assays showed that Trolox restored a normal mitochondrial function preventing the ROS-mediated damaging events on this organelle and on contractile proteins.

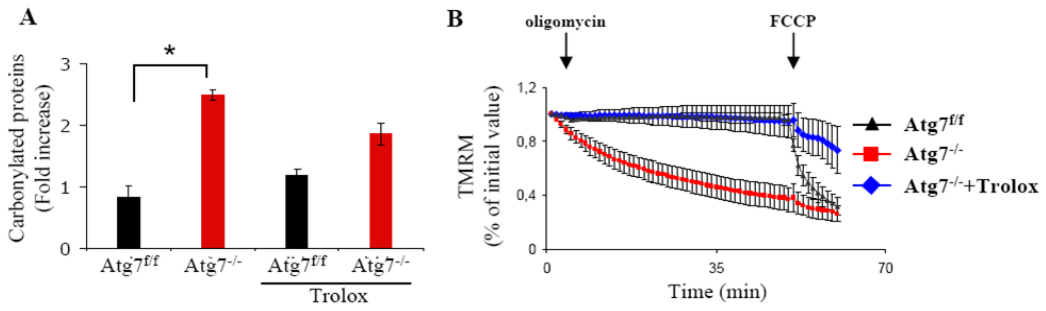

*Fig. 7: (A) Trolox treatment reduces the level of overall protein carbonylation in Atg7$^{-/-}$ muscles, thus abolishing the difference with Atg7$^{f/f}$ (n=4 mice per condition, * p<0.05). (B) Trolox treatment restores the ability of Atg7$^{-/-}$ mitochondria to maintain membrane potential (n>20 fibers per group, ** p<0.001)*

Then we asked which aspects of sarcopenia among atrophy, weakness and NMJ degeneration were affected by the blunting of oxidative stress. The treatment did not rescue myofibre size (Figure 8A) but reduced the drop of specific force in isolated Atg7-deficient myofibres (Figure 8B). Importantly, Trolox completely prevented carbonylation of purified myosin and actin (Figure 8C) and restored a normal acto-myosin interaction (Figure 8D). Concerning NMJ we found that inhibition of ROS in adult Atg7$^{-/-}$ mice only slightly reduced NMJ instability while did not ameliorate NMJ fragmentation (Figure 8E). In conclusion, these findings strongly suggest that ROS production directly affects acto-myosin interaction and force generation but shows a limited involvement on NMJ and no effect on atrophy.

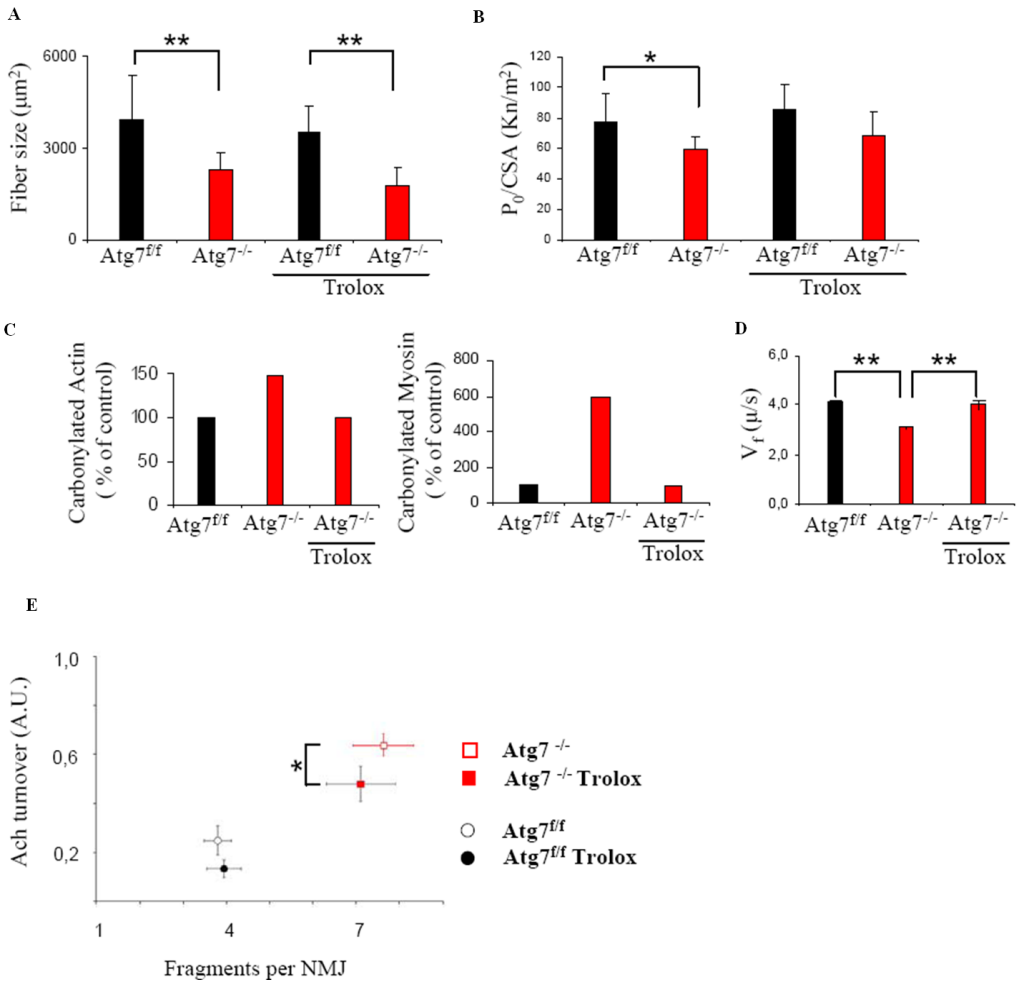

*Fig. 8: (A) Trolox treatment does not affect fiber size in both Atg7$^{f/f}$ and Atg7$^{-/-}$ muscles (n=4 mice per condition, * p<0.05). (B) In vitro isolated skinned fibers analysis: Trolox treatment*

*rescues the specific muscle force of isolated Atg7$^{-/-}$ myofibers, n=4 mice per condition, * p<0.05. (C) Trolox treatment reduces the level of actin (left panel) and myosin (right panel) protein carbonylation, in Atg7$^{-/-}$ muscles, thus abolishing the difference with Atg7$^{f/f}$ n=4 samples. (D) Trolox treatment rescues actin sliding velocity (Vf) in adult Atg7$^{-/-}$ muscles in in vitro motility assay, n=4 mice per condition, **p<0.01. (E) Confocal in vivo microscopy: Trolox treatment slightly reduces AChR turnover (data from at least 4 muscles per group, * p<0.05) but does not have any effect on NMJ fragmentation of adult Atg7$^{f/f}$ and Atg7$^{-/-}$ mice.*

3.4 AUTOPHAGY INHIBITION ALTERS THE RELEASE OF MUSCLE-DERIVED NEUROTROPHIC FACTORS

Our last findings indicate that even if oxidative stress and ROS generations contribute to precocious ageing phenotype of Atg7$^{-/-}$ mice, other factors have to be involved in NMJ degeneration. It is well known that NMJ development and maintenance is mediated by neurotrophic factors, that are either secreted by the nerve itself, or either derived from the post-synaptic muscle fibres. So we focused on the idea that, in our model, autophagy inhibition blocked the release of some factors that could be important for NMJ. For this reason we screened by qRT-PCR the expression of several factors that are important for NMJ. Since the changes of NMJ in autophagy-deficient muscles already occurred in adult mice, we looked for neurotrophins that were less expressed in both adult and aged Atg7$^{-/-}$mice. Among the different neurotrophins only Fibroblast Growth Factor Binding Protein 1 (FGFBP1) was strongly down-regulated in both adult and aged autophagy deficient mice compared with control counterpart (Figure 9A). Similarly, when we tested the levels of FGFBP1 in humans we found a significant reduction of its expression in muscle biopsies of old sedentary subjects (Figure 9B). Importantly, regular exercise partially counteracted the downregulation of FGFBP1. This data well correlate with the morphological analyses that showed denervation and atrophy in old sedentary. These features were strongly attenuated in old sportsmen (Zampieri S et al. Manuscript in press), which also showed numerous fibre type groupings, a characteristic sign of re-innervation.

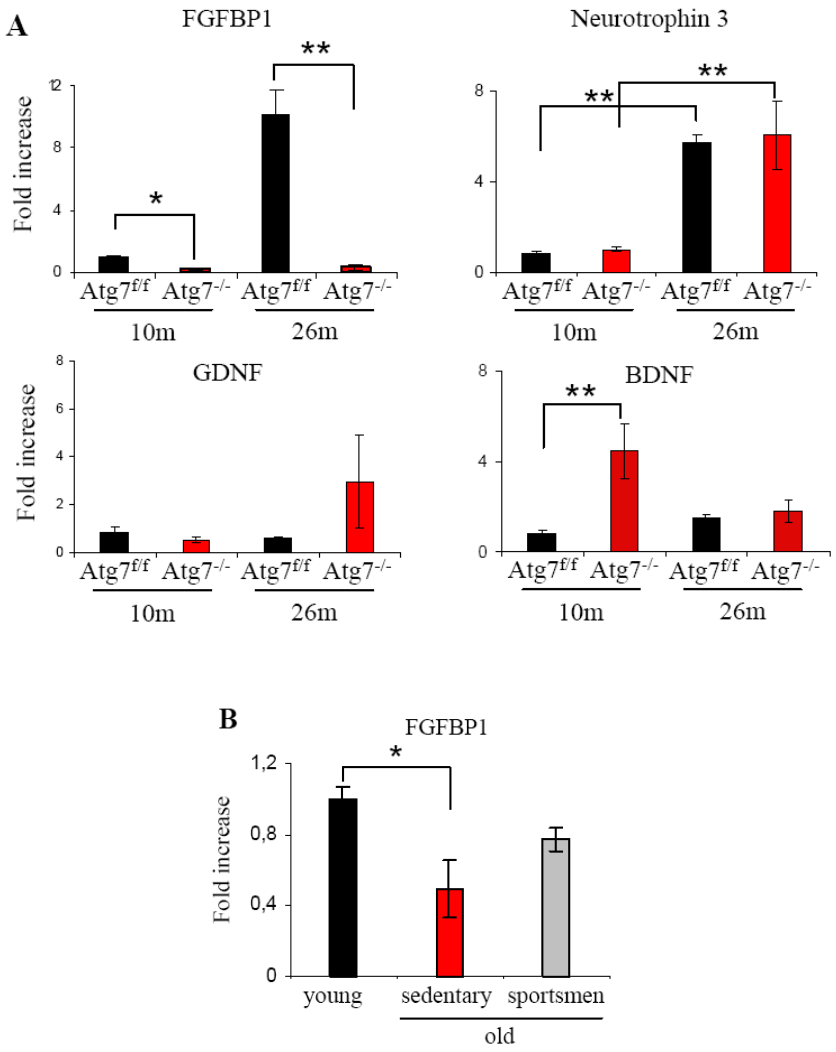

*Fig. 9: (A) qRT-PCR screening of some neurotrophic factors involved in NMJ development reveals a suppression of FGFBP1 in adult and aged Atg7$^{-/-}$ muscles (n=4 mice per condition, **p<0.01). (B) qRT-PCR of FGFBP1 in muscle biopsies of young, old sedentary and senior sportsmen, n=4 young, n=4 old sedentary and n=9 senior sportsmen, * p<0.05.*

To further get insight the role of autophagy in age-related NMJ alterations we used the inducible muscle specific Atg7 knockout mice that we have recently generated (Masiero et al., 2009). Atg7 gene was acutely deleted in 22 months old mice and mice were sacrificed 4 months later. Western blots for p62 and LC3 revealed that autophagy was successfully blocked in aged mice (Figure 10A). Then we proved that acute autophagy block was sufficient to induce an atrophic and myophatic phenotype, in fact we observed a trend concerning: reduction in fibres CSA and an

increased number of central-nucleated fibres (Figure 10B-C). Next we monitored NMJ to determine whether few months of autophagy inhibition in old mice were sufficient to destabilize muscle-nerve interaction. We found an up-regulation of MuSK and an increased number of NCAM positive fibres (Figure 10D-E). qRT-PCR revealed a suppression of FGFBP1 in muscles of inducible Atg7$^{-/-}$ (Figure 10D right panel). Importantly, acute inhibition of autophagy in aged mice caused a significant loss of MuSK on the myofiber plasma membrane and a concomitant enrichment of internalised MuSK protein (Figure 10F).

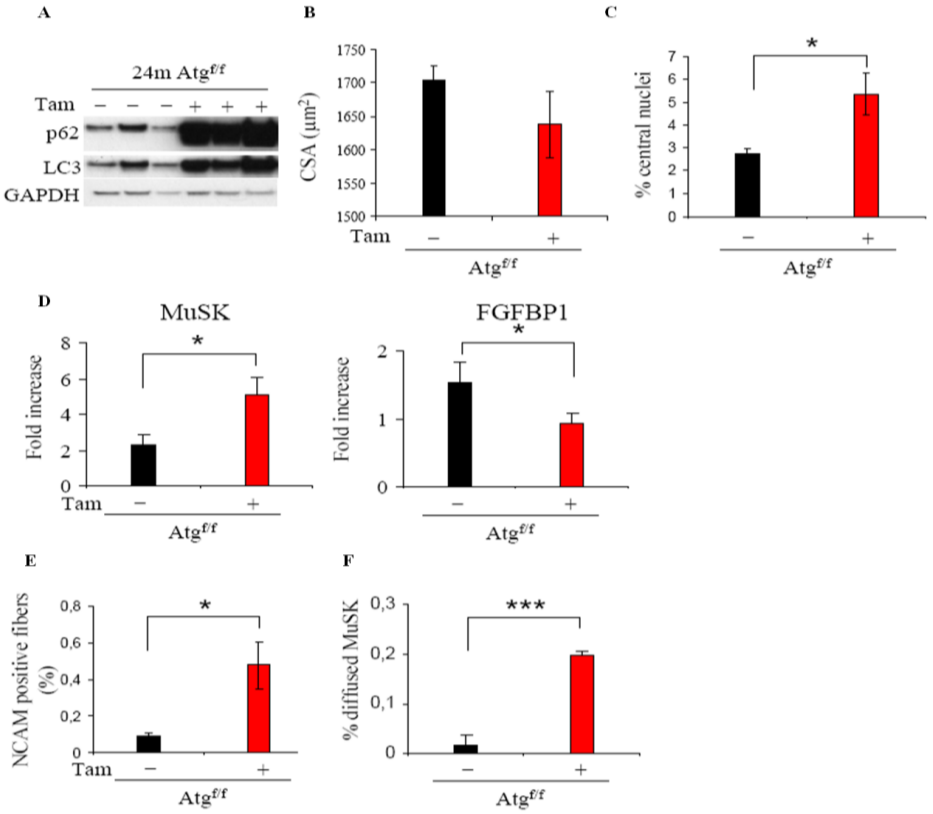

*Fig. 10: (A) Immunoblotting for Atg7, LC3 and p62 proteins on muscle extracts from 24 months old inducible Atg7$^{-/-}$ female mice. Three months after the tamoxifen treatment, skeletal muscles were collected and analysed. (B) Acute inhibition of autophagy in old mice induces muscle degeneration. Quantification of CSA of myofibers in TA muscles of aged inducible Atg7$^{-/-}$ and Atg7$^{f/f}$ mice. Values are mean +/- s.e.m., at least 5 muscles per group were analysed, *p<0.05. (C) Quantification of center-nucleated myofibers in TA of inducible Atg7$^{-/-}$. (n> 5 for each group, **p<0.01).(D) Expression levels of MuSK (left) and FGFBP1 (right) after acute inhibition of Atg7 in old mice. MuSK is up-regulated while FGFBP1 is down-regulated in aged inducible Atg7$^{-/-}$*

*muscles (*p<0.05, n>5). (E) Quantification of NCAM-positive fibers. Values were normalized for the total number of myofibers in muscle section (at least 5 muscles per group were analysed, *p<0.05). Acute inhibition of Atg7 in aged female mice increases the number of denervated N-CAM positive fibers when compared to age-matched controls (at least 4 muscles per group were analysed, *p<0.05). (F) Acute inhibition of autophagy in aged mice led to an increased amount of diffused MuSK staining; at least 4 muscles per group were analysed ***p<0.001.*

The next step was to understand the role of FGFBP1. FGFBP1 is a secreted factor that interacts and potentiates the bioactivity of FGF-7, FGF-10, and FGF-22 family members. Because FGF-7, FGF-10, and FGF-22 are muscle-derived regulators that promote pre-synaptic differentiation at the NMJ (Jang and Van Remmen, 2011; Williams et al., 2009), we hypothesized that alterations of FGFBP1 expression might affect NMJ maintenance. To address this point we performed both loss and gain of function approaches. First we mimicked autophagy-deficient muscle by knocking down FGFBP1 in adult muscles of control mice. Four different shRNAs were tested to specifically reduce FGFBP1 protein levels. C2C12 cell were transfected for 24 hours with the different oligos, and then western blot was performed on C2C12 protein extract. Two of them efficiently knocked down FGFBP1 (Figure 11A). For *in vivo* transfection experiments we used bicistronic vectors that simultaneously encode shRNAs and GFP. Therefore, detection of GFP fluorescence allows us to monitor the efficiency of transfection and the changes that occur on NMJ of transfected fibres. We then monitored that oligos 3 efficiently reduced *FGFBP1* transcript *in vivo*, also on isolated single fibres (Figure 11B).

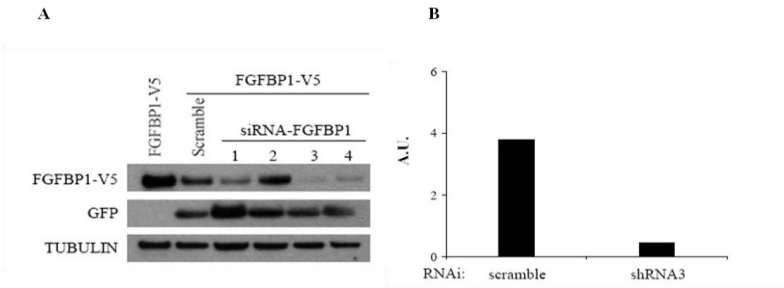

Fig. 11: (A) Four different shRNAs were tested against FGFBP1 expression. Western blot of C2C12 protein extract revealed that shRNA 3 and 4 successfully blocked FGFBP1 expression.(B) In vivo transfection of FDB fibers confermed that oligo 3 was able to reduce FGFBP1 expression.

We then transfected shRNAs into adult TA muscles for two weeks. In order to evaluate NMJ morphology and stability, after 4 days from transfection we injected α-bungarotoxin (BGT) coupled to AlexaFluor647 to label old acetylcholine receptors and 10 days later we injected BGTAF555 to label new receptors. After 14 days from transfection old receptors, new receptors, and synapse morphologies were monitored using confocal *in vivo* microscopy. Interestingly, knockdown of FGFBP1 *in vivo* induced significant changes in NMJ morphology, increasing NMJ instability and fragmentation (Figure 12A). Similar to Atg7$^{-/-}$, AChR clusters were fragmented and showed a higher turnover than those in myofibres expressing scramble oligos. Moreover, we quantified the number of NCAM positive fibres and it was significantly increased in muscles where FGFBP1 was down-regulated (Figure 12B).

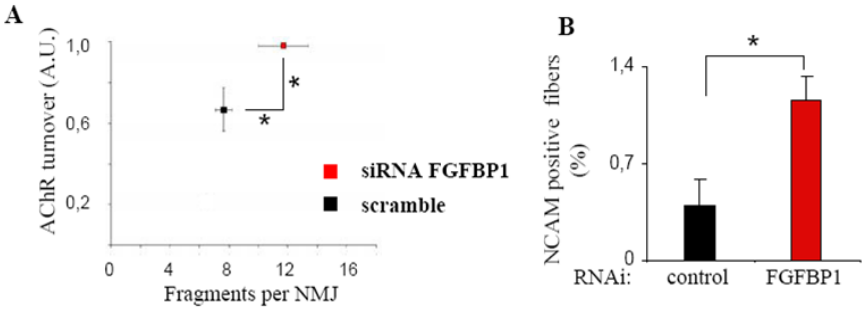

*Fig. 12: (A) AChR turnover and NMJ fragmentation increase in control mice transfected with shRNA-3 against FGFBP1, * p<0.05. (B) Quantification of NCAM-positive fibers in control and in FGFBP1 knocked down fibers. Values were normalized for the total number of myofibers in muscle section (n=9 muscles per group were analysed, *p<0.05)*

Then we decided to rescue FGFBP1 expression in Atg7$^{-/-}$ mice and monitor whether this could reduce the changes in NMJ and the number of denervated fibres. Adult TA muscles of Atg7$^{-/-}$ and control mice were co-transfected with vectors encoding FGFBP1 and GFP. Over-expression of FGFBP1 in autophagy-deficient muscle significantly reduced to control level the number of NCAM-positive fibres as the level of AChR turnover (Figure 13A-C). Moreover, MuSK localization was ameliorated after FGFBP1 over-expression (Figure 13D), suggesting that FGFBP1 elicited a protective action on NMJ.

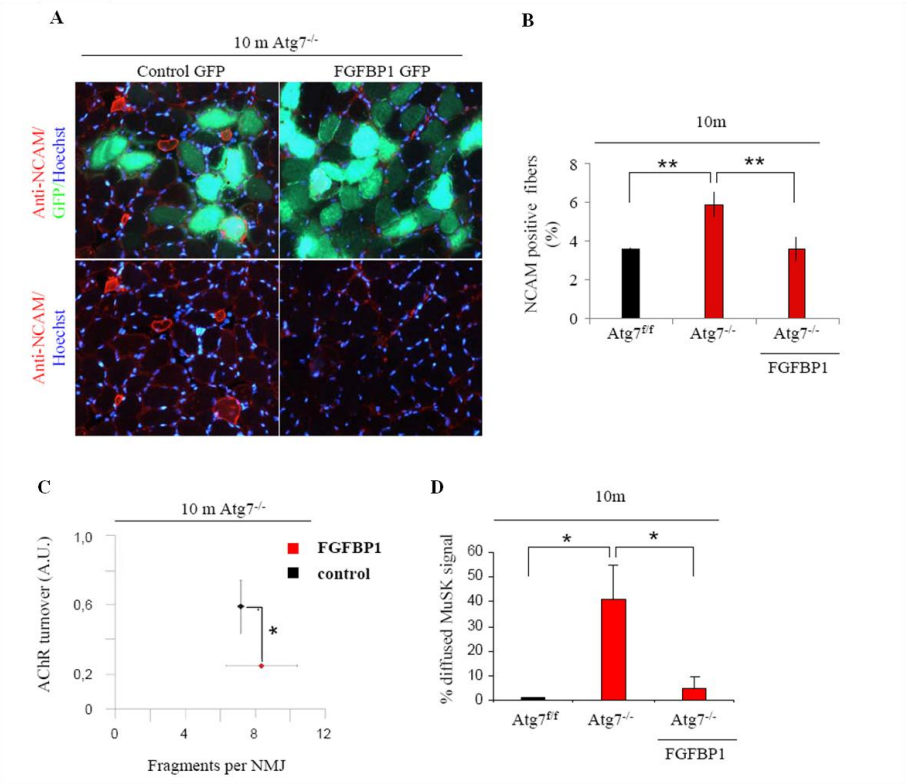

*Fig. 13: (A) Overexpression of FGFBP1in Atg7$^{-/-}$ reduces the number of NCAM positive fibers. Muscles of Atg7 $^{f/f}$ and Atg7 $^{-/-}$ were co-transfected in vivo with plasmids coding for FGFBP1 and GFP (green); fourteen days later NCAM expression (red) was evaluated. (B)The number of N-CAM positive fibers was quantified and normalized with the total number of myofibers per muscle section (at least four muscle for each condition have been analysed. ** p>0.001). (C) Confocal in vivo microscopy: FGFBP1 expression for two weeks greatly reduces AChR turnover (* p<0.05) but does not ameliorate NMJ fragmentation of Atg7$^{-/-}$ mice. (D) Expression of FGFBP1 in Atg7$^{-/-}$ significantly restored normal MuSK localization; n=4 Atg7$^{f/f}$ and n=16 Atg7$^{-/-}$ muscles per group were analysed *p<0.05.*

Therefore, FGFBP1 is a muscle-derived synaptic organizing factor that is required for NMJ maintenance.

3.5 DEFINING THE LINK BETWEEN AUTOPHAGY INHIBITION AND FGFBP1 ALTERATION

Since MuSK is a critical kinase that affects pathways involved in NMJ stability and since autophagy impairment resulted in abnormal internalization of AChR and MuSK, we reasoned that the downregulation of FGFBP1 is a consequence of MuSK inhibition. To mimic such situation we knocked down MuSK in adult tibialis anterior (TA) muscles, *in vivo,* and monitored FGFBP1 expression. We designed functional shRNAs against MuSK and transfected them *in vivo* for fourteen days. We confirmed a significant reduction of MuSK that led to downregulation of FGFBP1 (Figure 14A). Consistent to the data of FGFBP1 downregulation, acute inhibition of MuSK in adult control mice caused a significant increase of denervated NCAM-positive fibers (Figure 14B). These results indicated that MuSK impairment determines the suppression of FGFBP1 expression causing NMJ instability and myofiber denervation.

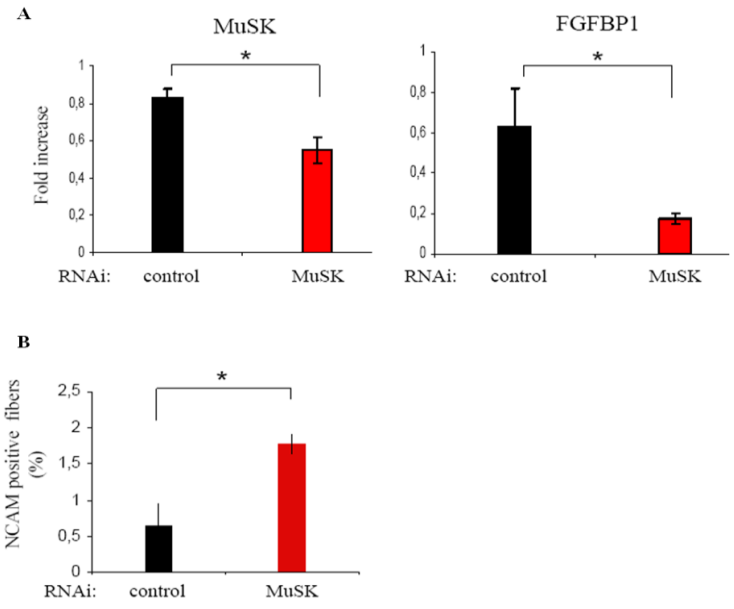

*Fig. 14: (A) qRT-PCR of MuSK in TA muscles transfected with shRNA against MuSK or scramble. MuSK was efficiently downregulated (at least 3 muscles per condition were analysed, *p<0.05). qRT-PCR of FGFBP1 in TA muscles that were transfected with shRNAs against MuSK or*

*scramble (at least 3 muscles per condition were analyzed, *p<0.05). (B) Knockdown of MuSK increases the number of denervated N-CAM positive fibers when compared to age-matched controls (at least 3 muscles per group were analysed, *p<0.05).*

PART II

3.6 AUTOPHAGY IS NOT REQUIRED TO SUSTAIN CONTRACTIONS DURING PHYSICAL ACTIVITY

Physical activity has been demonstrated to improve glucose and lipid homeostasis, maintain muscle mass and delay ageing. Moreover it has been reported that autophagy is activated upon exercise, but is still unclear whether the beneficial effects of exercise are due to autophagy induction. For this reason it is essential to define the link between autophagy and exercise. Previous works have reported controversial data, so it would be very important clarify the role of specific skeletal muscle autophagy during physical activity.

To address the role of skeletal muscle autophagy during physical activity we acutely deleted the Atg7 gene in adult animals (3 months old and sacrificed at 7 months) by treating inducible muscle-specific Atg7 knockout mice with tamoxifen ($Atg7HSA^{-/-}$) (Masiero et al., 2009). This inducible model was used in order to minimize the chance of any adaptations and compensations that occur with constitutive or conditional deletion of genes embryonically or at a very young age. First, we verified by western blot that block of autophagy had occurred, indeed after Tamoxifen treatment both p62 and non lipidated form of LC3 (LC3-I) did accumulate.

In order to investigate whether the acute block of autophagy in muscle affects exercise performance, control and inducible $Atg7^{-/-}$ mice performed exercise on a treadmill. We used a standard concentric exercise protocol while monitoring the maximum distance ran to exhaustion. Surprisingly, we did not find any significant difference in running capacity between controls and $Atg7^{-/-}$. Even looking at gender specific results, no differences were revealed between the $Atg7^{f/f}$ and $Atg7^{-/-}$ (Figure

15), suggesting that autophagy is not required to sustain muscle contraction during physical activity.

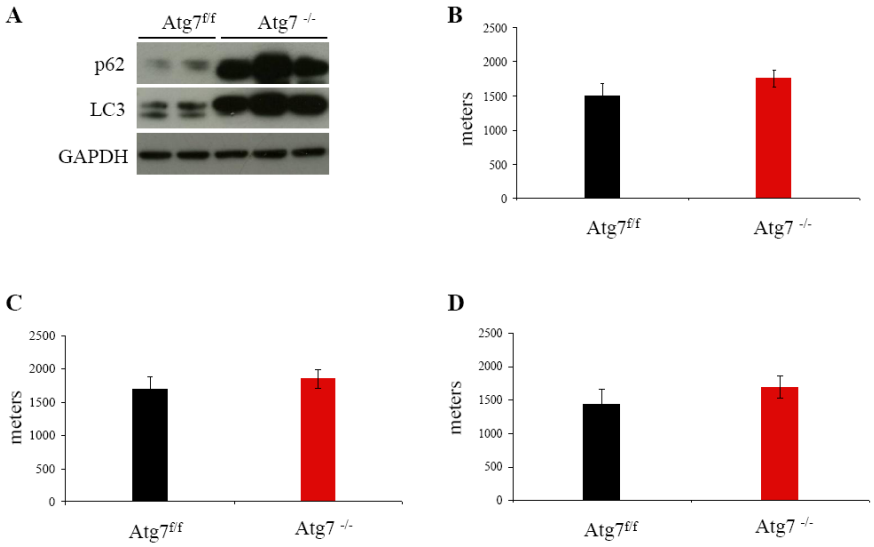

*Fig. 15: (A) Representative western blot analyse, it confirmed p62 and LC3-I accumulation in Atg7$^{-/-}$ after Tamoxifen treatment. (B) No differences observed in the maximal running distance during concentric exercise between control and Atg7$^{-/-}$(at least 10 mice per group were analysed, *p<0.05); this result was confirmed evaluating also the gender-specific issue, thus females (C) and males (D).*

3.7 AUTOPHAGY IS IMPORTANT TO SUSTAIN PHYSICAL ACTIVITY THAT PROVOKE DAMAGING CONTRACTIONS

Since autophagy is important for effective protein and organelle turnover as well as for survival under cellular stress, we tested whether autophagy could have a role in repairing muscle after damaging contraction. To address this, we performed a downhill running exercise to induce damaging eccentric contraction in Atg7$^{f/f}$ and Atg7$^{-/-}$ animals while recording maximal running distance achieved.

We confirmed that autophagy was induced upon exercise in control animals, as indicated by the lipidation of LC3 and a decrease in p62 in the muscle of Atg7$^{f/f}$. Conversely, Atg7$^{-/-}$ maintained their high levels of LC3-I and p62 protein, confirming the efficient inhibition of autophagy (Figure 16A).

On average autophagy-deficient mice ran less than wild type. However, when we took gender into consideration we found that Atg7 deficient females but not males ran less than their wild type counterparts (Figure 16B). Next, we investigated whether this result was maintained after prolonged physical activity, that induce an additive detrimental effect on muscle performance, as a consequence of cumulative damage. So, control and Atg7$^{-/-}$ mice performed repeated bouts of eccentric exercise to exhaustion for three consecutive days, that generate damaging eccentric contraction. As expected, both genotypes performed progressively worse over time (Figure 16C). However, autophagy-deficient females ran less than their littermate controls on all three days of exercise.

Next, we focused on the reason of this reduced performance, so we looked first at morphological alterations. H&E did not reveal any structural impairment or inflammation (Figure 16D). To assess whether eccentric contraction had caused damage to plasma membranes we stained myofibres for serum immunoglobulins. However, we did not find any positive staining inside myofibres, confirming that plasma membrane integrity was retained after eccentric contraction in both genotypes (Figure 16E), thus suggesting that autophagy knockout weakness was not due to major structural alterations.

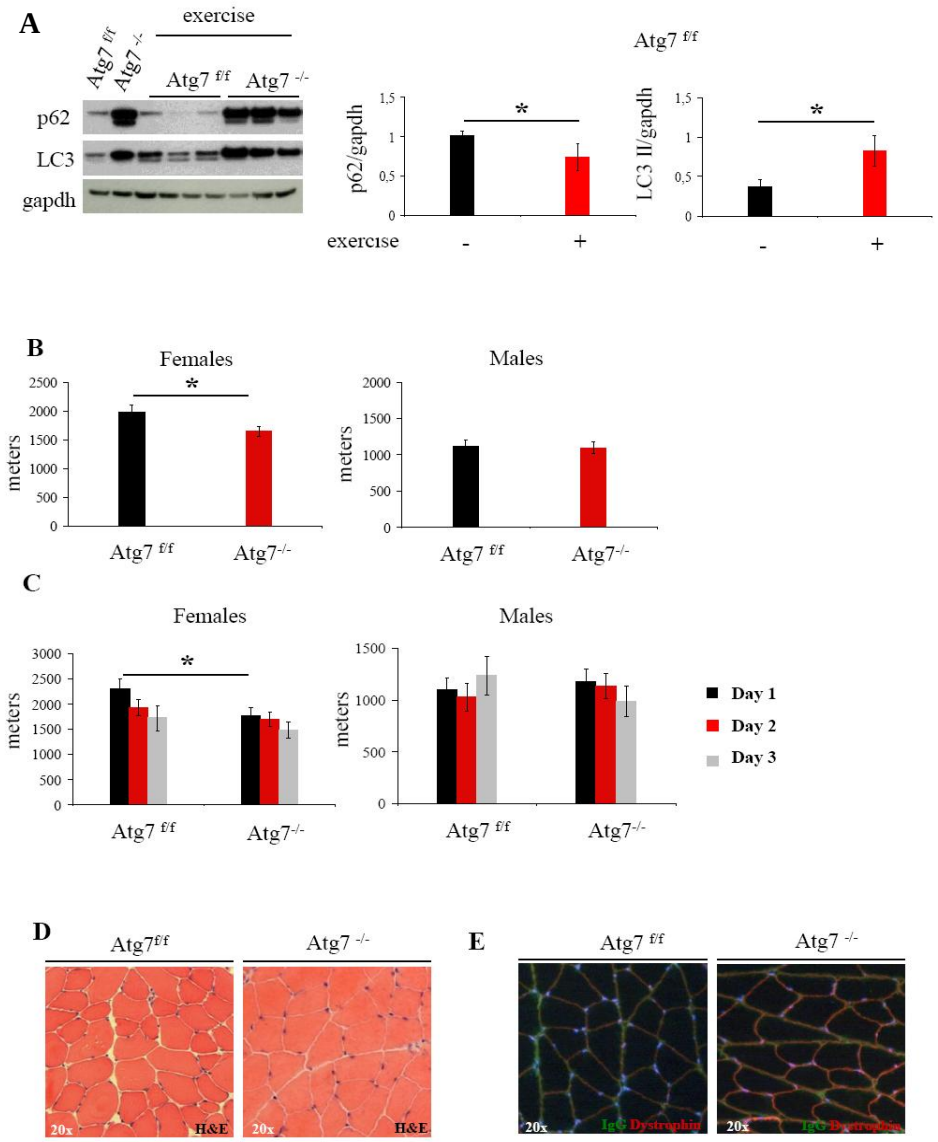

*Fig. 16: (A) A representative western blot showed decrease of p62 and increase of LC3-II upon exercise in control animals, quantification analyses are reported on the right (n>5 for each group) , moreover the same western blot confirmed p62 and LC3-I accumulation in Atg7$^{-/-}$ after Tamoxifen treatment. (B) Maximal running distance during eccentric exercise between control and Atg7$^{-/-}$ (at least 10 mice per group were analysed, *p<0.05), Atg7$^{-/-}$ females (on the left) run significantly less than controls, no differences observed between males (on the right; (C) Maximal running distance reported for each day of exercise, both genotypes performed progressively worse over time. (D-E) H&E and IgG staining did not reveal any structural impairment or inflammation.*

3.8 AUTOPHAGY IS NOT REQUIRED FOR AMPK ACTIVATION AND FOR EXERCISE-MEDIATED GLUCOSE UPTAKE

It has been reported that exercise-induced autophagy plays a critical role in AMPK activation and glucose homeostasis. It is therefore conceivable that the energy imbalance caused by exercise may explain the exercise intolerance observed in autophagy-deficient females. We monitored phosphorylation the level of AMPK and its direct downstream target ACC but no significant differences were observed between Atg7$^{f/f}$ and Atg7$^{-/-}$ (Figure 17).

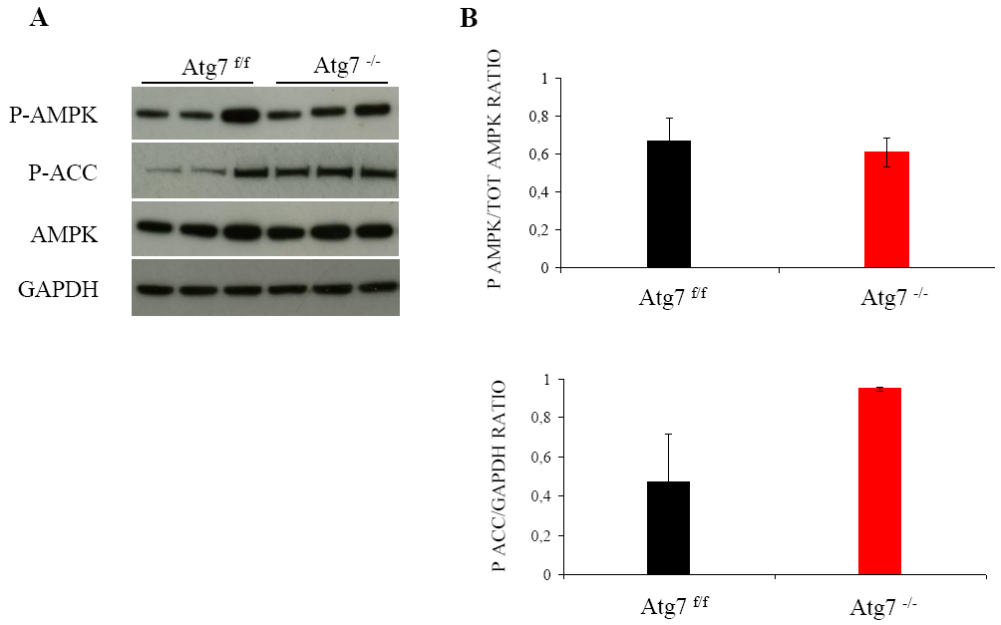

Fig. 17: (A) A representative western blot showed no differences in P-AMPK and P-ACC between control and Atg7$^{-/-}$ after exercise. (B) Quantification analyses are reported as ratio between P-AMPK/Total-AMPK and P-ACC/GAPDH (n=4 for each group).

To further investigate the presence of a possible energy imbalance, we measured blood levels of glucose and lactate in males (Figure 18A) and females (Figure 18B). After exercise, blood glucose was reduced along with a concomitant increase in blood lactate. Interestingly this metabolic profile was unaltered by the block in autophagy, as free fatty acid and cheton bodies content.

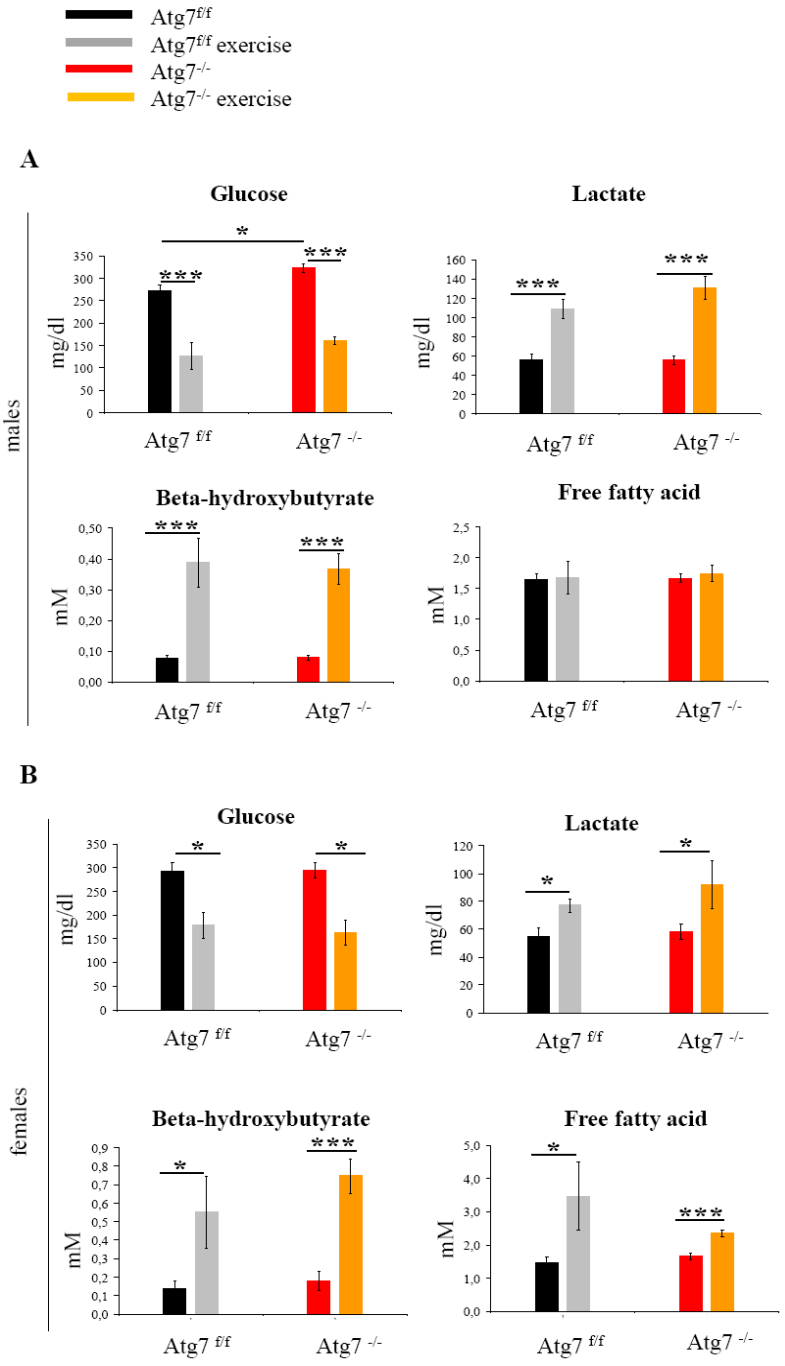

*Fig. 18: Blood metabolites levels quantification in females (A) and males (B), no major differences were observed between controls and Atg7$^{-/-}$ before and after exercise (n>5 for each group, *p<0.05, ***p<0.001).*

Accordingly, we did not find any significant changes in Glut4 expression or localization in Atg7$^{-/-}$ myofibres (data not shown) when compared to controls. Moreover, PAS and OIL RED staining did not reveal any glycogen or lipid accumulation in Atg7$^{-/-}$ mice (data not shown).

Altogether, these data suggest that muscle autophagy is not required for metabolic regulation during exercise, being unaltered both AMPK activation as well as glucose and lipid utilization.

3.9 AUTOPHAGY IS IMPORTANT TO PREVENT ACCUMULATION OF DYSFUNCTIONAL MITOCHONDRIA DURING DAMAGING CONTRACTION

Since autophagy is important for organelle quality control, we tested whether mitochondrial homeostasis was altered in wild type and autophagy deficient animals following exercise. Interestingly, flexor digitorum brevis (FDB) myofibers isolated from Atg7$^{-/-}$ showed a significant increase in depolarized mitochondria following treatment with the F_1F_0-ATPase blocker, oligomycin (Figure 19A). Interestingly, while eccentric exercise did not affect mitochondrial membrane potential in wild type animals, it exacerbated the percentage of depolarised fibres in Atg7$^{-/-}$ mice (Figure 19B, C). These alterations in mitochondrial membrane potential correlated with the impairment in physical performance.

Males lacking autophagy also demonstrated an increase in the number of fibres with depolarized mitochondria, however, to a lesser extent than females. Eccentric exercise did not alter the ability of Atg7$^{f/f}$ mitochondria to respond to exercise and indeed their mitochondria showed a slight hyperpolarization immediately after exercise which was completely restored to normal 3 days later (data not shown).

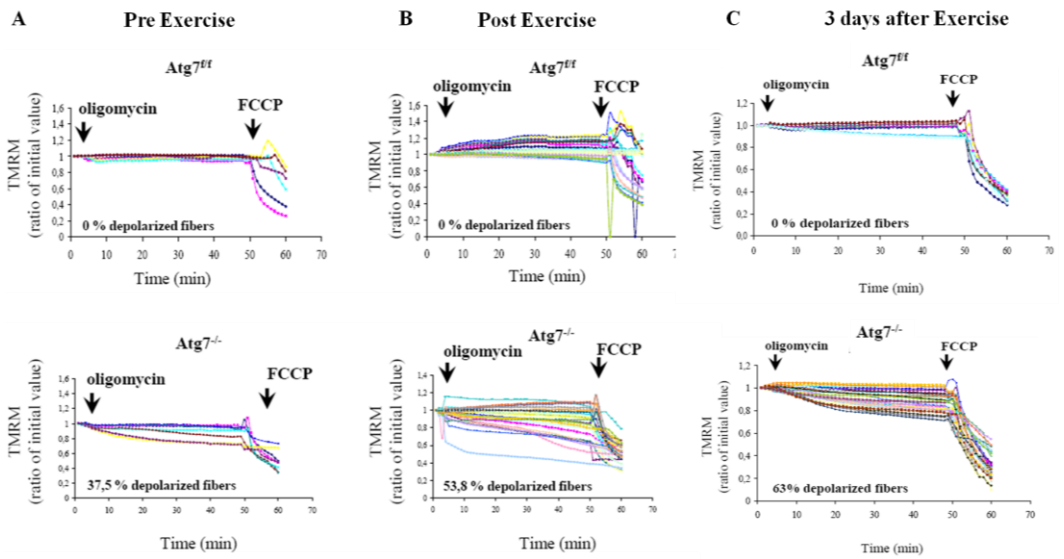

Fig. 19: Mitochondria membrane potential measurements in control and Atg7$^{-/-}$ females: before exercise (A), immediately after exercise (B), three days after exercise (C). While mitochondria of control mice are able to maintain their functionality upon exercise, Atg7$^{-/-}$ dissipate the potential, worsening the percentage of depolarized fibres with time (n>10 fibres for each group).

During contraction, skeletal muscle is a major source of ROS, as well as one of the main targets (Powers and Jackson, 2008). Since mitochondria are the main source and effectors of ROS in the cell it is feasible that oxidative stress may play a role in the observed results. Therefore, we measured total protein carbonylation in exercised muscles. As expected, Atg7 null muscles showed more carbonylated proteins than exercise-matched controls (Figure 20A).

To further investigate the source of ROS in these mice we used a mitochondrial targeted ROS-sensor (Dooley et al., 2004). The sensor was transfected in adult FDB muscles and 7 days later mice were exercised and sacrificed. FDB fibres were isolated and fluorescence changes were monitored and quantified. Atg7$^{-/-}$ mice produced more ROS compared to controls and this increase become significant after exercise (Figure 20B). Moreover, it is interesting to underline that after exercise ROS level in control mice was similar to the level present in Atg7$^{-/-}$ mice before exercise.

This result confirmed that dysfunctional mitochondria are the source of ROS that generate an oxidative stress in Atg7$^{-/-}$.

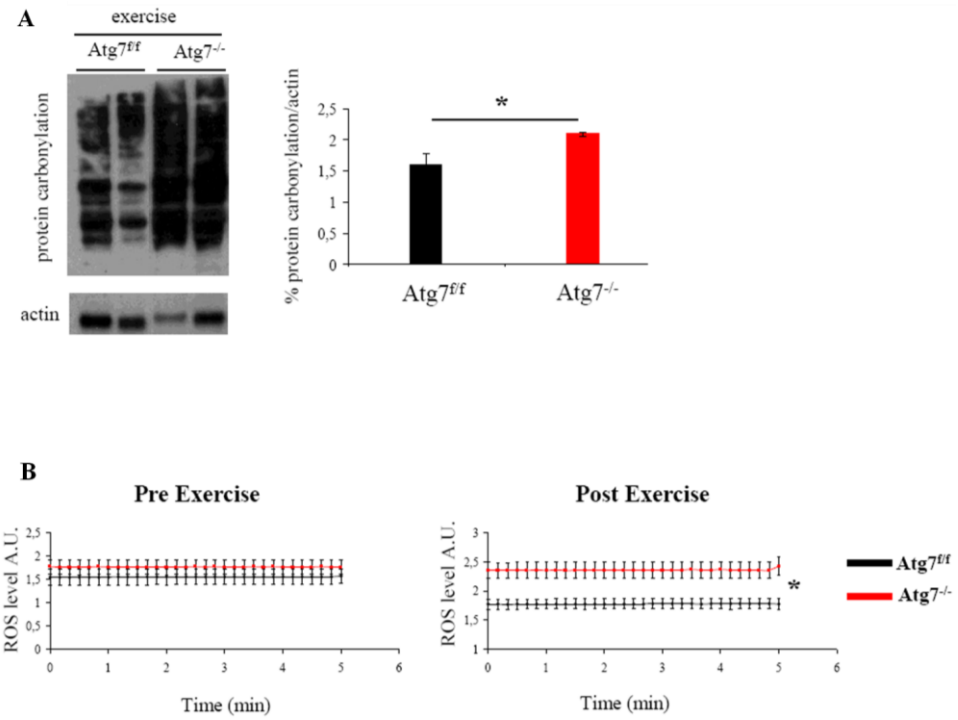

*Fig. 20: (A) Oxiblot analysis showed an increased level of carbonylated proteins in Atg7$^{-/-}$ compared to controls, as confirmed by quantification analyses (on the right. (B) ROS production measurements supported the evidence that in Atg7$^{-/-}$ there is an high ongoing oxidative stress compared to control mice and this difference increases after exercise. (n=5 for each group *p<0.05).*

Therefore, acute inhibition of autophagy led to accumulation of dysfunctional mitochondria, increased oxidative stress and reduced physical performance during eccentric contraction.

3.10 ANTI-OXIDANT TREATMENT DID NOT AMELIORATE THE PHYSICAL PERFORMANCE OF ATG7 KNOCKOUT BUT BLOCKED AUTOPHAGY IN CONTROLS WORSENING MITOCHONDRIAL FUNCTION AND RUNNING CAPACITY

Excessive oxidative stress has been documented to impair muscle function, which could potentially explain the reduced physical performance of Atg7$^{-/-}$ mice. (Peternelj and Coombes, 2011; Powers and Jackson, 2008).

In order to evaluate whether reducing oxidative stress could ameliorate their physical performance, we treated female Atg7$^{-/-}$ and control mice with the antioxidant N-Acetyl-Cysteine (NAC) for 6 weeks. and then subjected them to eccentric exercise. Surprisingly, NAC treatment severely impaired performance of control but did not elicit any benefit in inducible Atg7$^{-/-}$ mice (Figure 21). Indeed, the difference in the running distance between control and Atg7$^{-/-}$ mice was abolished at both one and three days of exercise.

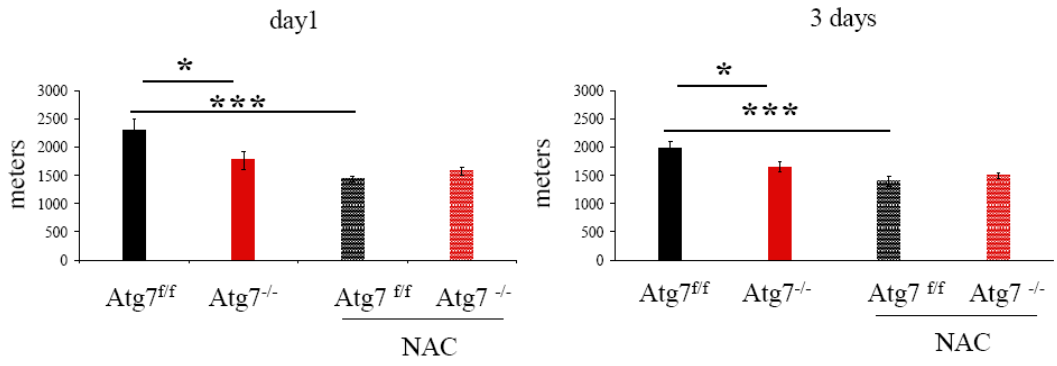

*Fig. 21: The maximal running distance of females control mice decreased after NAC treatment from the first day (on the left) till the end (on the right) of the protocol. No difference between maximal running distance between control and Atg7$^{-/-}$ mice (n>5 for each group *p<0.05, ***p<0.001).*

We first checked whether NAC treatment affected general protein carbonylation. The level of carbonylated proteins was reduced both in control and Atg7$^{-/-}$ mice after

the treatment, suggesting that NAC preserved control mice from ROS and reduced the ongoing oxidative stress present in Atg7$^{-/-}$ mice (Figure 22).

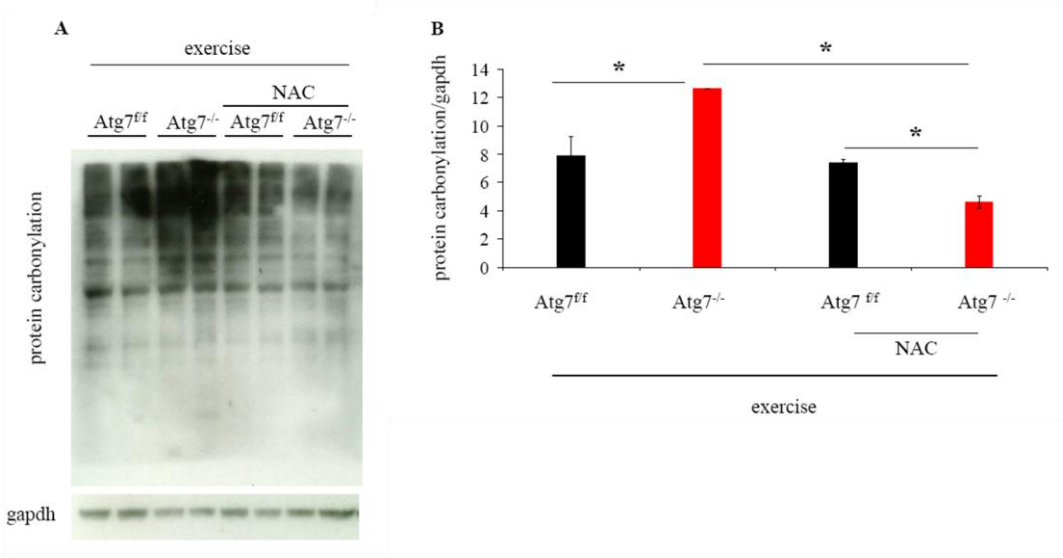

*Fig. 22: (A) Oxiblot analysis showed an increased level of carbonylated proteins in Atg7$^{-/-}$ compared to controls, as confirmed by quantification analyses (B). Oxidative stress was significantly reduced in Atg7$^{-/-}$ mice after NAC treatment (n=3 for each group, *p<0.05).*

Then, we wanted to further investigate the unexpected effect of NAC in control mice, so we monitored mitochondrial function in control mice before and after exercise. Interestingly, NAC treatment resulted in impaired ability to retain mitochondrial membrane potential in controls (Figure 23). In fact, NAC treated control mice exhibited a percentage of depolarized fibres prior to exercise that was similar to that of Atg7$^{-/-}$ mice (Figure 23A). Interestingly, exercise slightly reduced the amount of fibres with abnormal mitochondria from 62,5% to 42,1%. Therefore, exercise appears to have differential effects on mitochondrial membrane potential, where it exacerbates depolarization in Atg7$^{-/-}$ (compare with figure 19B), while improving that of NAC treated Atg7$^{f/f}$, respectively (Figure 23B).

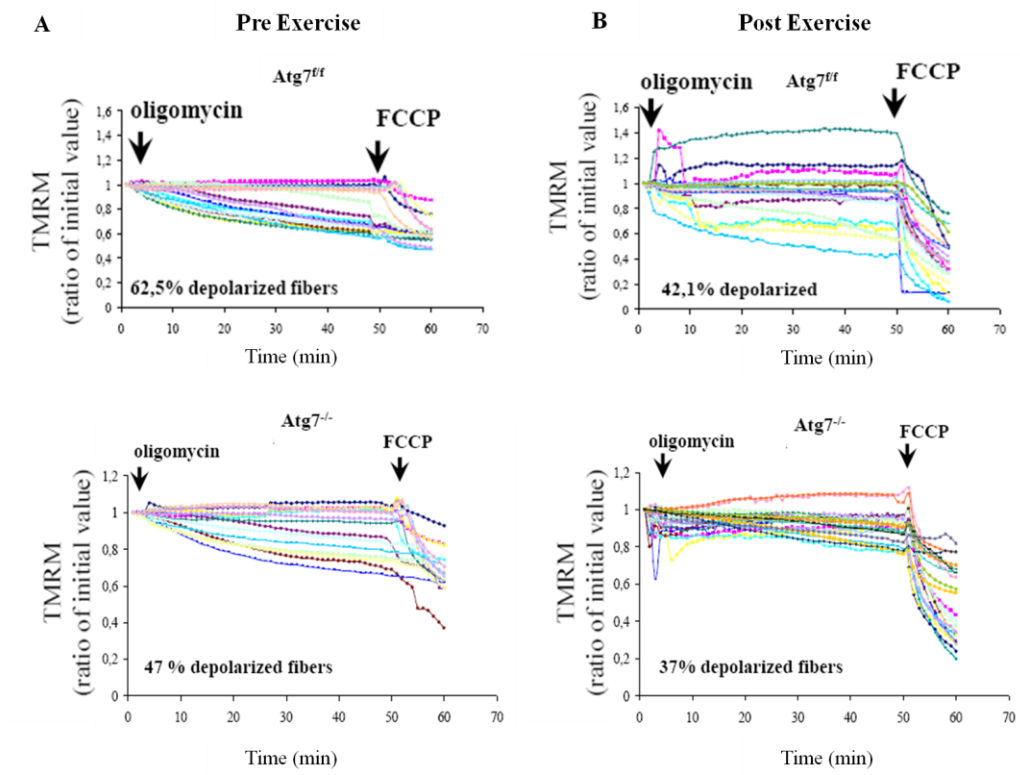

Fig. 23: Mitochondria membrane potential analyses after NAC treatment, before (A)and after (B) exercise. (n>15 fibres for each group). After NAC treatment, control and Atg7$^{-/-}$ mice showed similar level of depolarized fibres, that ameliorates after exercise in both conditions.

For this reason we further investigated the signalling events mediating this seemingly differential regulation.

We confirmed that even if AMPK is heavily implicated in exercise autophagy and mitochondrial regulation, in this case it is not the metabolic link. In fact, we observed no difference in exercise triggered AMPK and ACC phosphorylation between control and inducible Atg7$^{-/-}$ mice, indicating that AMPK is not responsible for the alteration in mitochondrial function reported (Figure 24).

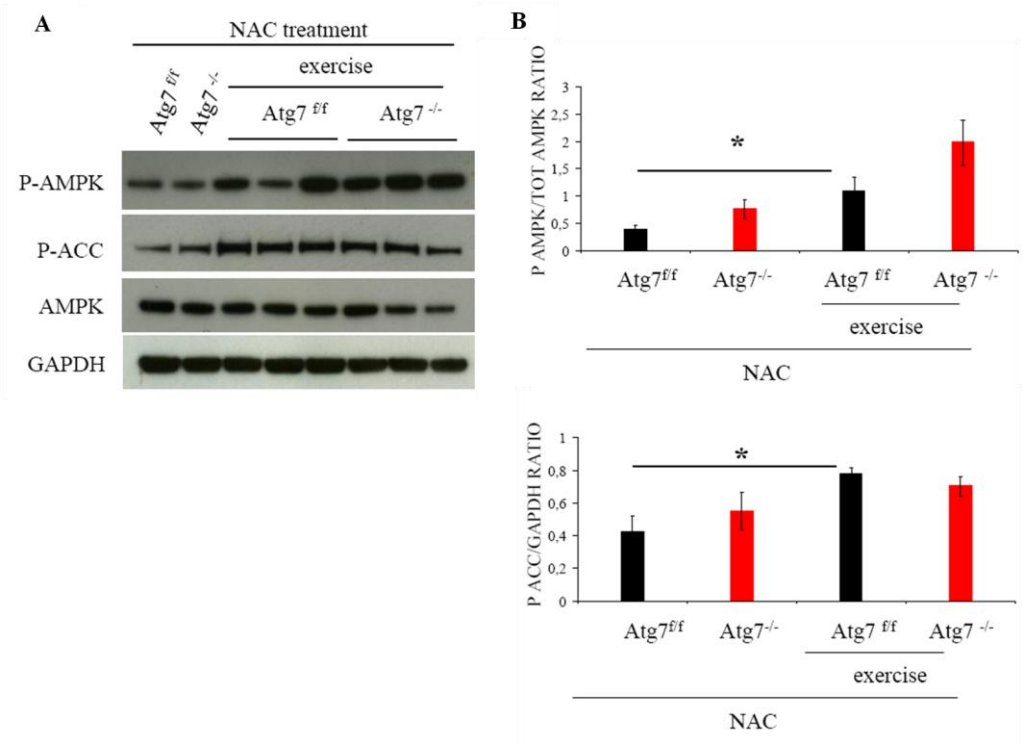

*Fig. 24: (A) Representative western blot and quantification analyses (B) of phosphorylation levels of AMPK and ACC confirmed that there are no major differences between control and Atg7$^{-/-}$ mice, upon exercise, after NAC treatment (n=5 for each group, *p<0.05).*

We finished the metabolic analyses evaluating blood metabolites after NAC in both control and Atg7$^{-/-}$ mice, but again we did not observe significant changes between genotypes before and after exercise (data not shown), confirming that this is not a metabolic issue.

In order to further investigate this point we tested a different anti-oxidant, called Mito-TEMPO, that acts specifically on mitochondria. Control and Atg7$^{-/-}$ mice were treated with Mito-TEMPO for 7 days and then performed the same protocol of 3 days eccentric exercise.

Analyzing the maximal distance run, we obtained the same results observed with the previous treatment with NAC. Also in this case, Mito-TEMPO treated control mice run less than no treated mice, showing similar distance than Atg7$^{-/-}$ mice treated with Mito-TEMPO (Figure 25).

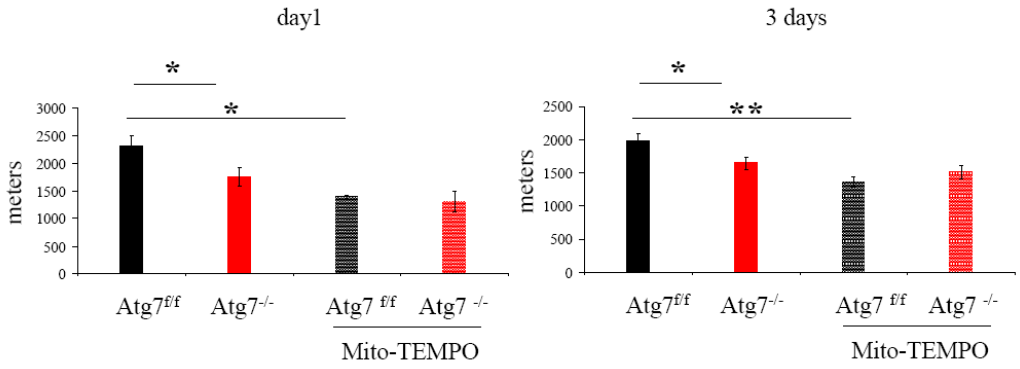

*Fig. 25: The maximal running distance of females control mice decreased after NAC treatment from the first day (on the left) till the end (on the right) of the protocol. No difference between maximal running distance between treated control and Atg7$^{-/-}$ mice (n>3 for each group, *p<0.05, **p<0.01).*

Moreover, we analyzed mitochondria functionality and found that again mitochondria of control mice treated with Mito-TEMPO were dysfunctional in basal condition, as the Atg7$^{-/-}$ mice (Figure 26).

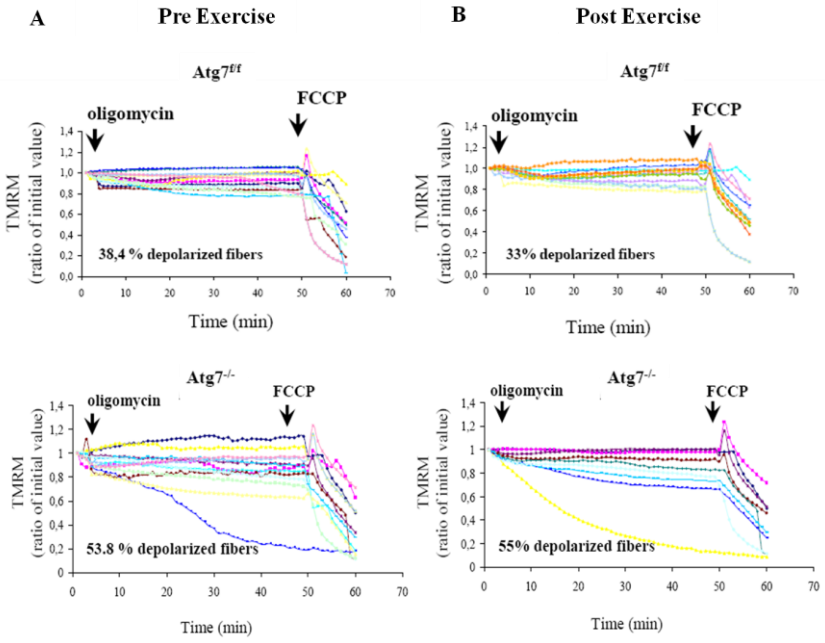

Fig. 26: Mitochondria membrane potential analyses after Mito-TEMPO treatment, before (A) and after (B) exercise. After Mito-TEMPO treatment, control and Atg7$^{-/-}$ mice showed similar

level of depolarized fibres, that ameliorates after exercise in both conditions (n>15 fibres for each group).

At this point we focused on the common results found with different anti-oxidant to understand the reduced performance of control treated mice.

It has been reported that treatment with anti-oxidant, such as NAC, impairs basal autophagy process in control animals (Underwood et al., 2010), so we wondered whether the reduced physical performance of NAC treated control mice was due to an impaired autophagy activation.

We monitored LC3 lipidation, as the major marker of autophagy, and the level of p62 protein in control and treated mice, before and after exercise. We observed that NAC treated control mice display a reduced LC3-II level, both in basal condition and upon exercise, compared to no treated control mice (Figure 27A-B). Moreover, p62 accumulates in NAC treated control mice in basal condition, indicating that NAC treatment reduced autophagy (Figure 27C). Upon exercise, we observed reduced level of p62, both in no treated and treated control mice, suggesting that exercise promotes autophagy induction even if it is reduced by NAC treatment.

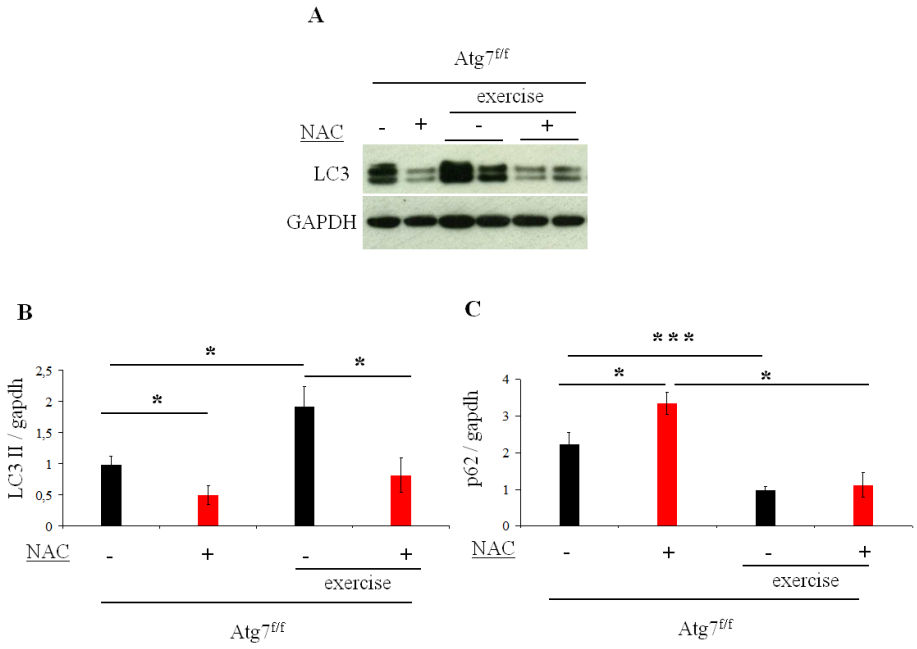

*Fig. 27: Representative western blot(A) and quantification analyses of LC3-II (B) and p62 (C) in no- and NAC treated control mice, before and after exercise. NAC treatment causes autophagy reduction (n=5 for each group, *p<0.05, ***p<0.001).*

These findings suggest that impaired physical performance of NAC treated control mice was due to a reduction in autophagy process, mediated by NAC treatment.

Altogether, these findings underline the critical role of autophagy in the maintenance of proper mitochondrial function. Moreover, we highlight an important physiological role of oxidative stress for basal autophagy regulation in skeletal muscle.

4. DISCUSSION

In this work, by using muscle specific autophagy-deficient (Atg7$^{-/-}$), we investigated the role of autophagy in skeletal muscle during ageing and exercise. We analyzed how decreased autophagy is related to ageing and the reason why autophagy reactivation can lead to ameliorated ageing features and increased lifespan.

PART I

In the first part of the work, we studied the role of autophagy during ageing in muscle tissue. Our results highlight two important functions of autophagy in sarcopenia, in fact it is responsible for the removal of damaged mitochondria that produce ROS, and for the signalling that induces the release of the neurotrophic factor FGFBP1 to maintain NMJ and muscle–nerve interaction.

Ageing leads to the functional degeneration of tissues and this is mainly due to accumulation of damaged DNA, proteins and organelles. Autophagy is a catabolic process essential for the maintenance of tissue homeostasis. It is responsible for the removal of dysfunctional proteins that are prone to aggregate, and for proper organelle turnover, such as mitochondria, in order to reduce ROS production and preserve DNA stability (Sandri, 2010).

Due to these actions and to the fact that autophagy declines with age, there is consensus in considering autophagy as an anti- ageing system. Indeed, genetic evidences in flies and worms sustain this concept but this indication is still lacking in mammals (Lee et al., 2010b; Rubinsztein et al., 2011; Simonsen et al., 2008; Madeo et al., 2010).

For what concerns mammals, there is a more complicated scenario, because autophagy knockout mice die at newborn stage due to a general energy failure (Kuma et al., 2004) and most of the tissue specific knockouts (e.g. in brain or heart)(Hara et al., 2006; Komatsu et al., 2006; Nakai et al., 2007) show severe organ

dysfunctions that precludes ageing studies. For this reason the link between autophagy and ageing is still lacking in mammals.

Our conditional model of muscle-specific autophagy deficiency allowed us to analyse the role of autophagy in muscles of adult and aged animal. Our findings support the notion that autophagy failure contributes to ageing. Adult $Atg7^{-/-}$ mice are characterized by mitochondrial dysfunction, oxidative stress, weakness, atrophy and loss of innervations; those are typical features of the ageing state, thus suggesting that autophagy-deficiency leads to premature ageing. Moreover, we found that altogether these events did shorten the lifespan of autophagy-deficient animals.

Ageing is a multisystemic disorder that affects multiple organs leading to alterations of metabolism and tissue function. The post-mitotic tissues such as brain, heart and skeletal muscle are the most susceptible to age-related diseases and precocious ageing when some dysfunction occurs. Interestingly, among the different age-related features, only one is conserved in several species, such as C.elegans, Drosophila, and mammals, including humans, that is the loss of muscle force. Therefore, muscle is a proper tissue that can be used to investigate ageing mechanisms. Moreover, muscles play an important role in the regulation of glucose, lipids and therefore in the general control of metabolism. Recent studies in Drosophila sustained the important role of muscle in healthy ageing. It has been shown that the over-expression of FoxO transcription factor, (that leads to autophagy activation), in the muscles of flies, preserves muscle function and increases longevity (Demontis and Perrimon, 2010), decreasing the accumulation of protein aggregates also in other tissues. On the contrary the over-expression of FoxO in adipose tissue, did not induce any changes. These results confirm that maintenance of a normal autophagy level in skeletal muscle, is sufficient to induce positively effects on whole-body metabolism, suggesting an important regulatory role for muscle tissue (Demontis and Perrimon, 2010).

Muscle-specific autophagy deficient mice allowed us to dissect the role of autophagy during ageing. Our findings support the notion that autophagy is critical to prevent sarcopenia. Indeed autophagy inhibition is sufficient to trigger a precocious ageing state in adult mice. It has been shown that oxidative stress increases during ageing, because of a reduction in autophagy flux and accumulation of dysfunctional

mitochondria. Since mitochondria are the main producers of ROS, dysfunctional mitochondria are thought to play a key role in decline of muscle function. At old age, a significant proportion of the mitochondria are abnormally enlarged, more rounded in shape and display vacuolization in the matrix and shorter christae (Peterson et al., 2012). We found that block of autophagy leads to accumulation of mitochondria with altered morphology and function. Accordingly, in the previous work it was showed that energy-stress sensor, AMPK, is activated in Atg7$^{-/-}$ muscles (Masiero et al., 2009). Importantly, we showed that mitochondrial dysfunction can be reversed by inhibiting ROS production through the anti-oxidant Trolox. This finding is consistent with a recent report that showed amelioration of age-related deficit, including mitochondrial function, by expressing a mitochondrial-targeted human catalase (Lee et al., 2010a). An higher production of ROS, leads to increased protein carbonylation, that mainly affects mitochondrial and structural proteins, such as actin and myosin. This contributes to impaired muscle contraction and weakness, caused by an altered actin/myosin interaction and a reduction in force generation. Trolox treatment reverted both protein oxidation and actin sliding properties, ultimately ameliorating muscle force. It is well established that changes in muscle mass and strength tend to be dissociated in elderly persons, being the decline of muscle strength three times faster than the decrease of muscle mass (Peterson et al., 2012). This notion suggests that alteration in the quality of contractile proteins plays critical role during age-related decrease of muscle force. Importantly, while anti-oxidant ameliorates acto/myosin functionality, it does not protect from muscle atrophy. However we cannot exclude that extending Trolox treatment would counteract muscle atrophy as well. Autophagy impairment also causes instability and degeneration of NMJ. Previous studies reported that mitochondrial ROS production may contribute to NMJ instability (Dobrowolny et al., 2008; Jang et al., 2012; Jang et al., 2010). But in our hands anti-oxidant treatment only slightly ameliorated NMJ stability of autophagy deficient mice, with no effect on fragmentation suggesting that other players were necessarily involved in NMJ maintenance. Indeed muscle tissue itself plays an important role in the signalling for NMJ development and maintenance (Johnson-Venkatesh and Umemori, 2010). In particular, molecules are secreted retrogradely from muscle to nerve, thus affecting

motor neuron survival, growth and maintenance (Dobrowolny et al., 2005; Funakoshi et al., 1995). We found that FGFBP1 is required for NMJ maintenance and that a normal autophagic flux is critical for its correct regulation. Knocking down FGFBP1 expression for 14 days in control muscles was sufficient to trigger fragmentation of NMJs and to increase AChR turnover. Moreover, these effects appear after only 2 weeks of FGFBP1 inhibition. Prolonged FGFBP1 perturbation might even worsen NMJ instability and fragmentation. In the opposite situation, when we over-expressed FGFBP1 in Atg7$^{-/-}$ mice we observed an ameliorated NMJ stability and rescue in the number of NCAM positive fibres, thus confirming that FGFBP1 is a muscle-derived synaptic organizing factor that is required for NMJ maintenance.

The alteration of FGFBP1 expression is a consequence of the impairment of endocytic trafficking that impacts on AChR cluster and MuSK activity on downstream signalling. In fact surface expression of MuSK, a kinase that affects a plethora of signalling pathways that are important for NMJ stability, is regulated by the endocytic pathway (Punga and Ruegg, 2012). MuSK does not properly localize at the NMJ in Atg7 knockout, being internalized instead of being at the surface of the myofibre. However, it was re-localized at the NMJ when FGFBP1 was over-expressed in Atg7$^{-/-}$ mice.

Our data strongly support the concept that autophagy, in a post-mitotic tissue, is required for healthy ageing being critical for the correct interplay between muscle and nerve and for the quality-control of mitochondria. Moreover we have evidences to believe that the beneficial effects of caloric restriction and exercise on ageing are a consequence of autophagy reactivation. Future works will investigate the link between autophagy inhibition, altered expression of FGFBP1 and MuSK.

PART II

In the second part of the work, we investigated the connection between autophagy and physical exercise.

We found that autophagy is required for healthy ageing. Lifestyle adaptations, in particular caloric restriction and physical activity contributes to increase lifespan ameliorating some ageing features (Melov et al., 2007; Fontana et al., 2010; Sandri et al., 2013). In particular, we analyzed human biopsies of young, aged sedentary subjects or senior sportsmen. We confirmed that autophagy is reduced with ageing, but upon exercise it is reactivated also in elderly. So it is important to understand the role of autophagy during physical activity, and to investigate whether the beneficial effects of exercise (that are also visible in aged people) are directly due to autophagy reactivation.

Autophagy is activated upon exercise in several tissues, in particular it has been shown that acute bout of exercise activates autophagosome formation in skeletal muscles (Grumati et al., 2010; Grumati et al., 2011a; Grumati et al., 2011b; He et al., 2012; Rubinsztein et al., 2011; Wohlgemuth et al., 2010). It has previously reported that autophagy is required for proper energy provision and glucose homeostasis during muscle contraction potentially through AMPK activation and its downstream targets (He et al., 2012). However, another study reached the opposite conclusion indicating that autophagy inhibition results in an improved blood glucose profile (Kim et al., 2013). Therefore, up to now there is no general consensus about the metabolic impact of autophagy during exercise, whether this effect is cell-autonomous and the mechanism underlying has not been fully understood yet. In order to address this issue we used inducible muscle-specific autophagy knockout mice, that were recently generated in our laboratory (Masiero et al., 2009). In these mice a muscle-specific acute deletion of the Atg7 gene was induced upon Tamoxifen treatment just before exercise. We used this model to avoid any possible compensation mechanism, that occur in conditional models.

We observed that block of autophagy in skeletal muscle did not impact on physical performance, glucose homeostasis or AMPK activation in our mice. Accordingly, a recent report where heterozygous mice for BECLIN1 were subjected to exercise also

found no differences in running capacity, providing further evidence that autophagy is not required during an acute bout of exercise (Safdar et al., 2011). The same study also demonstrated that the absence of exercise-induced autophagy results in a lack of exercise training-induced adaptations; thus suggesting that autophagy is required for muscle adaptations to chronic exercise which need mitochondrial turnover and remodelling (Safdar et al., 2011). So we wondered whether reduced performance was caused by impaired mitochondria functionality. Our data, indeed, support the idea that autophagy is critical for removing dysfunctional mitochondria during damaging contraction, and in fact the absence of autophagy leads to reduced running performance mainly due to increased ROS production and accumulation of dysfunctional mitochondria. Interestingly, this effect is gender specific being females more affected than males. These data are in line with the concept that females are more prone to muscle wasting during catabolic conditions. Moreover, one possibility could be that impairment in protein and organelle turnover might manifest more rapidly in females than in males, as it is known that in different tissues, such as brown adipose tissue, or mechanisms, such as oxidative stress response and mitochondria biogenesis, there are sex-dependent differences. (Nadal-casellas et al., 2013; Huges and Hekimi, 2011). Nevertheless it is plausible that different exercise regimens or a more chronic autophagy inhibition may unravel alterations in muscle performance in males as well. Further research into gender difference is required in order to discern the mechanisms responsible for male protection and female predisposition.

We wondered then whether reduction of oxidative stress could ameliorate physical performance of $Atg7^{-/-}$ mice. The chronic use of the antioxidant N-acetyl-cysteine did not ameliorate $Atg7^{-/-}$ performance, but on the contrary impaired the one of control animals. Moreover control mice treated with NAC showed a decreased basal and exercise-induced autophagy level. This result suggest that a basal level of ROS is necessary as signal to maintain redox homeostasis and autophagy activation mechanisms. Other works reported that 'physiological ROS' are important to mediate autophagy activation, thus maintaining tissue homeostasis (Underwood et al., 2010; Owusu-Ansah et al., 2013). Moreover, our findings correlate with the notion that anti-oxidants are detrimental for exercise-induced benefits, that has

already been reported in humans, although the mechanisms remain unclear (Ristow et al., 2011). We did not found significant changes in AMPK activation nor in blood metabolites that could explain the reduced physical performance. Moreover these data were confirmed when we acutely treated mice with a mitochondria-specific antioxidant.

Since we did not observed metabolic changes, we thought that one possible explanation could involve mitochondria-derived metabolites, which play an important role in signalling and could therefore impinge on cellular adaptations to stress. In our case, dysfunctional mitochondria can release factors that damage muscle tissue or, on the contrary, mitochondria impairment can lead to lack of certain important secreted factors. For instance, alpha-ketoglutarate-derived glutamine has been found to inhibit mTOR activity and activate autophagy (van der Vos et al., 2012). Importantly a recent work reported that impaired mitochondrial function in muscle specific Atg7 knockouts is protective from diet-induced obesity due to the induction of a mitochondrial stress mitokine, FGF21 (Kim et al., 2013). Therefore, it is possible that dysfunctional mitochondria generate metabolites or myokines that are involved in pathways important for myofibres function during exhausting and damaging muscle contraction. Moreover, the detrimental effects of anti-oxidants on physical performance underline the important role of mild oxidative stress in regulating autophagy and mitochondrial network in skeletal muscles.

We can conclude that autophagy is required for quality control of mitochondria during damaging contraction. More studies are required for investigate whether block of autophagy leads to possible impaired mitochondrial factor that impinge on muscle contraction capacity.

FUTURE WORKS

These works went through several open questions of the autophagy field, solving or indicating possible mechanism for each of them. At the same time, some new interesting issues came out.

For what concerns constitutive autophagy deficient mice Atg7$^{-/-}$, now it is important to understand the mechanisms that link FGBP1 alteration and MuSK wrong localization. We will investigate downstream signals of MuSK, such as ERK pathway, that can impinge on transcription factors which possibly regulate FGFBP1 expression. For the same reason we will study the promoter region of FGFBP1, to identify players involved in its regulation.

The findings obtained with the inducible autophagy deficient mice underlined the important role of autophagy in the removal and quality control maintenance of mitochondria, during damaging contraction. Now we have to better address which type of mitophagy is involved, understanding whether Pink-Parkin, Bnip3 or Nix play a role.

Then it would be interesting to further investigate which are the signals mediated by the mitochondria during exercise that are important for muscle homeostasis.

5. BIBLIOGRAPHY

Anson M., Drummond D.R., Geeves M.A., Hennessey E.S., Ritchie M.D., and Sparrow J.C. (1995). Actomyosin kinetics and *in vitro* motility of wild-type Drosophila actin and the effects of two mutations in the Act88F gene. *Biophys J.* 68, 1991-2003.

Bechet D, Tassa A, Taillandier D, Combaret L, Attaix D. (2005). Lysosomal proteolysis in skeletal muscle. *Int J Biochem Cell Biol* 37(10):2098-114.

Blaauw B., Mammucari C., Toniolo L., Agatea L., Abraham R., Sandri M., Reggiani C., and Schiaffino S. (2008). Akt activation prevents the force drop induced by eccentric contractions in dystrophin-deficient skeletal muscle. *Hum Mol Genet* 17, 3686-3696.

Bodine S.C., Latres E., Baumhueter S., Lai V.K., Nunez L., Clarke B.A., Poueymirou W.T., Panaro F.J., Na E., Dharmarajan K., Pan Z.Q., Valenzuela D.M., DeChiara T.M., Stitt T.N., Yancopoulos G.D., Glass D.J. (2001). Identification of ubiquitin ligases required for skeletal muscle atrophy. *Science* 3;294(5547):1704-8.

Bjørkøy G., Lamark T., Brech A., Outzen H., Perander M., Overvatn A., Stenmark H., Johansen T. (2005). p62/SQSTM1 forms protein aggregates degraded by autophagy and has a protective effect on huntingtin-induced cell death. *J Cell Biol* 21;171(4):603-14.

Bottinelli R., CanepariM., Pellegrino M.A., and Reggiani C. (1996). Force-velocity properties of human skeletal muscle fibres: myosin heavy chain isoform and temperature dependence. *J Physiol* 495 (Pt 2), 573-586.

Boya P., Reggiori F., Codogno P. (2013). Emerging regulation and functions of autophagy. *Nat Cell Biol* 15(7):713-20.

Buchberger A., Bukau B., Sommer T. (2010). Protein quality control in the cytosol and the endoplasmic reticulum: brothers in arms. *Mol Cell.* 22;40(2):238-52.

Burden SJ. (2011). SnapShot: Neuromuscular Junction. *Cell* 4;144(5):826-826.

Burden SJ. (2000). Wnts as retrograde signals for axon and growth cone differentiation. *Cell* 3;100(5):495-7.

Burden SJ. (2002). Building the vertebrate neuromuscular synapse. *J Neurobiol.* 53(4):501-1.

Canepari M., Maffei M., Longa E., Geeves M., and Bottinelli R. (2012). Actomyosin kinetics of pure fast and slow rat myosin isoforms studied by in vitro motility assay approach. *Exp Physiol* 97, 873-881.

Canepari M., Rossi R., Pellegrino M.A., Bottinelli R., Schiaffino S., and Reggiani C. (2000). Functional diversity between orthologous myosins with minimal sequence diversity. *J Muscle Res Cell Motil* 21, 375-382.

Canepari M., RossiR., Pellegrino M.A., Reggiani C., and Bottinelli R. (1999). Speeds of actin translocation in vitro by myosins extracted from single rat muscle fibres of different types. *Exp Physiol* 84, 803-806.

Chai R.J., Vukovic J., Dunlop S., Grounds M.D., and Shavlakadze T. (2011). Striking denervation of neuromuscular junctions without lumbar motoneuron loss in geriatric mouse muscle. *PLoS One* 6, e28090.

Chabi B., Ljubicic V., Menzies K.J., Huang J.H., Saleem A., and Hood D.A. (2008). Mitochondrial function and apoptotic susceptibility in aging skeletal muscle. *Aging Cell* 7, 2-12.

Chen F., Liu Y., Sugiura Y., Allen P.D., Gregg R.G., and Lin W. (2011) Neuromuscular synaptic patterning requires the function of skeletal muscle dihydropyridine receptors. *Nat Neurosci.* 14(5):570-7.

Cheng A., Morsch M., Murata Y., Ghazanfari N., Reddel S.W., Phillips W.D. (2013) Sequence of Age-Associated Changes to the Mouse Neuromuscular Junction and the Protective Effects of Voluntary Exercise. *PLOS ONE* 3;8(7).

Cherednichenko G., Zima A.V., Feng W., Schaefer S., Blatter L.A., Pessah I.N. (2004). NADH oxidase activity of rat cardiac sarcoplasmic reticulum regulates calcium-induced calcium release. *Circ Res* 94:478–486.

Coen P.M., Jubrias S.A., Distefano G., Amati F., Mackey D.C., Glynn N.W., Manini T.M., Wohlgemuth S.E., Leeuwenburgh C., Cummings S.R., Newman A.B., Ferrucci L., Toledo F.G., Shankland E., Conley K.E., Goodpaster B.H. (2013). Skeletal muscle mitochondrial energetics are associated with maximal aerobic capacity and walking speed in older adults. *J Gerontol A Biol Sci Med Sci* 68, 447-455.

Courtney J., Steinbach J.H. (1981). Age changes in neuromuscular junction morphology and acetylcholine receptor distribution on rat skeletal muscle fibres. *J Physiol* 320: 435–447.

Cuervo A.M. (2011) Chaperone-mediated autophagy: Dice's 'wild' idea about lysosomal selectivity. *Nat Rev Mol Cell Biol.* 12(8):535-41.

Davies K.J., Quintanilha A.T., Brooks G.A., Packer L. (1982). Free radicals and tissue damage produced by exercise. *Biochem Biophys Res Commun*. 107:1198–1205.

Demontis F., and Perrimon N. (2010). FOXO/4E-BP Signaling in Drosophila Muscles Regulates Organism-wide Proteostasis during Aging. *Cell* 143, 813-825.

Desaphy J.F., Pierno S., Liantonio A., Giannuzzi V., Digennaro C., Dinardo M.M., Camerino G.M., Ricciuti P., Brocca L., Pellegrino M.A., Bottinelli R., Camerino D.C. (2010). Antioxidant treatment of hindlimb-unloaded mouse counteracts fiber type transition but not atrophy of disused muscles. *Pharmacol Res.* 61(6):553-63.

Deschenes M.R., Wilson M.H. (2003). Age-related differences in synaptic plasticity following muscle unloading. *J Neurobiol* 57:246–256.

Dikalova A.E., Bikineyeva A.T., Budzyn K., Nazarewicz R.R., McCann L., Lewis W., Harrison D.G., Dikalov S.I. (2010). Therapeutic targeting of mitochondrial superoxide in hypertension. *Circ Res.* 107(1):106-16.

Donà M., Sandri M., Rossini K., Dell'Aica I., Podhorska-Okolow M., Carraro U. (2003). Functional in vivo gene transfer into the myofibers of adult skeletal muscle. *Biochem Biophys Res Commun*. 312(4):1132-8.

Dodson M., Darley-Usmar V., Zhang J. (2013). Cellular metabolic and autophagic pathways: traffic control by redox signaling. *Free Radic Biol Med*. 63:207-21.

Dooley C.T., Dore T.M., Hanson G.T., Jackson W.C., Remington S.J., et al. (2004). Imaging dynamic redox changes in mammalian cells with green fluorescent protein indicators. *J Biol Chem* 279: 22284–22293.

Fontana L., Klein S., and Holloszy J.O. (2010). Effects of long-term calorie restriction and endurance exercise on glucose tolerance, insulin action, and adipokine production. *Age* (Dordr) 32, 97-108.

Fox M.A., Sanes J.R., Borza D.B., Eswarakumar V.P., Fässler R., Hudson B.G., John S.W., Ninomiya Y., Pedchenko V., Pfaff S.L., Rheault M.N., Sado Y., Segal Y., Werle M.J., Umemori H. (2007). Distinct target-derived signals organize formation, maturation, and maintenance of motor nerve terminals. *Cell*. 129(1):179-93.

Geisler S., Holmström K.M., Skujat D., Fiesel F.C., Rothfuss O.C., Kahle P.J., Springer W. (2010). PINK1/Parkin-mediated mitophagy is dependent on VDAC1 and p62/SQSTM1. *Nat Cell Biol*. 12(2):119-31.

Glass D.J. (2005). Skeletal muscle hypertrophy and atrophy signaling pathways. *Int J Biochem Cell Biol*.; 37(10):1974-84.

Gomes M.D., Lecker S.H., Jagoe R.T., Navon A., Goldberg A.L. (2001). Atrogin-1, a muscle-specific F-box protein highly expressed during muscle atrophy. *Proc Natl Acad Sci U.S.A*. 98(25):14440-5.

Gomes L.C., Di Benedetto G., Scorrano L. (2011). During autophagy mitochondria elongate, are spared from degradation and sustain cell viability. *Nat Cell Biol*. 13(5):589-98.

Gomez A.M., Burden S.J. (2011). The extracellular region of Lrp4 is sufficient to mediate neuromuscular synapse formation. *Dev Dyn* 240(12):2626-33.

Gozuacik D., Kimchi A. (2004) Autophagy as a cell death and tumor suppressor mechanism. *Oncogene*. 23(16):2891-906.

Green D.R., Kroemer G. (2009). Cytoplasmic functions of the tumour suppressor p53. *Nature* 458(7242):1127-30.

Grumati P., Coletto L., Sabatelli P., Cescon M., Angelin A., Bertaggia E., Blaauw B., Urciuolo A., Tiepolo T., Merlini L., et al. (2010). Autophagy is defective in collagen VI muscular dystrophies, and its reactivation rescues myofiber degeneration. *Nat Med* 16, 1313-1320.

Grumati P., Coletto L., Sandri M., and Bonaldo P. (2011a). Autophagy induction rescues muscular dystrophy. *Autophagy* 7, 426-428.

Grumati P., Coletto L., Schiavinato A., Castagnaro S., Bertaggia E., Sandri M., and Bonaldo P. (2011b). Physical exercise stimulates autophagy in normal skeletal muscles but is detrimental for collagen VI-deficient muscles. *Autophagy* 7, 1415-1423.

Guarente L. (2013) Calorie restriction and sirtuins revisited. *Genes Dev.* 27(19):2072-85.

Hanson G.T., Aggeler R., Oglesbee D., Cannon M., Capaldi R.A., Tsien R.Y., Remington S.J. (2004). Investigating mitochondrial redox potential with redox-sensitive green fluorescent protein indicators. *J Biol Chem* 279: 13044–13053.

Hall Z.W., Sanes J.R. (1993). Synaptic structure and development: the neuromuscular junction. *Cell.* 72 Suppl:99-121.

Hall A., Burke N., Dongworth R., Hausenloy D. (2013). Mitochondrial fusion and fission proteins: Novel therapeutic targets for combating cardiovascular disease. *Br J Pharmacol*.

Hara T., Nakamura K., Matsui M., Yamamoto A., Nakahara Y., Suzuki-Migishima R., Yokoyama M., Mishima K., Saito I., Okano H., et al. (2006). Suppression of basal autophagy in neural cells causes neurodegenerative disease in mice. *Nature* 441, 885-889.

He C., Bassik M.C., Moresi V., Sun K., Wei Y., Zou Z., An Z., Loh J., Fisher J., Sun Q., Korsmeyer S., Packer M., May H.I., Hill J.A., Virgin H.W., Gilpin C., Xiao G., Bassel-Duby R., Scherer P.E., Levine B. (2012). Exercise-induced BCL2-regulated autophagy is required for muscle glucose homeostasis. *Nature* 481, 511-515.

Henríquez J.P., Krull C.E., Osses N. (2011). The Wnt and BMP families of signaling morphogens at the vertebrate neuromuscular junction. *Int J Mol Sci.*12(12):8924-46.

Holloszy J.O. (2011). Regulation of mitochondrial biogenesis and GLUT4 expression by exercise. *Compr Physiol*. 1(2):921-40.

Hughes B.G, Hekimi S. (2011). A mild impairment of mitochondrial electron transport has sex-specific effects on lifespan and aging in mice. *PLoS One*. 6(10):e26116.

Ichimura Y., Komatsu M. (2010). Selective degradation of p62 by autophagy. *Semin Immunopathol.* 32(4):431-6.

Jang Y.C., Liu Y., Hayworth C.R., Bhattacharya A., Lustgarten M.S., Muller F.L., Chaudhuri A., Qi W., Li Y., Huang J.Y., Verdin E., Richardson A., Van Remmen H. (2012). Dietary restriction attenuates age-associated muscle atrophy by lowering oxidative stress in mice even in complete absence of CuZnSOD. *Aging Cell.* 11(5):770-82.

Jang Y.C., Lustgarten M.S., Liu Y., Muller F.L., Bhattacharya A., Liang H., Salmon A.B., Brooks S.V., Larkin L., Hayworth C.R., Richardson A., Van Remmen H. (2010). Increased superoxide in vivo accelerates age-associated muscle atrophy through mitochondrial dysfunction and neuromuscular junction degeneration. *FASEB J* 24, 1376-1390.

Jang Y.C., and Van Remmen H. (2011). Age-associated alterations of the neuromuscular junction. *Exp Gerontol* 46, 193-198.

Johansen T., Lamark T. (2011). Selective autophagy mediated by autophagic adapter proteins. *Autophagy*. 7(3):279-96.

Johnson-Venkatesh E.M., Umemori H. (2010). Secreted factors as synaptic organizers. *Eur J Neurosci*. 32(2):181-90.

Kanter M.M. (1994). Free radicals, exercise, antioxidant supplementation. *Int J Sport Nutr* 4:205–220.

Kenyon C.J. (2010). The genetics of ageing. *Nature* 464, 504-512.

Kim N., Stiegler A.L., Cameron T.O., Hallock P.T., Gomez A.M., Huang J.H., Hubbard S.R., Dustin M.L., Burden S.J. (2008). Lrp4 is a receptor for Agrin and forms a complex with MuSK. *Cell*. 135(2):334-42.

Kim N., Burden S.J. (2008). MuSK controls where motor axons grow and form synapses. *Nat Neurosci* 11(1):19-27.

Kim K.H., Jeong Y.T., Oh H., Kim S.H., Cho J.M., Kim Y.N., Kim S.S., Kim do H., Hur K.Y., Kim H.K., Ko T., Han J., Kim H.L., Kim J., Back S.H., Komatsu M., Chen H., Chan D.C., Konishi M., Itoh N., Choi C.S., Lee MS. (2013). Autophagy deficiency leads to protection from obesity and insulin resistance by inducing Fgf21 as a mitokine. *Nat Med* 19, 83-92.

Klionsky D.J., Cregg J.M., Dunn W.A. Jr, Emr S.D., Sakai Y., Sandoval I.V., Sibirny A., Subramani S., Thumm M., Veenhuis M., Ohsumi Y. (2003). A unified nomenclature for yeast autophagy-related genes. *Dev Cell*. 5(4):539-45.

Komatsu M., Waguri S., Ueno T., Iwata J., Murata S., Tanida I., Ezaki J., Mizushima N., Ohsumi Y., Uchiyama Y., Kominami E., Tanaka K., Chiba T. (2005). Impairment of starvation-induced and constitutive autophagy in Atg7-deficient mice. *J Cell Biol*. 169(3):425-34.

Komatsu M., Waguri S., Chiba T., Murata S., Iwata J., Tanida I., Ueno T., Koike M., Uchiyama Y., Kominami E., Tanaka K. (2006). Loss of autophagy in the central nervous system causes neurodegeneration in mice. *Nature* 441, 880-884.

Komatsu M., Waguri S., Koike M., Sou Y.S., Ueno T., Hara T., Mizushima N., Iwata J., Ezaki J., Murata S., Hamazaki J., Nishito Y., Iemura S., Natsume T., Yanagawa T., Uwayama J., Warabi E., Yoshida H., Ishii T., Kobayashi A., Yamamoto M., Yue Z., Uchiyama Y., Kominami E., Tanaka K. (2007). Homeostatic levels of p62 control cytoplasmic inclusion body formation in autophagy-deficient mice. *Cell*. 131(6):1149-63.

Kouroku Y., Fujita E., Tanida I., Ueno T., Isoai A., Kumagai H., Ogawa S., Kaufman R.J., Kominami E., Momoi T. (2007). ER stress (PERK/eIF2alpha phosphorylation) mediates the polyglutamine-induced LC3 conversion, an essential step for autophagy formation. *Cell Death Differ* 14(2):230-9.

Kroemer G., Galluzzi L., Brenner C. (2007). Mitochondrial membrane permeabilization in cell death. *Physiol Rev*. 87(1):99-163.

Kron S.J., Toyoshima Y.Y., Uyeda T.Q., and Spudich J.A. (1991). Assays for actin sliding movement over myosin-coated surfaces. *Methods Enzymol* 196, 399-416.

Kuma A., Hatano M., Matsui M., Yamamoto A., Nakaya H., Yoshimori T., Ohsumi Y., Tokuhisa T., and Mizushima N. (2004). The role of autophagy during the early neonatal starvation period. *Nature* 432, 1032-1036.

Kurth-Kraczek E.J., Hirshman M.F., Goodyear L.J., Winder W.W. (1999) 5' AMP-activated protein kinase activation causes GLUT4 translocation in skeletal muscle. *Diabetes* 48(8):1667-71.

Lecker S.H., Goldberg A.L., and Mitch W.E. (2006). Protein degradation by the ubiquitin-proteasome pathway in normal and disease states. *J. Am. Soc. Nephrol*. 17, 1807–1819.

Lee H.Y., Choi C.S., Birkenfeld A.L., Alves T.C., Jornayvaz F.R., Jurczak M.J., Zhang D., Woo D.K., Shadel G.S., Ladiges W., Rabinovitch P.S., Santos J.H., Petersen K.F., Samuel V.T., Shulman G.I. (2010a). Targeted expression of catalase to mitochondria prevents age-associated reductions in mitochondrial function and insulin resistance. *Cell Metab* 12, 668-674.

Lee J.H., Budanov A.V., Park E.J., Birse R., Kim T.E., Perkins G.A., Ocorr K., Ellisman M.H., Bodmer R., Bier E., Karin M. (2010b). Sestrin as a feedback inhibitor of TOR that prevents age-related pathologies. *Science* 327, 1223-1228.

Lee J., Giordano S., Zhang J. (2012). Autophagy, mitochondria and oxidative stress:cross-talk and redox signaling. *Biochem. J.* 441, 523–540.

Levine B., Klionsky D.J. (2004). Development by self-digestion: molecular mechanisms and biological functions of autophagy. *Dev Cell* 6(4):463-77.

Levine B., Kroemer G. (2008). Autophagy in the pathogenesis of disease. *Cell* 132, 27-42.

Li Y., Lee Y., Thompson W.J. (2011). Changes in Aging Mouse Neuromuscular Junctions Are Explained by Degeneration and Regeneration of Muscle Fiber Segments at the Synapse. *J Neurosci* 31: 14910–14919.

Libby P., Bursztajn S., and Goldberg A.L. (1980). Degradation of the acetylcholine receptor in cultured muscle cells: selective inhibitors and the fate of undegraded receptors. *Cell* 19, 481-491.

Lipinski M.M., Zheng B., Lu T., Yan Z., Py B.F., Ng A., Xavier R.J., Li C., Yankner B.A., Scherzer C.R., Yuan J. (2010). Genome-wide analysis reveals mechanisms modulating autophagy in normal brain aging and in Alzheimer's disease. *Proc Natl Acad Sci U.S.A.* 107(32):14164-9.

Madeo F., Tavernarakis N., Kroemer G. (2010). Can autophagy promote longevity?. *Nat Cell Biol* 12(9):842-6.

Majmundar A.J., Wong W.J., Simon M.C. (2010). Hypoxia-inducible factors and the response to hypoxic stress. *Mol Cell*. 40(2):294-309.

Mammucari C., Milan G., Romanello V., Masiero E., Rudolf R., Del Piccolo P., Burden S.J., Di Lisi R., Sandri C., Zhao J., Goldberg A.L., Schiaffino S., Sandri M. (2007). FoxO3 controls autophagy in skeletal muscle in vivo. *Cell Metab*. 6, 458–471.

Mammucari C., Schiaffino S., and Sandri M. (2008). Downstream of Akt: FoxO3 and mTOR in the regulation of autophagy in skeletal muscle. *Autophagy* 4, 524–526.

Margossian S.S., and Lowey S. (1982). Preparation of myosin and its subfragments from rabbit skeletal muscle. *Methods Enzymol* 85 Pt B, 55-71.

Masiero E., Agatea L., Mammucari C., Blaauw B., Loro E., Komatsu M., Metzger D., Reggiani C., Schiaffino S., and Sandri M. (2009). Autophagy is required to maintain muscle mass. *Cell Metab* 10, 507-515.

Mazure N.M., Pouysségur J. (2010). Hypoxia-induced autophagy: cell death or cell survival? *Curr Opin Cell Biol* 22(2):177-80.

Melendez A., Talloczy Z., Seaman M., Eskelinen E.L., Hall D.H., and Levine B. (2003). Autophagy genes are essential for dauer development and life-span extension in C. elegans. *Science* 301, 1387-1391.

Melov S., Tarnopolsky M.A., Beckman K., Felkey K., and Hubbard A. (2007). Resistance exercise reverses aging in human skeletal muscle. *PLoS ONE* 2(5):e465.

Mizushima N. (2011). Autophagy in protein and organelle turnover. *Cold Spring Harb Symp Quant Biol.* 76:397-402.

Mizushima N., and Komatsu M. (2011). Autophagy: renovation of cells and tissues. *Cell* 147, 728-741.

Mizushima N., Levine B., Cuervo A.M., and Klionsky D.J. (2008). Autophagy fights disease through cellular self-digestion. *Nature* 451, 1069-1075.

Morrison J.H., and Hof P.R. (1997). Life and death of neurons in the aging brain. *Science* 278, 412-419.

Murgia M., Serrano A.L., Calabria E., Pallafacchina G., Lomo T., Schiaffino S. (2000). Ras is involved in nerve-activity-dependent regulation of muscle genes. *Nat Cell Biol*. 2(3):142-7.

Nadal-Casellas A., Bauzá-Thorbrügge M., Proenza A.M., Gianotti M., Lladó I. (2013). Sex-dependent differences in rat brown adipose tissue mitochondrial biogenesis and insulin signaling parameters in response to an obesogenic diet. *Mol Cell Biochem*. 373(1-2):125-35.

Nakai A., Yamaguchi O., Takeda T., Higuchi Y., Hikoso S., Taniike M., Omiya S., Mizote I., Matsumura Y., Asahi M., Nishida K., Hori M., Mizushima N., Otsu K. (2007). The role of autophagy in cardiomyocytes in the basal state and in response to hemodynamic stress. *Nat Med* 13, 619-624.

Narendra D.P., Jin S.M., Tanaka A., Suen D.F., Gautier C.A., Shen J., Cookson M.R., Youle R.J. (2010). PINK1 is selectively stabilized on impaired mitochondria to activate Parkin. *PLoS Biol*. 8(1):e1000298.

Newham D.J., McPhail G., Mills K.R., Edwards R.H. (1983) Ultrastructural changes after concentric and eccentric contractions of human muscle. *J Neurol Sci* 61 (1): 109-22.

Numberger M., Dürr I., Kues W., Koenen M., Witzemann V. (1991). Different mechanisms regulate muscle-specific AChR gamma- and epsilon-subunit gene expression. *EMBO J*. 10(10):2957-64.

Owusu-Ansah E., Song W., Perrimon N. (2013). Muscle mitohormesis promotes longevity via systemic repression of insulin signaling. *Cell*. 155(3):699-712.

Pankiv S., Clausen T.H., Lamark T., Brech A., Bruun J.A., Outzen H., Øvervatn A., Bjørkøy G., Johansen T. (2007). p62/SQSTM1 binds directly to Atg8/LC3 to facilitate degradation of ubiquitinated protein aggregates by autophagy. *J Biol Chem*. 282(33):24131-45.

Peternelj T.T., Coombes J.S. (2011). Antioxidant supplementation during exercise training: beneficial or detrimental? *Sports Med*. 41(12):1043-69.

Powers S.K., Jackson M.J. (2008). Exercise-induced oxidative stress: cellular mechanisms and impact on muscle force production. *Physiol Rev* 88 (4): 1243-76.

Peterson, C.M., Johannsen, D.L., and Ravussin, E. (2012). Skeletal Muscle Mitochondria and Aging: A Review. *J Aging Res* 194821.

Pette D., Heilmann C. (1979). Some characteristics of sarcoplasmic reticulum in fast- and slow-twitch muscles. *Biochem Soc Trans*. (4):765-7.

Pfaffl M.W., Lange I.G., Daxenberger A., Meyer H.H. (2001). Tissue-specific expression pattern of estrogen receptors (ER): quantification of ER alpha and ER beta mRNA with real-time RT-PCR. *APMIS*. 109(5):345-55.

Punga A.R., and Ruegg M.A. (2012). Signaling and aging at the neuromuscular synapse: lessons learnt from neuromuscular diseases. *Curr Opin Pharmacol* 12, 340-346.

Ristow M., Zarse K., Oberbach A., Klöting N., Birringer M., Kiehntopf M., Stumvoll M., Kahn C.R., Blüher M. (2009). Antioxidants prevent health-promoting effects of physical exercise in humans. *Proc Natl Acad Sci U.S.A.* 106, 8665-8670.

Roder I.V., Choi K.R., Reischl M., Petersen Y., Diefenbacher M.E., Zaccolo M., Pozzan T., and Rudolf R. (2010). Myosin Va cooperates with PKA RIalpha to mediate maintenance of the endplate in vivo. *Proc Natl Acad Sci U.S.A.* 107, 2031-2036.

Roder I.V., Petersen Y., Choi K.R., Witzemann V., Hammer J.A. 3rd, and Rudolf R. (2008). Role of Myosin Va in the plasticity of the vertebrate neuromuscular junction in vivo. *PLoS One* 3, e3871.

Romanello V., Guadagnin E., Gomes L., Roder I., Sandri C., Petersen Y., Milan G., Masiero E., Del Piccolo P., Foretz M., Scorrano L., Rudolf R., Sandri M. (2010). Mitochondrial fission and remodelling contributes to muscle atrophy. *EMBO J.* 29(10):1774-85.

Rossi P., Marzani B., Giardina S., Negro M., Marzatico F. (2008). Human Skeletal muscle aging and the oxidative system:cellular events. *Current aging science* 1: 182-191.

Rubinsztein D.C., Marino G., and Kroemer G. (2011). Autophagy and aging. *Cell* 146, 682-695.

Safdar A., Bourgeois J.M., Ogborn D.I., Little J.P., Hettinga B.P., Akhtar M., Thompson J.E., Melov S., Mocellin N.J., Kujoth G.C., Prolla T.A., Tarnopolsky M.A. (2011). Endurance exercise rescues progeroid aging and induces

systemic mitochondrial rejuvenation in mtDNA mutator mice. *Proc Natl Acad Sci U.S.A.* 108, 4135-4140.

Sandri M., Sandri C., Gilbert A., Skurk C., Calabria E., Picard A., Walsh K., Schiaffino S., Lecker S.H., Goldberg A.L. (2004). Foxo transcription factors induce the atrophy-related ubiquitin ligase atrogin-1 and cause skeletal muscle atrophy. *Cell* 117(3):399-412.

Sandri M. (2010). Autophagy in skeletal muscle. *FEBS Lett* 584, 1411-1416.

Sandri M., Sandri C., Gilbert A., Skurk C., Calabria E., Picard A., Walsh K., Schiaffino S., Lecker S.H., and Goldberg A.L. (2004). Foxo transcription factors induce the atrophy-related ubiquitin ligase atrogin-1 and cause skeletal muscle atrophy. *Cell* 117, 399-412.

Sandri M. (2008). Signaling in muscle atrophy and hypertrophy. *Physiology (Bethesda)*. 23:160-70.

Sandri M. (2010). Autophagy in health and disease. 3. Involvement of autophagy in muscle atrophy. *Am J Physiol Cell Physiol*. 298(6):C1291-7.

Sandri M., Barberi L., Bijlsma A.Y., Blaauw B., Dyar K.A., Milan G., Mammucari C., Meskers C.G., Pallafacchina G., Paoli A., Pion D., Roceri M., Romanello V., Serrano A.L., Toniolo L., Larsson L., Maier A.B., Muñoz-Cánoves P., Musarò A., Pende M., Reggiani C., Rizzuto R., Schiaffino S. (2013). Signalling pathways regulating muscle mass in ageing skeletal muscle: the role of the IGF1-Akt-mTOR-FoxO pathway. *Biogerontology*. 14(3):303-23.

Sartori R., Schirwis E., Blaauw B., Bortolanza S., Zhao J., Enzo E., Stantzou A., Mouisel E., Toniolo L., Ferry A., Stricker S., Goldberg A.L., Dupont S., Piccolo S., Amthor H., Sandri M. (2013). BMP signaling controls muscle mass. *Nat Genet.* 45(11):1309-18.

Schiaffino S., Hanzlíková V. (1972a). Autophagic degradation of glycogen in skeletal muscles of the newborn rat. *J Cell Biol*. 52(1):41-51.

Schiaffino S., Hanzlíková V. (1972b). Studies on the effect of denervation in developing muscle. II. The lysosomal system. *J Ultrastruct Res*. 39(1):1-14.

Schiaffino S., Reggiani C. (1996). Molecular diversity of myofibrillar proteins: gene regulation and functional significance. *Physiol Rev*. 76(2):371-423.

Schiaffino S., Sandri M., Murgia M. (2007). Activity-dependent signaling pathways controlling muscle diversity and plasticity. *Physiology (Bethesda).* 22:269-78.

Schiaffino S., Dyar K.A., Ciciliot S., Blaauw B., Sandri (2013). Mechanisms regulating skeletal muscle growth and atrophy. *M.FEBS J. 280*(17):4294-314.

Schuler M., Ali F., Metzger E., Chambon P., Metzger D. (2005). Temporally controlled targeted somatic mutagenesis in skeletal muscles of the mouse. *Genesis* 41(4):165-70.

Scorrano L. (2013). Keeping mitochondria in shape: a matter of life and death. *Eur J Clin Invest* 43(8):886-93.

Shi L., Fu A.K., Ip NY. (2012). Molecular mechanisms underlying maturation and maintenance of the vertebrate neuromuscular junction. *Trends Neurosci.* 35(7):441-53.

Simonsen A., Cumming R.C., Brech A., Isakson P., Schubert D.R., and Finley K.D. (2008). Promoting basal levels of autophagy in the nervous system enhances longevity and oxidant resistance in adult Drosophila. *Autophagy* 4, 176-184.

Tan C.C., Yu J.T., Tan M.S., Jiang T., Zhu X.C., Tan L. (2013). Autophagy in aging and neurodegenerative diseases: implications for pathogenesis and therapy. *Ageing Res Rev*. 12(1):237-52.

Toledo F.G., and Goodpaster B.H. (2013). The role of weight loss and exercise in correcting skeletal muscle mitochondrial abnormalities in obesity, diabetes and aging. *Mol Cell Endocrinol* 379(1-2):30-4.

Tracy K., and Macleod K.F. (2007). Regulation of mitochondrial integrity, autophagy and cell survival by BNIP3. *Autophagy* 3, 616–619.

Trinidad J.C., Fischbach G.D., Cohen J.B., (2000). The Agrin/MuSK Signaling Pathway Is Spatially Segregated from the Neuregulin/ErbB Receptor Signaling Pathway at the Neuromuscular Junction. *J Neurosci.* 20(23):8762-70.

Underwood B.R., Imarisio S., Fleming A., Rose C., Krishna G., Heard P., Quick M., Korolchuk V.I., Renna M., Sarkar S., García-Arencibia M., O'Kane C.J.,

Murphy M.P., Rubinsztein D.C. (2010). Antioxidants can inhibit basal autophagy and enhance neurodegeneration in models of polyglutamine disease. *Hum Mol Genet.* 19(17):3413-29.

Urso M.L., Clarkson P.M. (2003). Oxidative stress, exercise, antioxidant supplementation. *Toxicology* 189:41–54.

Vainshtein A., Kazak L., and Hood D.A. (2011). Effects of endurance training on apoptotic susceptibility in striated muscle. *J Appl Physiol* 110, 1638-1645.

Valdez G., Tapia J.C., Kang H., Clemenson G.D., Jr. Gage F.H., Lichtman J.W., and Sanes, J.R. (2010). Attenuation of age-related changes in mouse neuromuscular synapses by caloric restriction and exercise. *Proc Natl Acad Sci U.S.A.* 107, 14863-14868.

Van der Vos K.E., Eliasson P., Proikas-Cezanne T., Vervoort S.J., van Boxtel R., Putker M., van Zutphen I.J., Mauthe M., Zellmer S., Pals C., Verhagen L.P., Groot Koerkamp M.J., Braat A.K., Dansen T.B., Holstege F.C., Gebhardt R., Burgering B.M., Coffer P.J. (2012). Modulation of glutamine metabolism by the PI(3)K-PKB-FOXO network regulates autophagy. *Nat Cell Biol* 14, 829-837.

Visser M., and Schaap L.A. (2011). Consequences of sarcopenia. *Clin Geriatr Med* 27, 387-399.

Wenz T., Rossi S.G., Rotundo R.L., Spiegelman B.M., and Moraes C.T. (2009). Increased muscle PGC-1alpha expression protects from sarcopenia and metabolic disease during aging. *Proc Natl Acad Sci U.S.A.* 106, 20405-20410.

Whidden M.A., Smuder A.J., Wu M., Hudson M.B., Nelson W.B., Powers S.K. (2010). Oxidative stress is required for mechanical ventilation-induced protease activation in the diaphragm. *J Appl Physiol* 108(5):1376-82.

Williams A., Jahreiss L., Sarkar S., Saiki S., Menzies F.M., Ravikumar B., Rubinsztein D.C. (2006). Aggregate-prone proteins are cleared from the cytosol by autophagy: therapeutic implications. *Curr Top Dev Biol.* 76:89-101.

Williams A.H., Valdez G., Moresi V., Qi X., McAnally J., Elliott J.L., Bassel-Duby R., Sanes J.R., and Olson E.N. (2009). MicroRNA-206 delays ALS progression

and promotes regeneration of neuromuscular synapses in mice. *Science* 326, 1549-1554.

Wohlgemuth S.E., Seo A.Y., Marzetti E., Lees H.A., and Leeuwenburgh C. (2010). Skeletal muscle autophagy and apoptosis during aging: effects of calorie restriction and life-long exercise. *Exp Gerontol* 45, 138-148.

Wu H., Xiong W.C., Mei L. (2010). To build a synapse: signaling pathways in neuromuscular junction assembly. *Development* 137(7):1017-33.

Xia R., Webb J.A., Gnall L.L., Cutler K., Abramson J.J. (2003). Skeletal muscle sarcoplasmic reticulum contains a NADH-dependent oxidase that generates superoxide. *Am J Physiol Cell Physiol* 285:C215–C221.

Yumoto N., Kim N., Burden S.J. (2012). Lrp4 is a retrograde signal for presynaptic differentiation at neuromuscular synapses. *Nature* 489(7416):438-42.

Zhao J., Brault J.J., Schild A., Cao P., Sandri M., Schiaffino S., Lecker S.H., and Goldberg A.L. (2007). FoxO3 coordinately activates protein degradation by the autophagic/lysosomal and proteasomal pathways in atrophying muscle cells. *Cell Metab*. 6, 472–483.

Zhao J., Brault J.J., Schild A., and Goldberg A.L. (2008). Coordinate activation of autophagy and the proteasome pathway by FoxO transcription factor. *Autophagy* 4, 378–380.

Zhou J., Yi J., Fu R., Liu E., Siddique T., Rios E., Deng H.X. (2010). Hyperactive intracellular calcium signaling associated with localized mitochondrial defects in skeletal muscle of an animal model of amyotrophic lateral sclerosis. *J. Biol. Chem*. 285, 705–712.